

**16th
Caribbean
Geological
Conference**



June 16th – 21st, 2002

Barbados

West Indies

FIELD GUIDES

FIELD TRIP #1

FIELD GUIDE TO **THE SUB-QUATERNARY OF BARBADOS**

Field Guide and Author:

Robert C. Speed

Northwestern University
Department of geological Sciences
Evanston, Illinois 60208
U.S.A.

GEOLOGIC BACKGROUND

The island of Barbados is the only emergent peak of the Barbados Ridge, which is an extensive, NS-trending submarine mountain belt (Fig.1). The Barbados Ridge is the accretionary prism of the Lesser Antilles forearc. It lies above the subduction zone between the Caribbean and South America plates (Fig.1).

Quaternary Limestone: Some 80% of the island is covered by limestone of known and presumed Quaternary age (Fig.2) (Mesollela, 1968; Mesollela and others, 1970; Matthews, 1973; Taylor, 1974; Fairbanks and Matthews, 1978; Bender and others, 1979; Gallup and others, 1994; Speed and Barker, 1997). The Quaternary limestone is composed principally of biogenic grainstone and coral boundstone. It records shorezone deposition during sea level changes due to tectonic uplift and eustatic oscillation. The limestone cap, also known as the coral cap, varies irregularly in thickness between 1 and 150m. The formation formerly covered all of Barbados and has been widely eroded from the island's eastern margin.

Sub-Quaternary: Below the limestone cap and exposed over 20% of the island is the sub-Quaternary, the focus of this field guide. The sub-Quaternary is divided among four major tectonic-stratigraphic units, named in Table 1, on the basis of outcrop and well data. The major units are further divided into subunits, whose names and depositional age ranges are in Table 1. Figure 3 illustrates a diagrammatic tectonostratigraphic stacking among the major and minor units. Figure 4 shows schematically a depth array of the major units in a NW-SE section.

Basal Complex: The basal complex is the lowest exposed unit (Speed, 1979, 1982, 1986; Poole and Barker, 1982; Speed and Larue, 1982; Larue and Speed, 1985; Sedlock and Speed, 1986; Jansma and Speed, 1986). It is constituted by fault-bound packets of two types: terrigenous strata and radstone-hemipelagic strata (Table 1, Fig. 3). The terrigenous strata are quartzose turbidites of wide facies spectrum (Speed and Larue, 1982; Pudsey and Reading, 1982; Larue and Speed, 1983; Larue, 1985). The strata are poorly dated. Correlations of strata from packet to packet are not generally possible, and there is no island-wide stratigraphy. The radstones occupy discrete fault packets in the basal complex (Gortner and Larue, 1987). The age of accretion of the basal complex is probably late Eocene.

Prism Cover: Prism cover consists of sediments deposited on the basal complex after its accretion and before (Woodbourne Fm, Cambridge beds) or after (Conset Marl) the arrival of the Oceanic allochthon. The subsurface Woodbourne Fm is the thickest deposit of prism cover owing to its probable syntectonic deposition in the Woodbourne Trough (Barker and others, 1986; Speed, 1986).

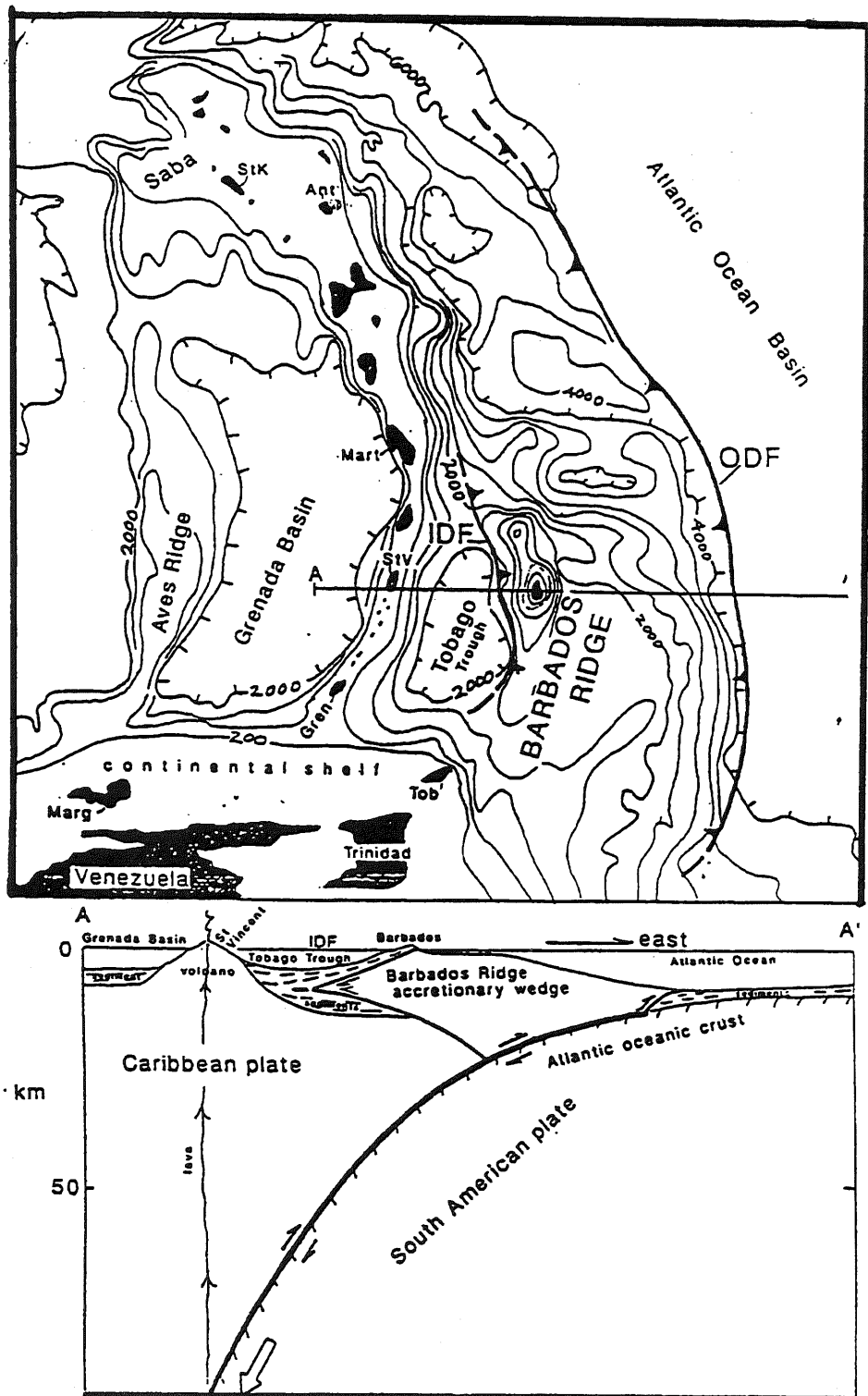


Figure 1: Map and section of Lesser Antilles forearc; Barbados Ridge is the accretionary prism and Tobago Trough is the forearc basin. Water depths in m. ODF is outer deformation front and IDF is inner deformation front of accretionary prism.

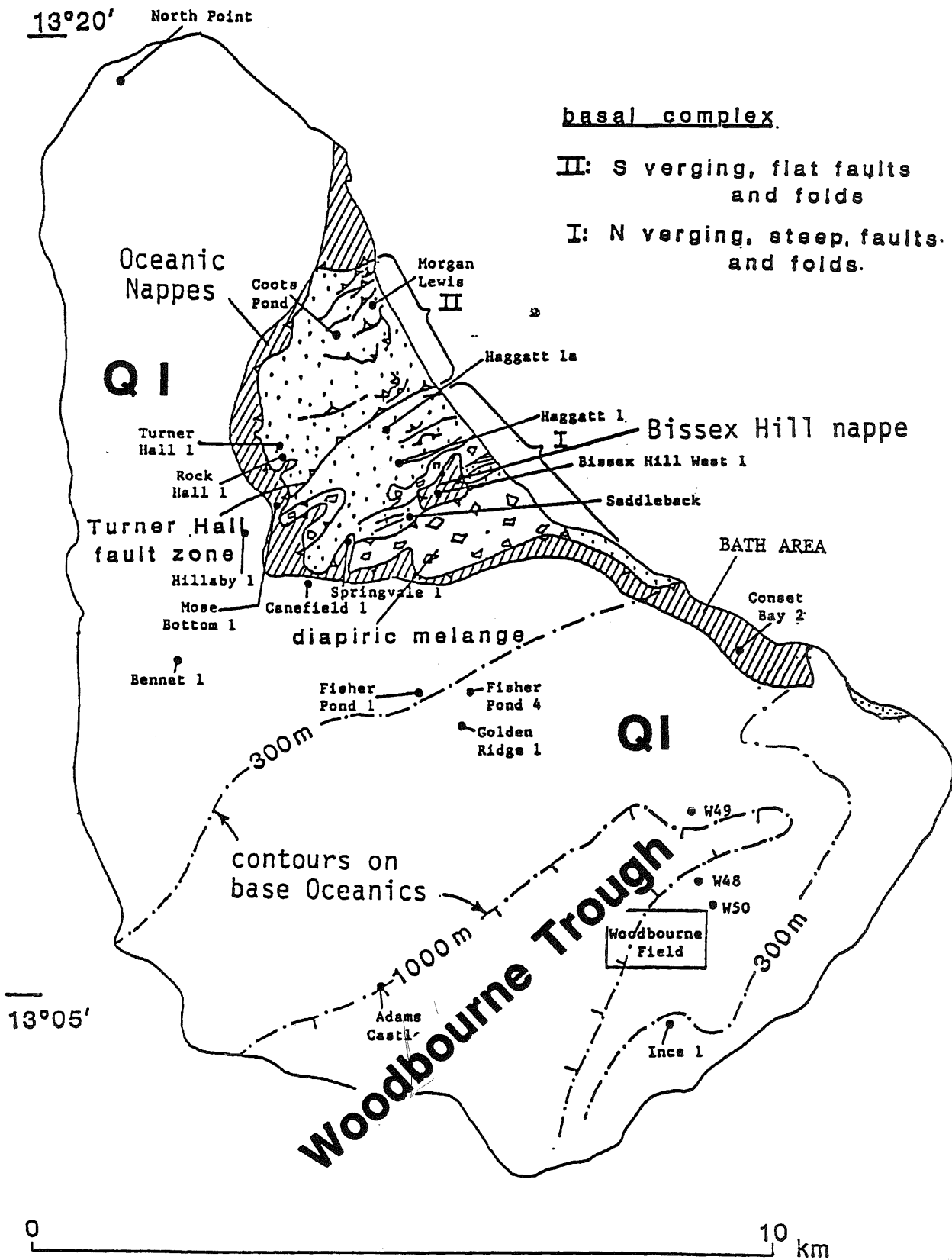


Figure 2: Outcrop map of Barbados

Table 1. Tectonic – stratigraphic units of the sub-Quaternary of Barbados

<u>Major Units</u>	<u>Sub units</u>	<u>Depositional Age Range</u>
Diapirs	—	—
Oceanic allochthon	Oceanic nappes Bissex Hill nappe Cattlewash nappe	mid-middle Eocene to late Oligocene late-middle Eocene to early Oligocene late-middle Eocene
Prism Cover	Woodbourne Fm Conset Marl Bissex Hill Fm Cambridge beds Kingsley beds unnamed (subsurf)	late Oligocene (?) to middle Miocene middle Miocene middle Miocene late Oligocene(?) to early Miocene late Miocene to Pliocene (?) Miocene
Basal Complex	terrigenous radstone or hemipelagic	middle Eocene to late Eocene early Eocene to mid-middle Eocene

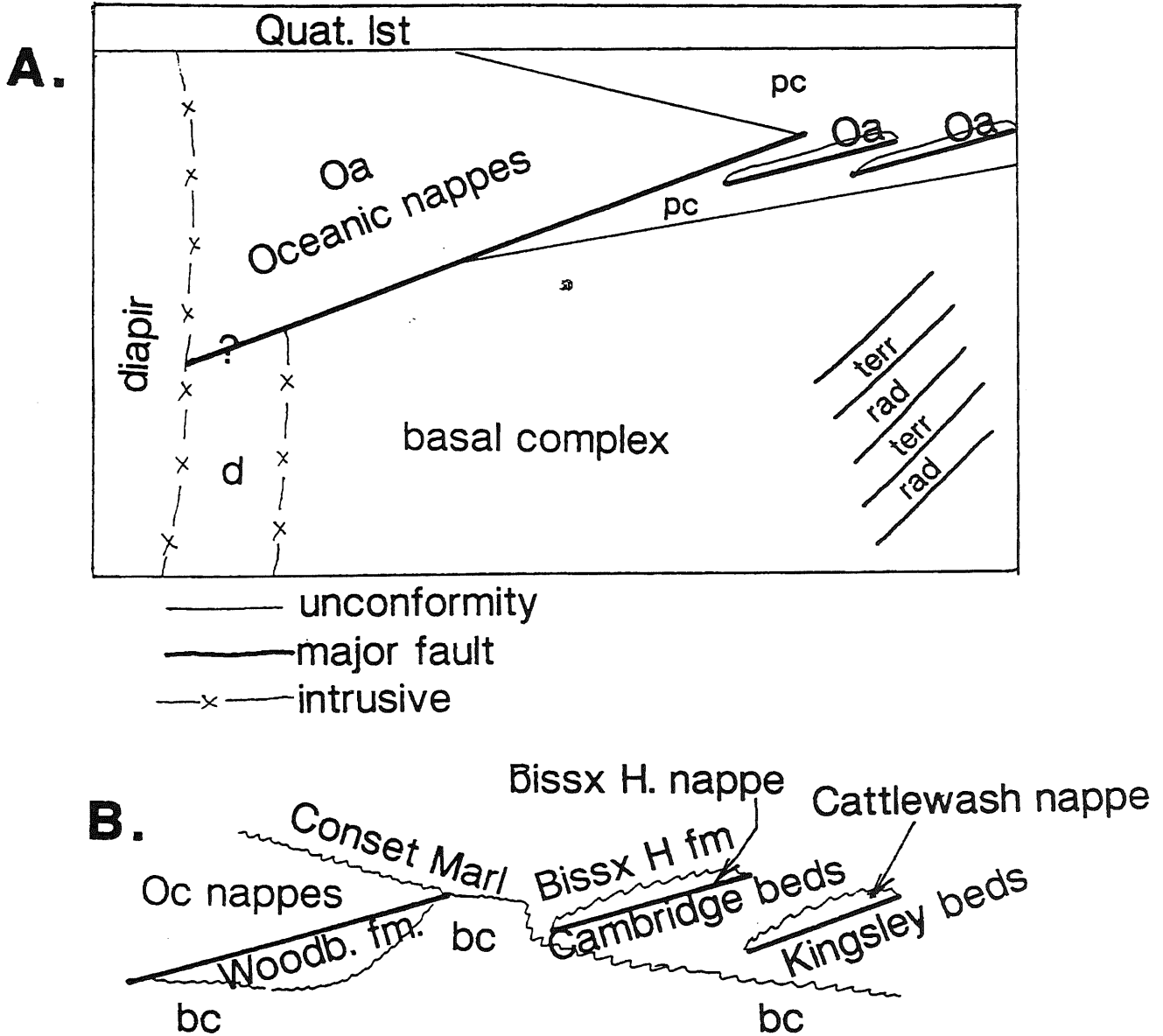


Figure 3: Stacking diagram for some major and minor tectonic- stratigraphic units. A: shows total stacking. B: shows detail among minor units of prism cover (pc), Oceanic allochthon (Oa), and basal complex (bc). Heavy lines are faults; wiggly lines are unconformities; dash-x are intrusive contacts.

Oceanic Allochthon: The Oceanic allochthon was emplaced from west to east above the inner (western) front of the Barbados accretionary prism in middle Miocene time. The allochthon is constituted by pelagic marl and ash, which was deposited in forearc basins precursor to the present Tobago Trough (Senn, 1948; Torrini and others, 1985; Torrini, 1986; Torrini and Speed, 1989). The Oceanic allochthon is divided in two ways. First is by structural position and rock composition. Here the main body of the allochthon is assigned as the Oceanic nappes (Figs. 3, 4); it is the structurally highest and contains no terrigenous sediment. Two outlying subunits of the allochthon are, the Bissex Hill and Cattlewash nappes, each of whose marl successions includes minor quartz sandstone and whose structural positions are below that of the Oceanic nappes (Speed, 1986; Larue, 1986). The second division scheme applies only to the Oceanic nappes subunit and separates a lower and upper tier (Fig.4). The lower tier is an imbricate of marl-ash slices, probably a duplex. The upper tier appears to be a single nappe that includes a continuous stratigraphic section of Eocene and Oligocene beds.

The sole fault of the Oceanic allochthon is a generally distinctive zone of deformed rock, concentionary limestone with organic carbon, and fluid seeps. This is called the SOFZ (sub-oceanic fault zone) (Fig.4).

Diapirs: The diapir tectonic-stratigraphic unit crops out in at least nine bodies that are discrete at the surface. The diapirs are constituted by lithic blocks, green mud granules, matrix, and rarely, clams (Kugler and others, 1984; Larue, 1986). The blocks are as large as 25m and composed mainly of hard rocks of the basal complex. The matrix comprises smectitic mud, quartz sand, and bitumen. Green mud granules are angular or faceted mudstone fragments which are alien to the surface units. Diapir bodies have varied forms: thick (3km) vertical dike, plug, thin (10m) subhorizontal sill, thin (10m) inclined dike, and probably others. Eocene pollen has been obtained from the matrix.

Structures: Structures of the basal complex are fault zones that bound the accretionary packets and major and minor folds. The fault zones are of varied structure: narrow or discrete surfaces to thick (20m) belts of broken sandstone and mudstone foliated with spaced, scaly cleavage. Some fault zones have had reactivation where early structures are truncated by later ones. Folds exist within packet interiors as first phase structures and in some fault zones as late phase structures. Sets of flat packets are folded at places. In general, fault zones and major folds of the northern Scotland district are shallowly inclined whereas those of the southern Scotland District are subvertical. The prevailing direction of tectonic transport is between NNW–SSE and NW–SE, including fold contraction and net slip of faults. Reactivated fault zones are mainly thrusts with SSE slip.

Prism cover is slightly to strongly deformed, depending on time of deposition relative to emplacement of the Oceanic allochthon. Some prism cover is structurally embedded within the basal complex of northern Barbados (Fig.4).

BARBADOS ISLAND

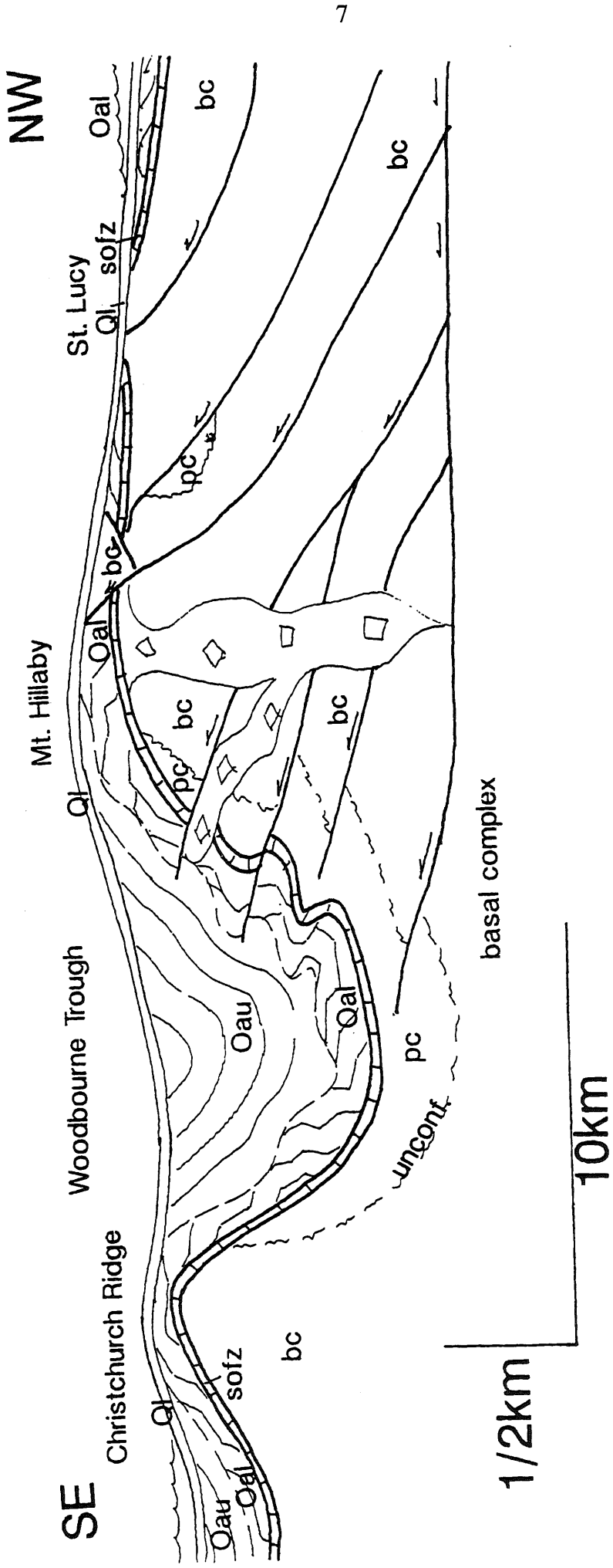


Figure 4: Schematic cross section through Barbados showing major tectonic-stratigraphic units. Oceanic allochthon nappes subunit divided into lower (Oal) and upper (Oau) tiers. SOFZ is sub-Oceanic fault zone. Diapir identified by block pattern.

The only major structure associated with deposition of prism cover is the Woodbourne Trough (Fig. 2) which trends SW–NE in the subsurface of southern Barbados. The Trough was a one–or two–sided subsiding basin in the early Miocene, in which more than 1km of the Woodbourne formation accumulated on the basal complex. Northeast of the Woodbourne field (Fig.2), the Woodbourne Trough plunges SW such that the basal complex is at sea level at the East Coast and the Woodbourne Formation pinches out northeastward. It is not certain whether the plunge is primary or was superposed on the Trough in middle Miocene time.

Structures of the Oceanic allochthon are low-angle fault imbricates in the lower third of the Oceanic nappes (Oal, Fig.4) and in the Bissex Hill and Cattlewash nappes. Such faults are commonly cm–thick zones of bituminous foliated clay, implying dissolution and fluid conduction as well as fault slip. The sub-Oceanic fault zone (SOFZ) varies in thickness from 1 to 25 m. It contains lenses of rocks from both walls wherein mudrocks are strongly deformed by singular and conjugate faults and by spaced cleavage. The tectonic transport inferred from such structures is top ESE (Torrini; 1986). Another characteristic of the SOFZ is the concentration of calcite concretions with distinctive replacement textures and veinwork. The carbon in such calcite came from petroleum–methane mixtures. The SOFZ also includes vent communities and major concentration of bitumens (Torrini and others, 1990).

The form of the Woodbourne Trough is mainly defined by the vertical thickness of the Oceanic allochthon (Fig.1), which exceeds 1km in the SW reach of the Trough. Beyond the flanks of the Trough in central and northern Barbados, the Oceanic allochthon is generally less than 100m thick. The thickness distribution is probably due to denudation in the northern two-thirds of the island and to relative preservation in the Woodbourne Trough by emplacement of the Oceanic allochthon in a deep marine basin.

The SOFZ, the contact between the Oceanic allochthon and the basal complex or prism cover, is locally folded on NE–trending axes. Such folds are major and minor and locally overturned. Their existence implies that the Woodbourne Trough continued subsidence, probably as a syncline, after emplacement of the Oceanic allochthon.

The history and mechanisms of emplacement of the diapirs are uncertain. Some appear to have taken up regional NNW–SSE contraction by local development of spaced cleavage. One thin (20m) inclined dike evidently filled an extension crack without related fault motions. The Oceanic allochthon was in place before some of the diapirs reached their present level. The allochthon exerts control on the diapiric process. One diapir (packet 8) tops at the base of the Bissex Hill nappe (Fig. 5). The largest diapir (packet 18) overlies that nappe but domes up and spreads laterally below the higher Oceanic nappes unit (Fig.5).

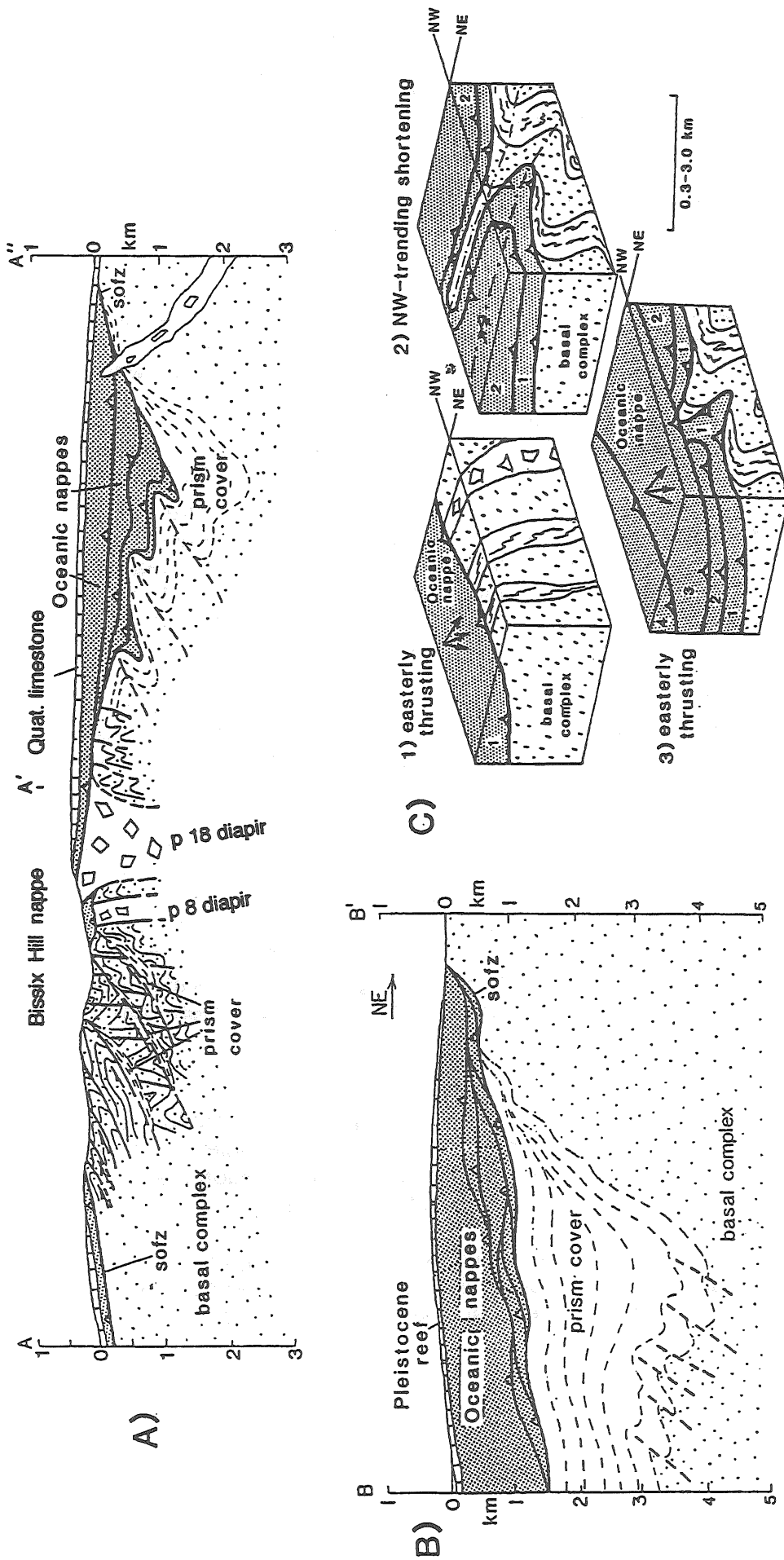


Figure 5: Section A (NW-SE along length of island) showing late imbrication of basal complex and prism cover, folding of SOFZ, and flap structures at top of central diapir (packet 18). Section B (SW-NE along axis of Woodbourne Trough) showing upper and lower divisions of Oceanic nappes unit. Block diagrams C showing sequence of emplacement and folding of Oceanic allochthon.

The youngest structures are normal faults with easterly throw. These are concentrated in the Oceanic allochthon and Quaternary limestone in eastern Barbados. They are apparently rare in the basal complex. Such normal faults are apparently a mechanism of denudation concurrent with uplift of eastern Barbados.

Structural History: Structures can be placed in a 3-phase history. The first phase is the development of fault-bound packets and first folds of the basal complex. This was probably late Eocene.

A number of different structures are included in the second phase, which was Miocene, perhaps extending to the present. The second phase is illustrated in Figure 6. It begins with the development of a major fold set with NW-SE axis over what is now Barbados island. Synclines developed in northern and southern Barbados, the latter being the Woodbourne Trough. Both synclines received deposits of prism cover (wedge cover of Fig. 6). Central Barbados was anticlinal. In mid-Miocene (15 my ago), the basal complex and prism cover of northern Barbados developed into an emergent thrust belt, the Woodbourne Trough continued subsidence as a foreland basin, and diapirism began and was concentrated in the central arch. The Oceanic allochthon was emplaced from the west, oblique to the line of section of Figure 6, just after the middle section. The allochthon covered the structures of the middle section but then underwent progressive deformation with them.

The third phase of structuring was the uplift of present-day Barbados, causing denudation of the northern two-thirds of the island. The mechanisms of denudation were both normal faulting and marine erosion. The possible scene at 1 my ago is illustrated by the third section of Figure 6.

Turbidite Lithofacies of the Basal Complex: The terrigenous beds of the basal complex are interpreted to be entirely submarine fan deposits (Speed, 1979; Larue and Speed, 1983; Larue, 1985). Evidence is the existence of classic turbidite beds, intraclasts of open marine aspect, ichnofossils of deep water aspect, and certain microfossil types within mudstone intervals. The microfossils are agglutinated benthic forams which suggest deeper water, and radiolarians and rare calcareous nannofossils, which indicate an open marine environment.

The basal complex includes a broad array of fan layer types (Fig. 7), including single (nonamalgamated) sandstones, amalgamated sandstones, and multilayers of mudstone and sandstones. Among turbidite facies (Mutti and Ricci-Lucchi, 1972), reviewed in Figure 8, facies D and C are predominant; facies B and E are less prevalent, and facies A and F are rare.

Analysis within fault packets of vertical changes of layer types and thicknesses and of fan facies indicates several different fan sequence types. These include progradation, abandonment, and retrogradation (Larue, 1985).

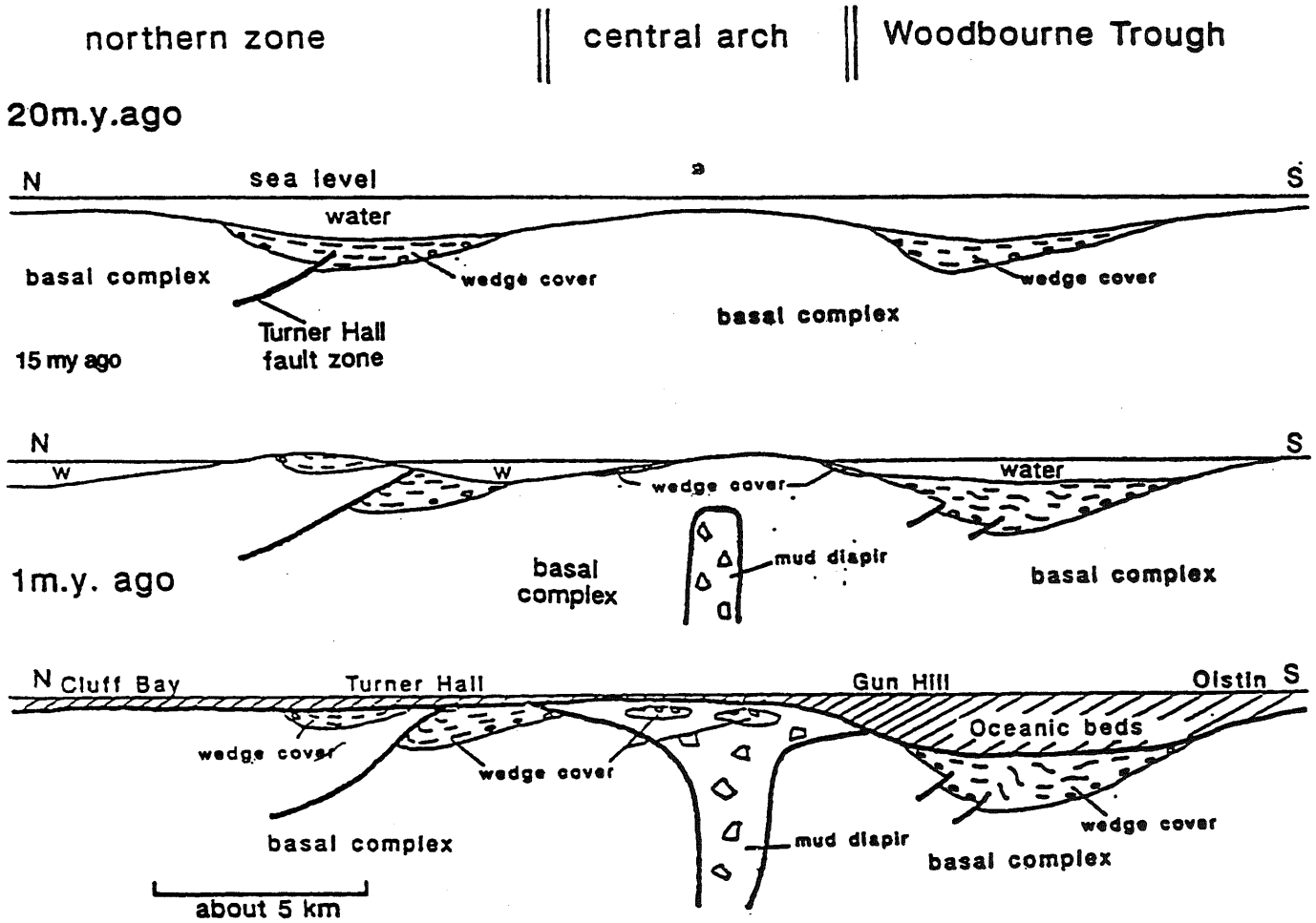
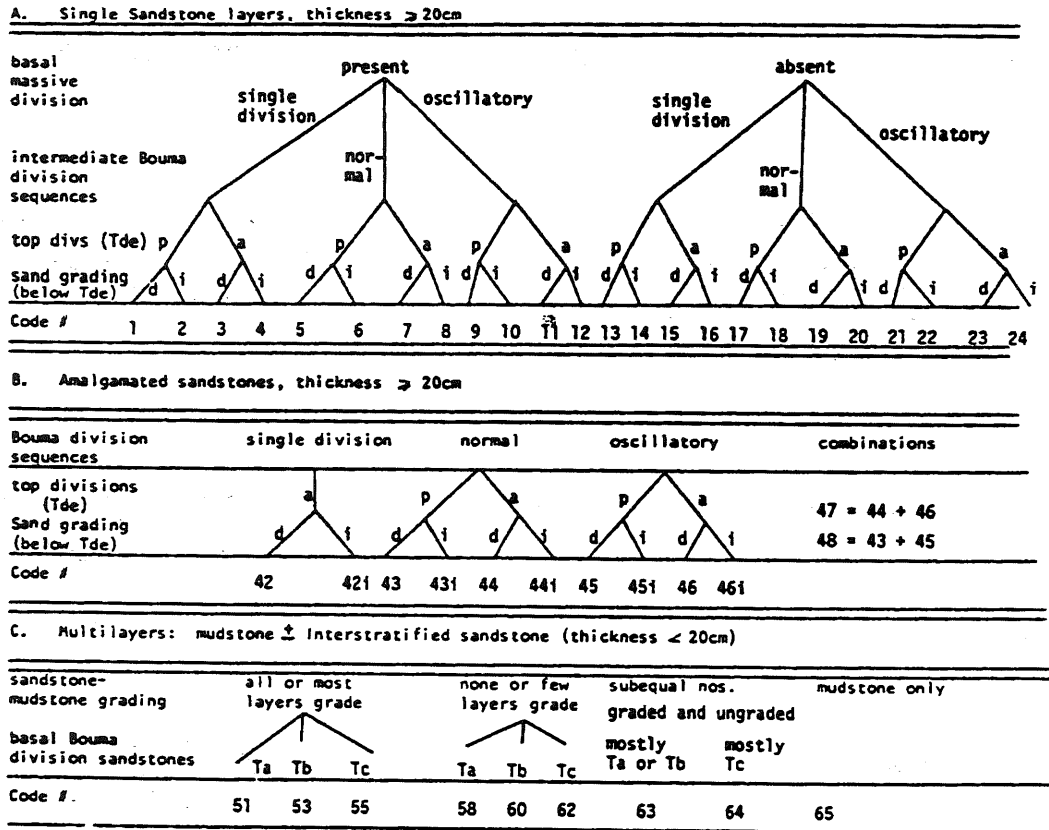


Figure 6: Time serial sections through Barbados Island, showing interpretive structural history at 20 ma, 15 ma, and 1 ma.



Bedding types. Abbreviations: p, present; a, absent; d, distinct; i, indistinct.

Major bedding types in different facies associations

Facies association	Location	Single	Amalgamated	Multilayered	Mudstone
Basin plain	The Choyce			62(30%)	65(51%)
	Packet 5A			62(45%)	65(50%)
Distal outer fan	Green Hill	24(28%)			65(42%)
	Green Hill (R)*	24(29%)		62(23%)	
	Packet 12	16(44%)		62(17%)	
	The Choyce	16(21%)		62(37%)	65(16%)
		20(21%)			
	Packet 5A	16(30%)		62(27%)	65(23%)
Proximal outer fan	Green Hill	24(35%)			65(17%)
	Green Hill (R)*	24(27%)		62(16%)	
				64(16%)	
	Packet 12	16(42%)		62(17%)	
	Packet 6	24(55%)			
	Monkey Hill	16(17%)		62(15%)	
		24(24%)		63(15%)	
	Packet 5A		42(22%)	58(22%)	
		44(22%)			
Midfan	Packet 5B	20(14%)		62(24%)	65(12%)
	Packet 12	7(33%)			
	Breedy's	7(21%)	42(23%)		
Inner fan(?)	Packet 6	7(14%)		58(21%)	
	Monkey Hill	4(15%)		58(30%)	65(15%)
	Ragged Point	3(6%)	48(18%)	62(7%)	65(35%)
		7(6%)			

* (R) = revisited, second occurrence in section.

Figure 7: Classification of turbidite layer types in terrigenous beds of basal complex.

Sequences of contiguous facies within some better exposed fault packets have been interpreted as to position in a submarine fan using the radial fan model. The five standard radial fan divisions: basin plain, distal outer fan, proximal outer fan, midfan, and innerfan, are illustrated in Figure 8, with example sites and proportions of principal layer types in Figure 7.

The distal outer fan associations are thicker bedded and sandier than the basin plain associations. Both are flat-bottomed and base-absent. Outer fan sandstones are noteworthy for oscillations of Tb and Tc Bouma zones within single graded beds. Proximal outer fan associations have thicker, sandier beds than distal, are commonly base-present, and have scoured bases. Midfan association has generally single layer sandstones whereas inner fan sandstones are mostly amalgamated. Midfan sandstones include coarse grained sand whereas those of the proximal outer fan are medium grained or finer. This difference may mark the transition from channelized to sheet sandstones.

The radial fan model provides a useful and applicable context for turbidites of the basal complex. There is, however, no strong support that such geometry existed. Other models such as a long channel-levee type may also be applicable.

Fault Packets of the Basal Complex: The deepest denudation of Barbados has occurred in the northeast, in what is called the Scotland District. There, the surface has moved down into the basal complex, probably by sliding, faulting, and surface water erosion. Exposures are best along the coastal strip, and it is there the structure of the basal complex has been most thoroughly studied. The fault packets and their internal structures strike at high angles to the shoreline.

Some 43 fault-bound packets have been identified and numbered along the coastal strip (Fig.9). These include two packets of diapir (8 and 18). Owing to poor exposure inland, the packets cannot be traced west with confidence. The inland region of the basal complex is simply divided between terrigenous (t) and radiolarian/hemipelagic (r) rock.

Generalized facies and facies associations¹

Facies A	Groups of conglomeratic or pebbly to coarse sandy layers, high sandstone/mudstone.
Facies B	Groups of massive sandstone layers, may be weakly laminated.
Facies C	Groups of base-present turbidites, medium to thick-bedded.
Facies D	Groups of base-absent turbidites, medium to thin-bedded.
Facies E	Groups of thin-bedded, coarse-grained to fine-grained turbidites, lenticular beds.
Facies F	Groups of pebbly mudstone layers, slumped units.
Facies G	Groups of hemipelagic layers.
Facies H	High bioturbation of layer makes distinction of above facies difficult to impossible.
Inner Fan	Facies B, C (minor D, E). Total association thickness, 50-200 m. Sandstone/mudstone is greater than 10.
Middle Fan	Facies B, C, D, E, (minor A, F). Interlayered sand-rich and mud-rich units 2-20 m thick. Sand units have erosional bases and thin upward into mud-rich units.
Outer Fan	Facies C, D (minor B, E). Interlayered sand-rich and mud-rich units 2-20 m thick. Mud units typically coarsen and thicken upward into sand units.
Basin Plain	Facies D. Mud-rich facies. Sand beds occur without evidence of upward thinning or thickening.

¹ Modified after Underwood (1984); Mutti and Ricci Lucchi (1972). Facies H from Larue (1985).

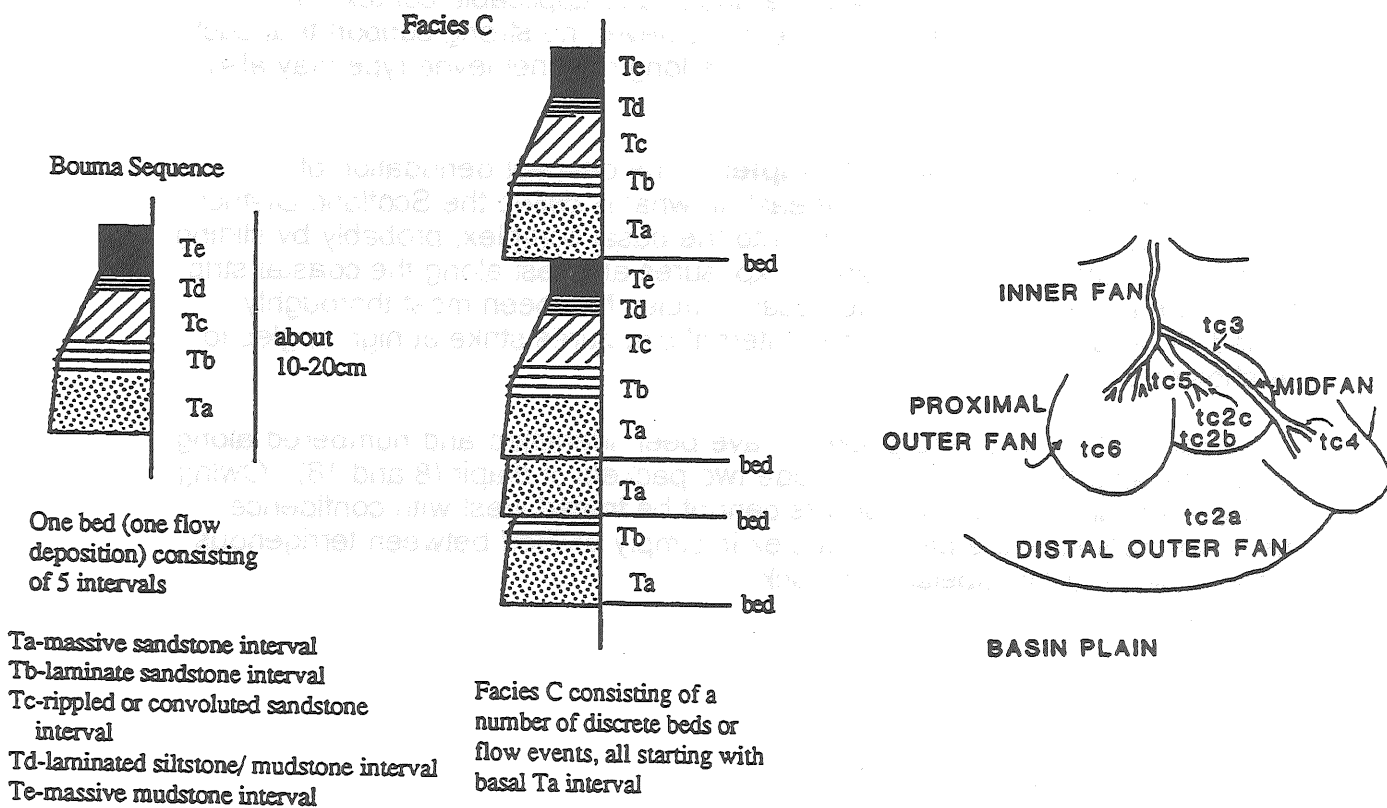


Figure 8: Review of characteristics of Ricci-Lucchi turbidite facies, facies associations, and of Bouma sequence.

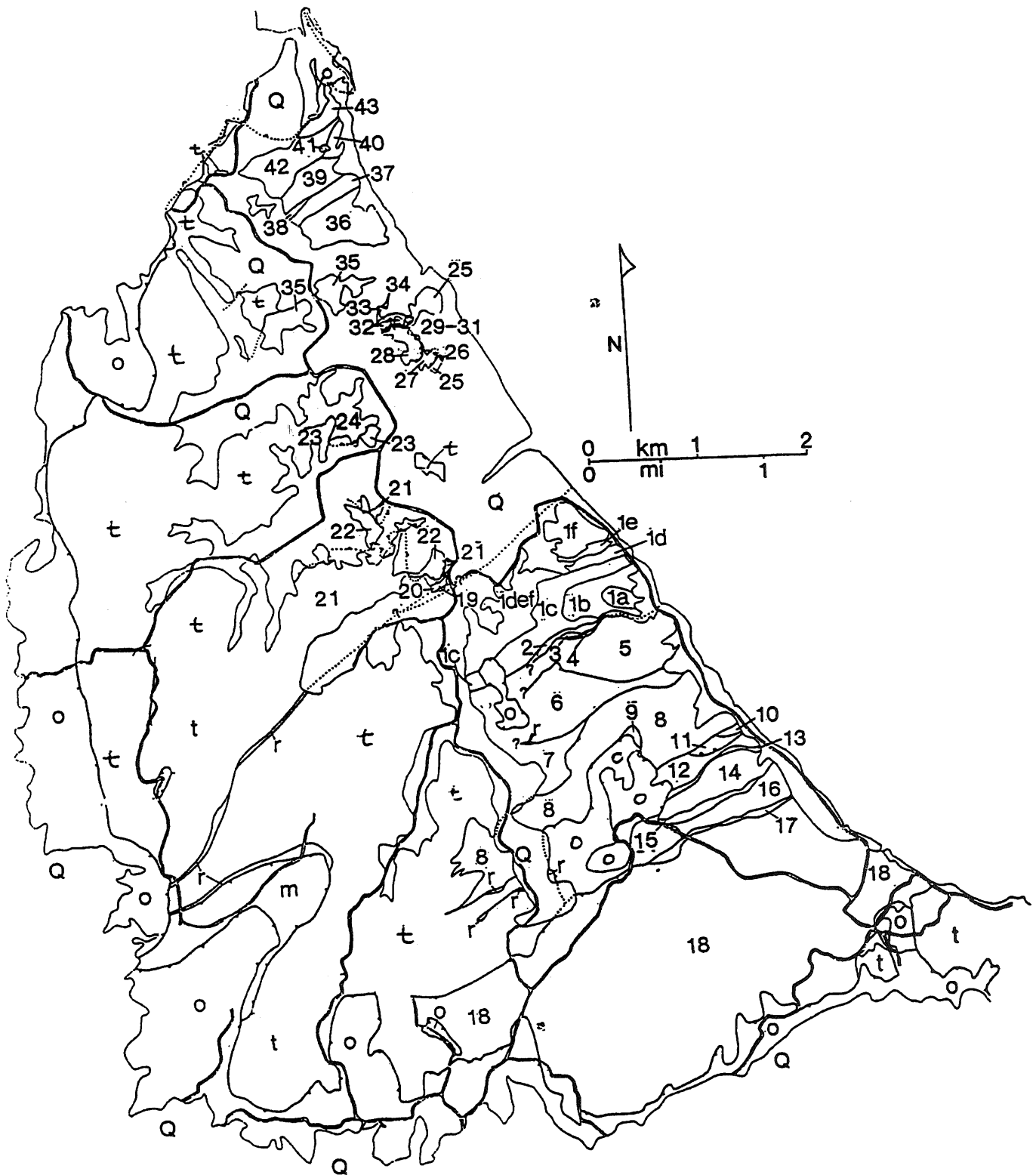


Figure 9: Map of Scotland district showing principal surface units and packets 1-43 within basal complex and diapirs in coastal strip. Inland units divided among Oceanic allochthon (O), terrigenous rocks of basal complex (t), and radstone of basal complex (r). Packet 1 (Chalky Mt.) subdivided by stratigraphic units (1a-1f = tc1-tc6). Q is Quaternary limestone and alluvium.

FIELD SITE INTRODUCTION

Sites are indicated on Figures 10 and 11. The sites are grouped as follows:

Sites 1-6: Scotland District

1. **Chalky Mt.:** structure, stratigraphy, and turbidite facies (progradational, channel-fill, and abandonment) of terrigenous rocks largest recognized fault packet.
2. **Bissex Hill:** Bissix Hill nappe of the Oceanic allochthon above basal complex and diapir; deformed Oceanic beds and prism cover (Bissex Hill Formation) within nappe.
3. **Breedy's-River Estate:** traverse through muddy basin-plain facies – sandy channel fill; thin, inclined melange diapir; and Walker's beds (many classic turbidites).
4. **Walker's Savannah:** complex of large and small fault packets with varied terrigenous lithofacies; duplex structure; progradational fan facies at Green Hill.
5. **Mt. Hillaby:** flap form of melange diapir above basal complex and below Oceanic allochthon.
6. **Coconut Grove:** deeply eroded valley in largest diapir (packet 18) of Barbados; this diapir is a 3km-wide vertical dike.

Sites 7-10: Below Cliffs

7. **Martin's Bay:** SE-dipping contact of Oceanic allochthon and basal complex, which may be the northwestern flank of the Woodbourne Trough at its up-plunge end.
8. **Bath:** excellent exposure of Oceanic allochthon and sub-Oceanic fault zone above basal complex; major late folds of SOFZ; site is possibly on axis of Woodbourne Trough at up-plunge end.
9. **Codrington College:** thin, inclined melange diapir cutting Oligocene beds of Oceanic allochthon.
10. **St. Mark's Church:** prism cover (Conset Marl) which apparently covers contact of Oceanic allochthon and basal complex.

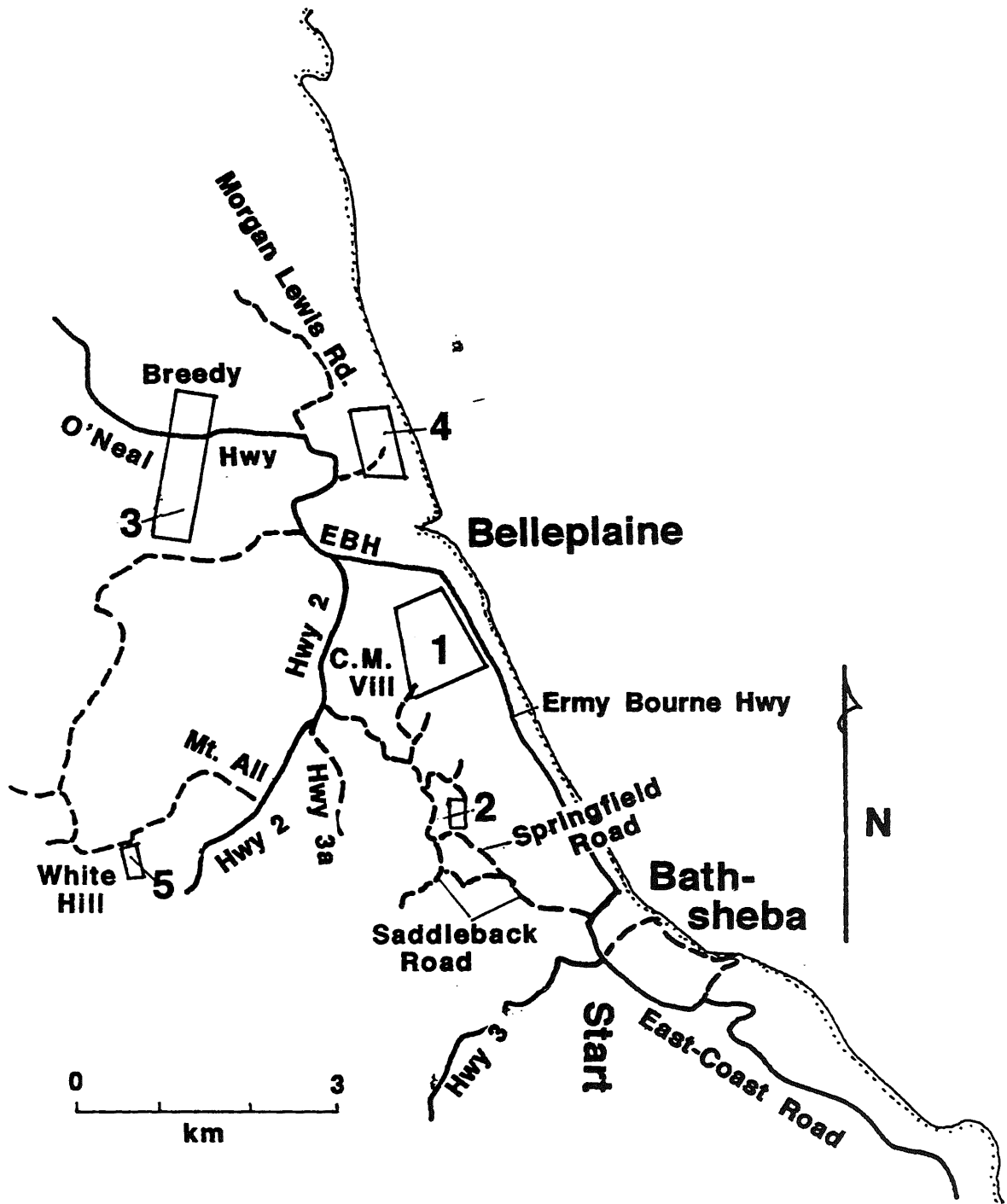


Figure 10: Roads and sites 1-5

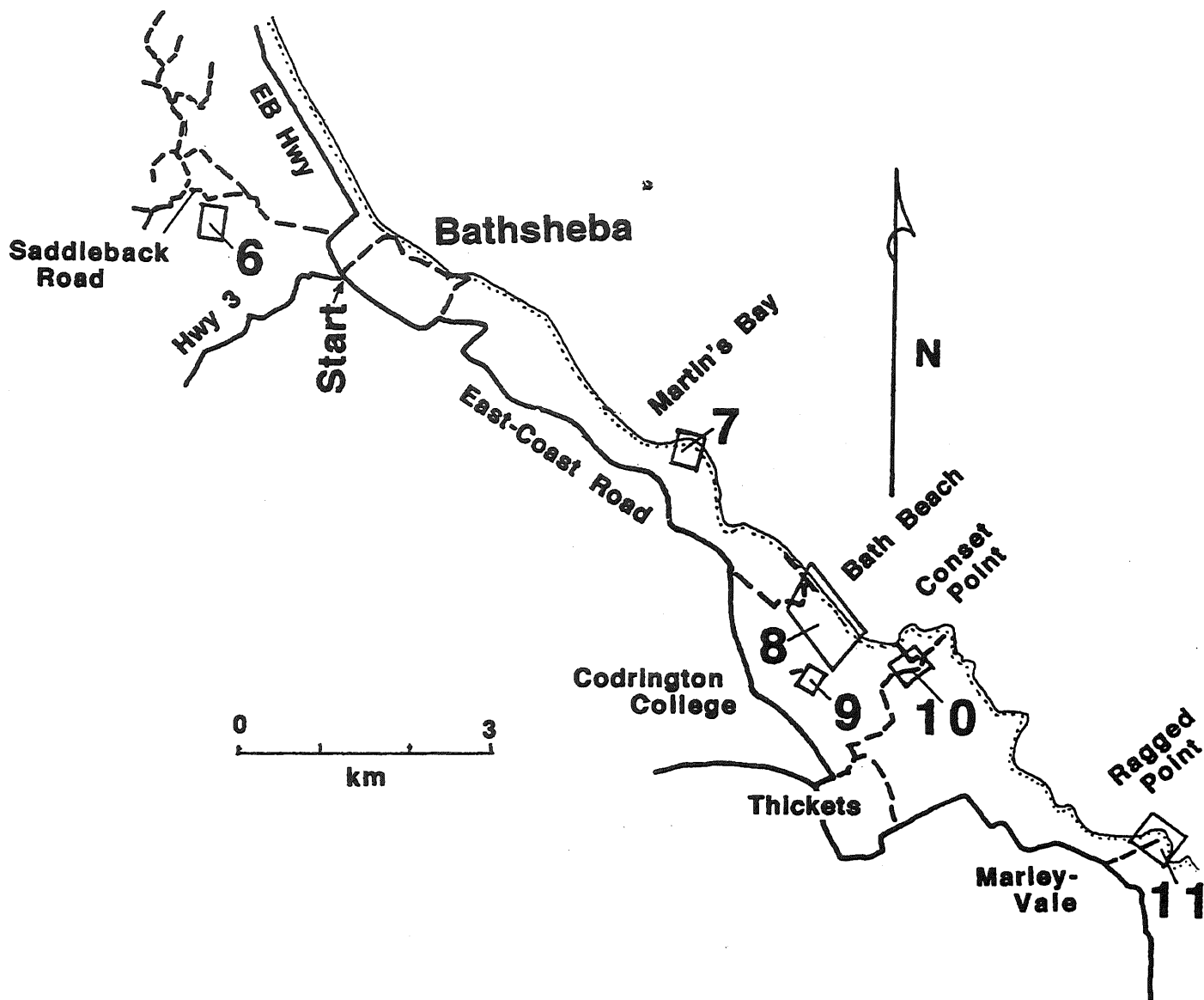


Figure 11: Roads and sites 6-11

Site 11: Southeastern Coast

- 11. Ragged Point:** southernmost exposure of basal complex in perpetually uplifting ridge that may represent deformation within the Woodbourne Trough; basal complex includes inner fan and facies.

Routes to sites begin in Bathsheba, at the 4-way intersection (Start Figs. 10, 11) of Highway 3, the Ermy Bourne Highway, and a road heading east (down) to the Edgewater Hotel. A landmark near the intersection is Martin's Bar.

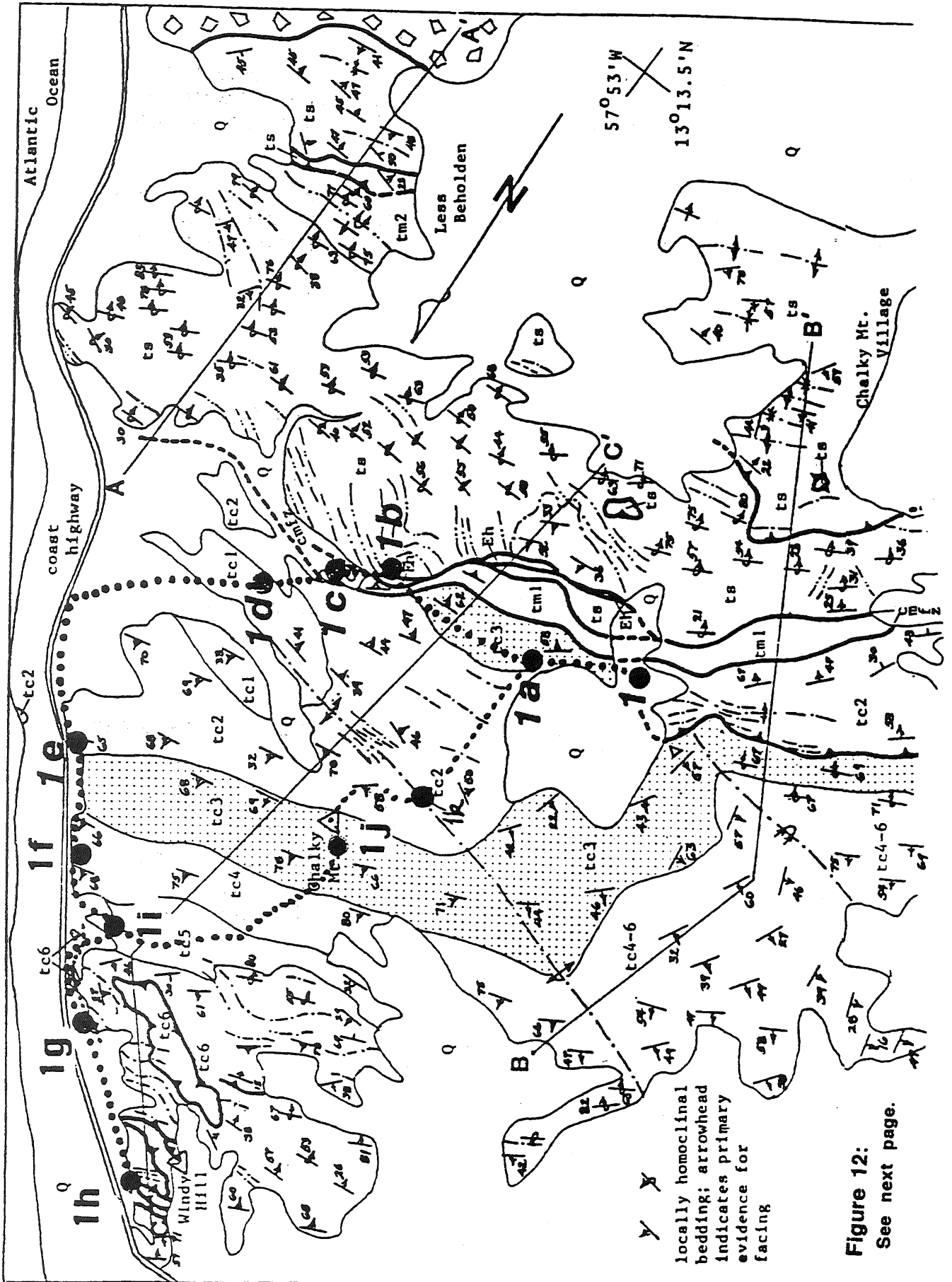
Site 1 Chalky MountRoute (Fig. 10)

0. km: Start; drive north from Bathsheba on Ermy Bourne Hwy
- 3.5 km: Pass Barclay's Park.
- 6.4 km: Intersection; turn left on Hwy 2.
- 8.4 km: Intersection; turn left on Chalky Mount road.
- 9.8 km: Intersection; turn left on Chalky Mount Village road; school on left, Chalky Mt. Bar on right.
- 11.0 km: Road ends; park.

This trip is a circuit, requiring about three hours and a gain and loss of 175m elevation.







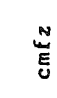










General: Chalky Mount and its northern arm, Windy Hill, provide the best exposures of terrigenous rocks of the basal complex on Barbados (Fig. 12). Chalky Mount is underlain chiefly by fault packet 1 (Figs. 9, 13). This packet contains the thickest stratal section (600m) identified so far on Barbados (Fig. 14). The section is divided among 6 lithostratigraphic units, named tc1 – tc6 (Figs. 12, 14). The layer characteristics and facies associations (Figs. 15,16) of the six units are interpreted as follows:

tc1	basin plain
tc2a, tc2b	progradational distal outerfan
tc 2c	progradational midfan
tc3, tc4	midfan, or/and innerfan channel
tc5	fan abandonment
tc6	outer fan rejuvenation



y x locally homoclinal bedding; arrowhead indicates primary evidence facing

Figure 12:
See next page.

-  cleavage
-  thrust fault
-  high angle fault
-  axial trace, first phase
-  axial trace, second phase
-  A-A' cross section trace
-  cmfz Chalky Mount fault zone
-  melange
-  Q Quaternary sediment
-  Eh Eocene hemipelagic rocks
-  t: terrigenous rocks
-  tc1,2,3,4,5,6 stratigraphic units of packet 1
-  tc4-6 units 4,5, and 6 undivided
-  tm1 mudstone of packet 2
-  tm2 mudstone unit of packet 5
-  ts undivided sandstone
-  tu undifferentiated

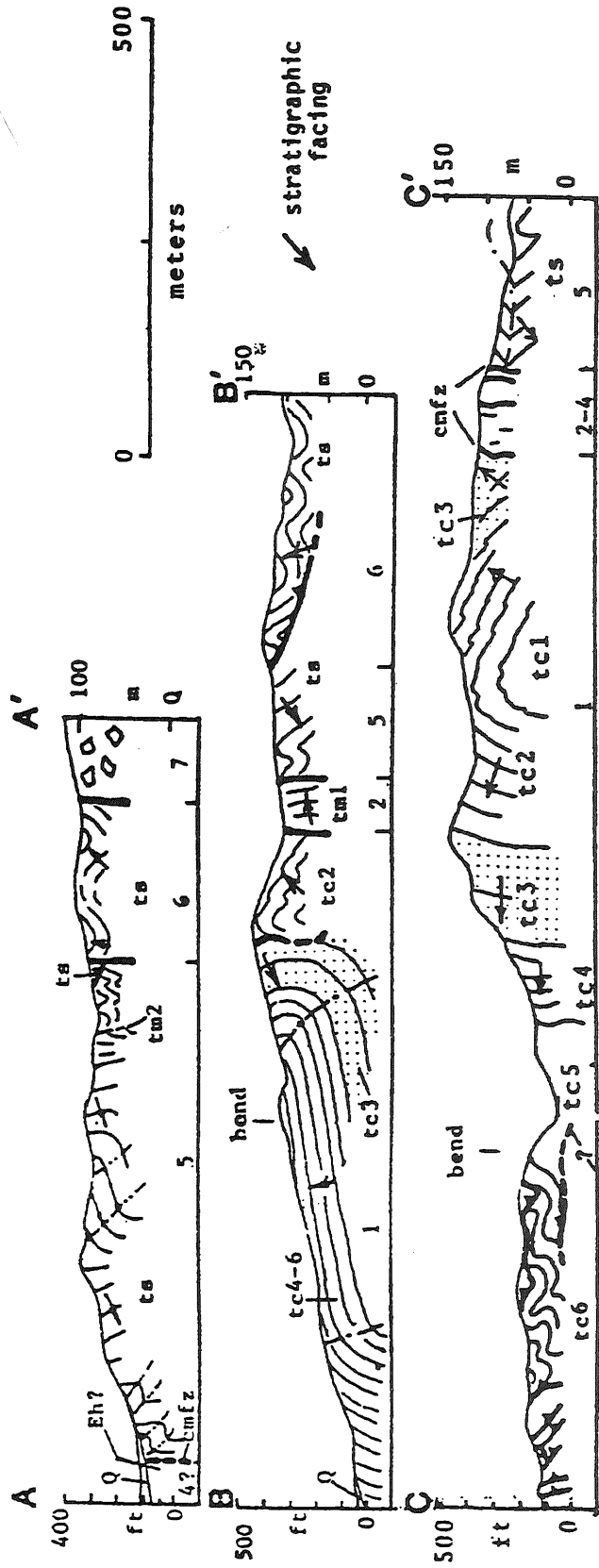


Figure 12: Geologic map and sections of Chalky Mount area. Walking tour follows dots; start at stop 1 at road's end in Chalky Mt. Village.

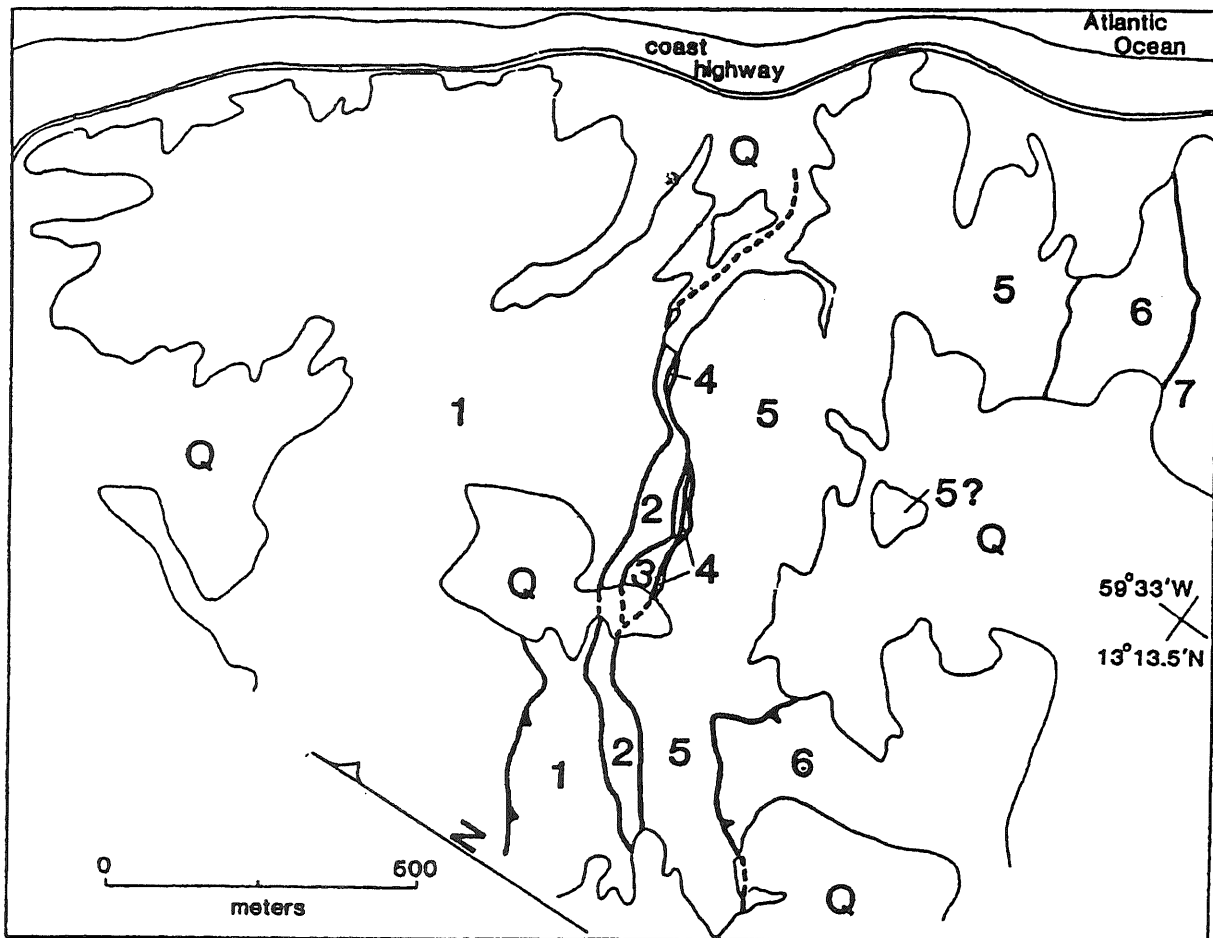


Figure 13: Map of same area of Chalky Mount as Figure 12, showing packet structure.

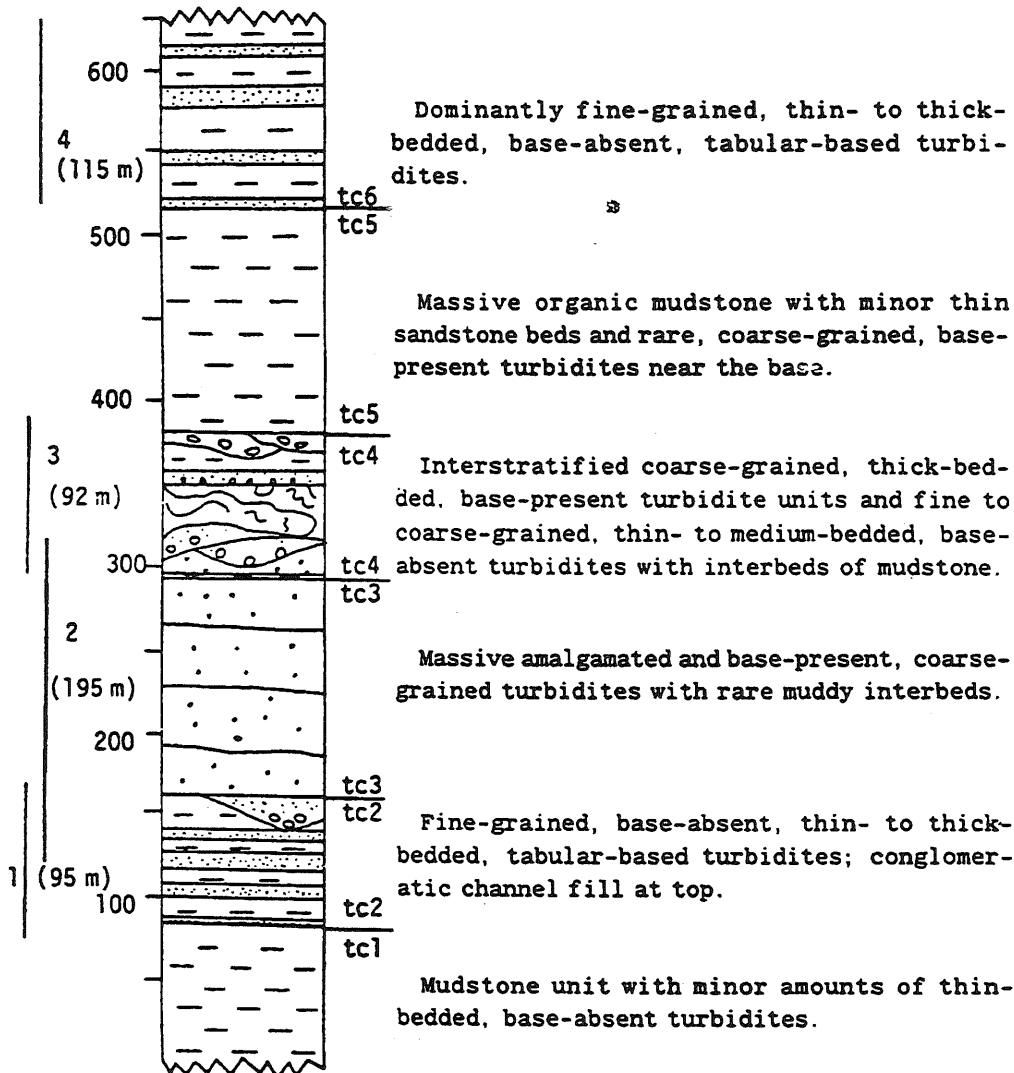


Figure 14: Stratigraphic column for packet 1; intervals on left are continuously measured sections; units are tc1-6; unit thicknesses in parentheses.

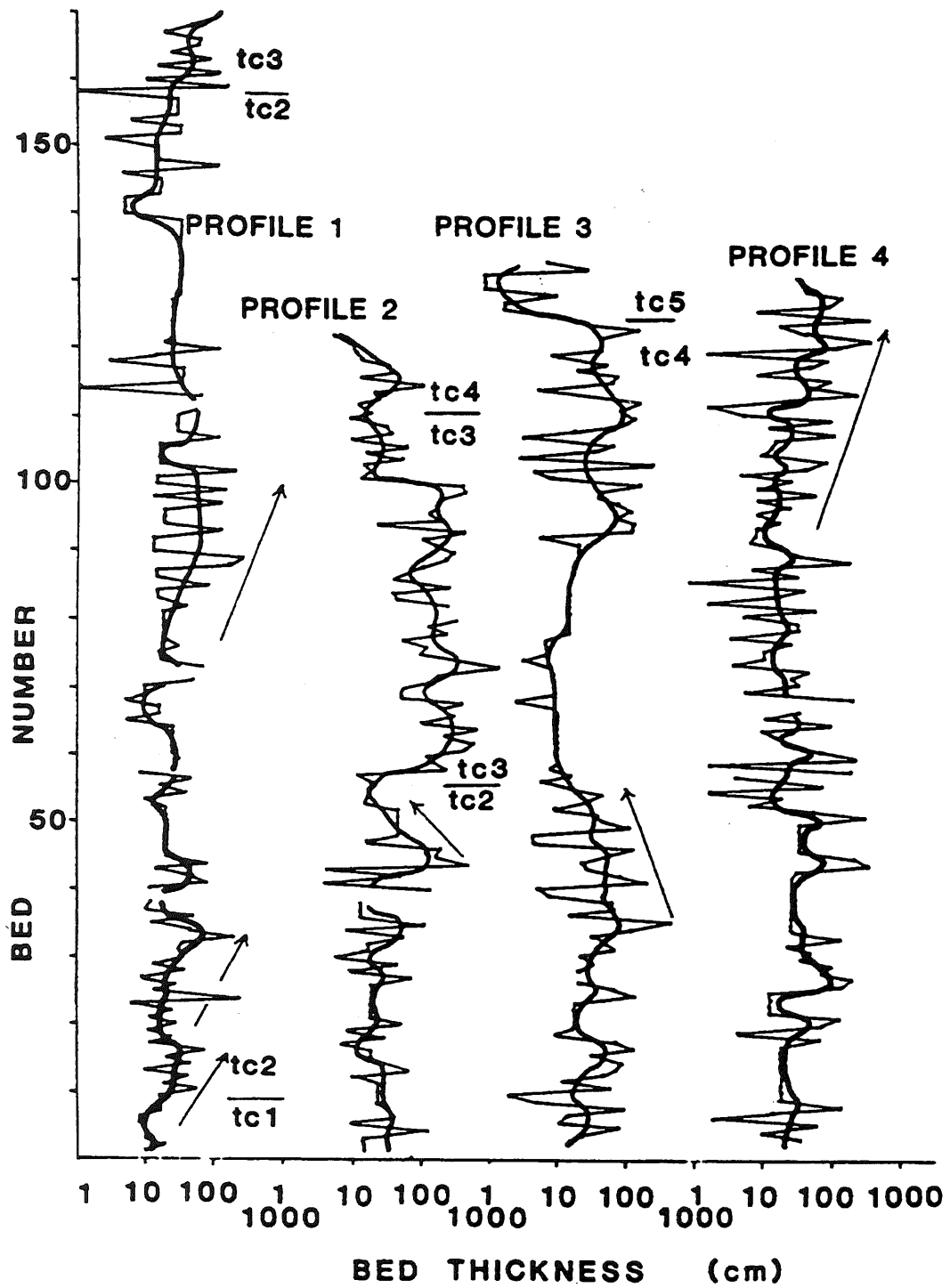


Figure 15: Layer thickness vs. height in packet 1; arrows indicate upward thinning or - thickening sequences.

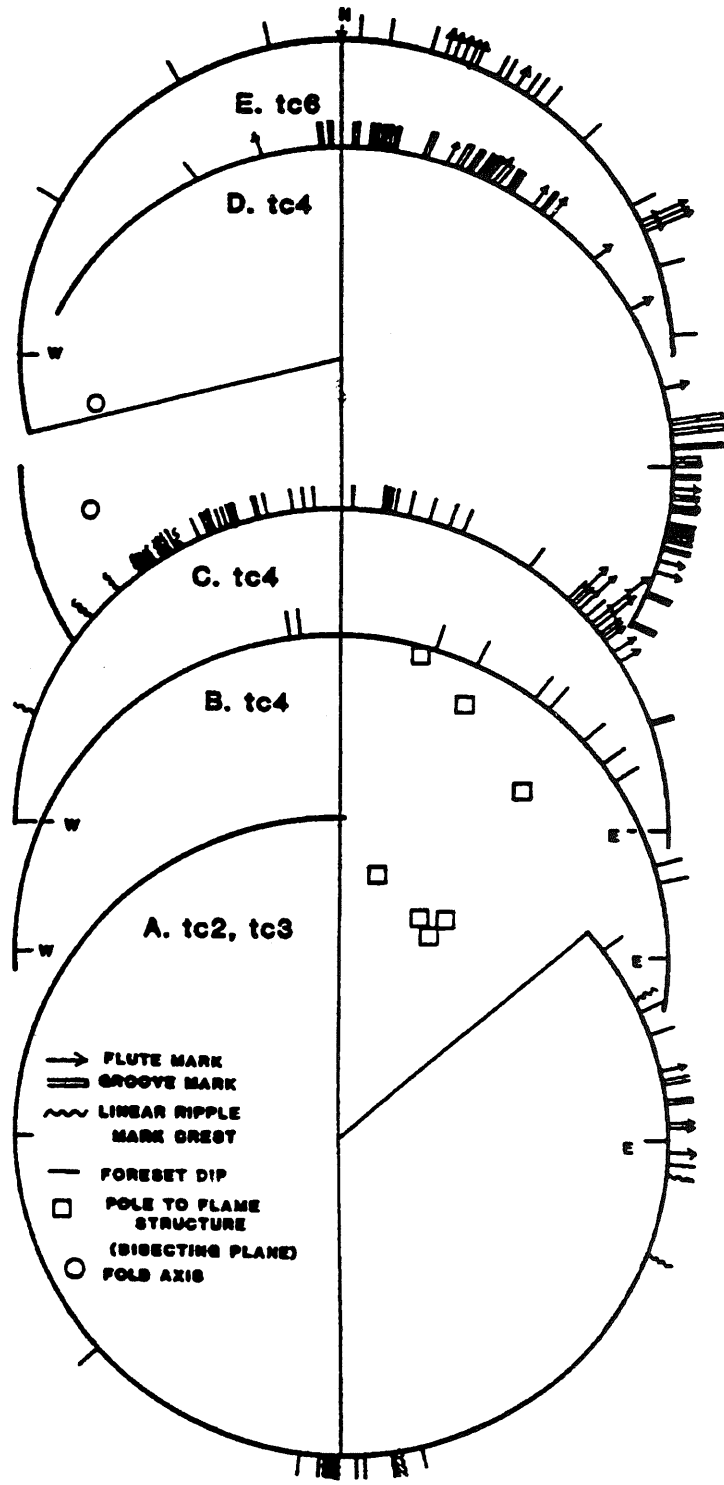


Figure 16: Paleocurrent data for packet 1; corrected only for layer dip.

Packet 1 is important in understanding the structure of the basal complex, because its internal structure is remarkably coherent.

Structural Highlights

- 1) The subvertical Chalky Mt. Fault Zone at its southern boundary (Fig. 17);
- 2) Major upright early phase anticline and syncline with northerly overturning (Fig. 12, sections BB', CC');
- 3) Transition northward from a coherent fold train to broken formation with refolded folds and reactivated thrusts (Fig. 25).

<u>Stops</u>		(Fig. 13, on foot, distance cumulative)
0	m. 1	Road end Chalky Mt. Village; head N 70°E on trail through massive sandstone.
200	m. 1a	Unit tc3 of packet 1. Mainly amalgamated layers of quartz sandstone up to 13m thick; facies B, probably inner fan channel. This stop is in the intermediate limb of the major fold pair (Fig. 12).
500	m. 1b	Chalky Mt. Fault Zone. This 20-50m wide zone truncates large packet 1 on its north wall and large packet 5 on its south wall (Figs 13, 17). The zone interior contains disrupted lenses of small packets 2,3,4. Here, packet 4 is seen; a middle Eocene radstone. Beds of packet 5 in south wall of CMFZ are closely folded. Such folds are second phase and due to reactivation of CMFZ with left-oblique slip.
650	m. 1c	Chalky Mt. Fault Zone. Outcrops show broken formation (Fig. 18) comprising conjugate extensional faults and brittle boudinage in sandstone and spaced cleavage in mudstone.
850	m. 1d	Unit tc1 of packet 1. Thin bedded, mudrich basin plain turbidites (Fig. 19) in lowest unit of packet 1 section (Figs. 12-14). Stop is in axial region of major anticline (Fig 12) whose profile is seen in a westerly view. Head north from stop 1d toward 1e, proceeding upsection through lower two-thirds of unit tc2. Upward-thickening and coarsening sequences (Fig. 20) of facies D are traversed. These represent outer fan progradation.



Figure 18: Chalky Mt. fault zone at stop 1b. Sandstone phacoids in foliated mudstone. Foliation, a spaced scaly cleavage, dips steeply to the right (south).

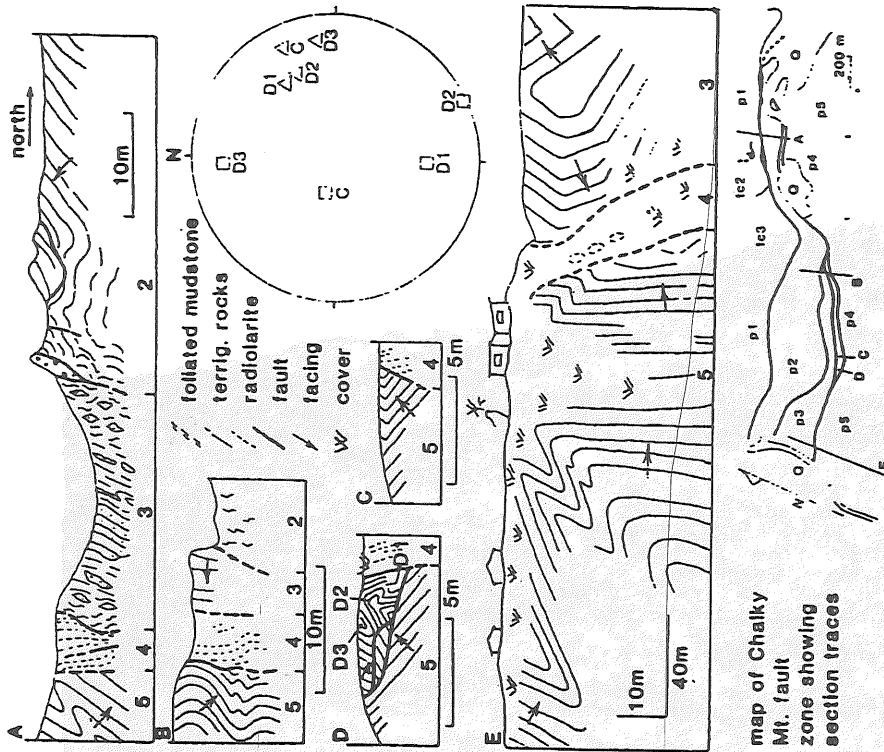


Figure 17: Cross sections through Chalky Mt. fault zone; packet 1 on right (north).



Figure 19: Unit tc1 in packet 1. Thin bedded muddy graded sets, a few underlain by graded or nongraded fine grained sandstone (white).

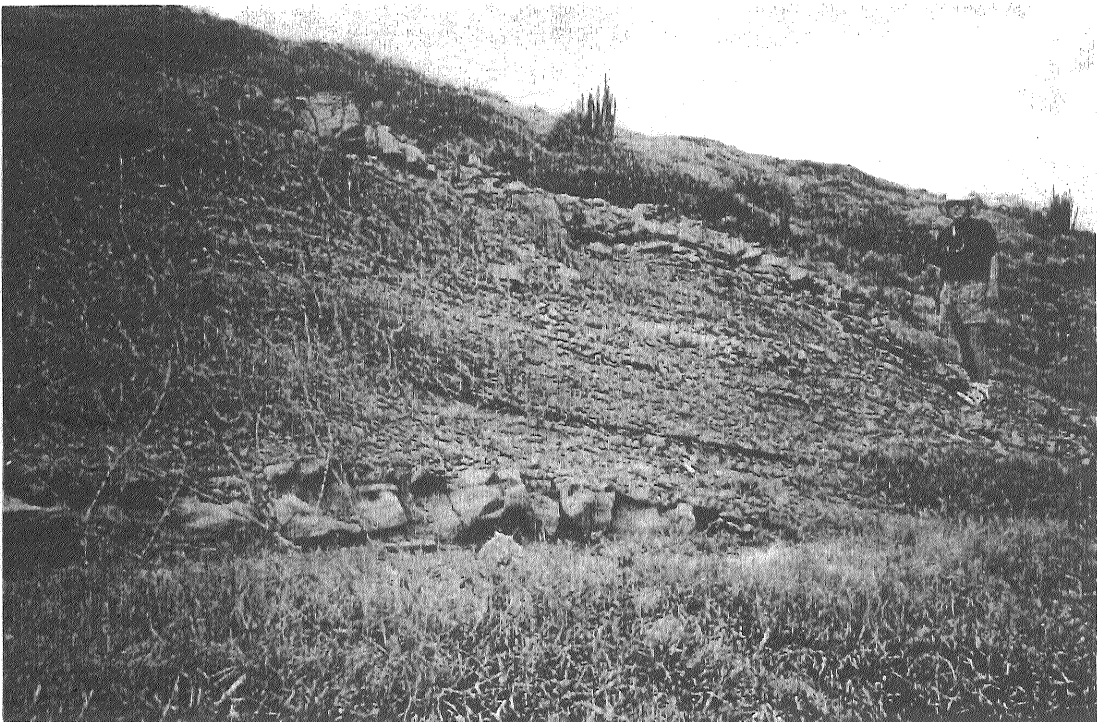


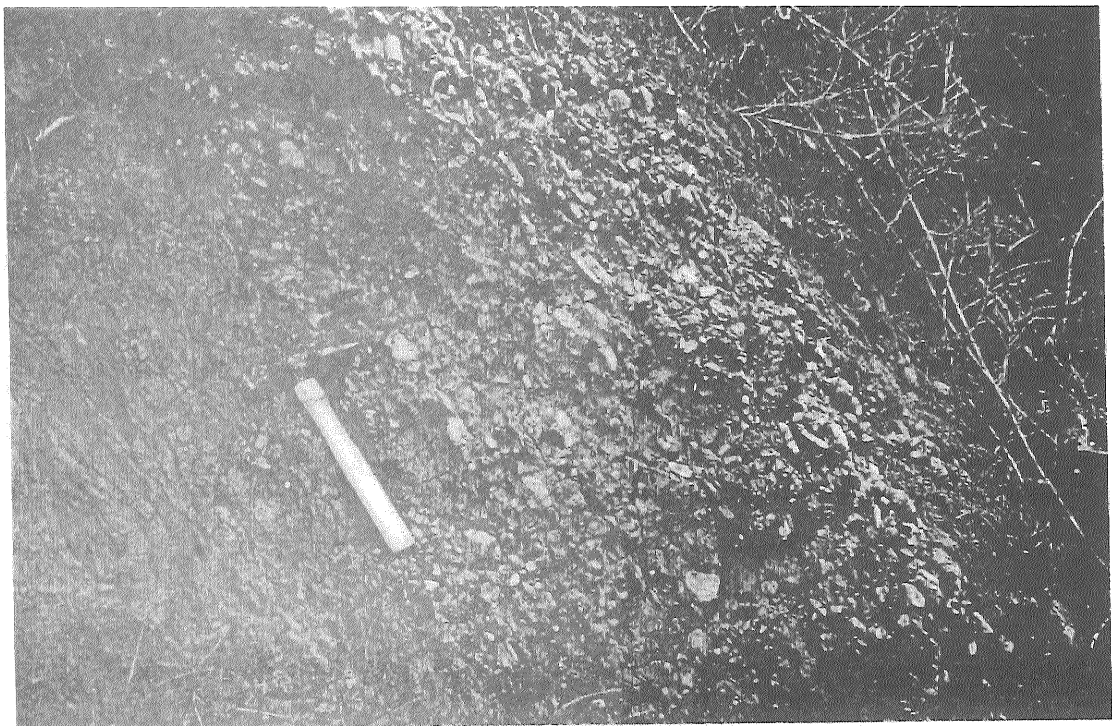
Figure 20: Unit tc2 (lower half) of packet 1. Upward-thickening sequence of fine grained sandstone beds beginning below feet of figure.

- 1150 m. 1e Unit tc2, top quarter, of packet 1. Roadcut on Ermy Bourne Highway. Thick and thin bedded turbidites of proximal outer fan overlain by channel-filling conglomerate (Figs. 21, 22) and associated thin and thick bedded turbidites of levee and thalweg deposition. Proceed NW on highway below Chalky Mt. and unit tc3, which is 130m of very thick bedded, mainly amalgamated coarse sandstone of midfan or inner fan channel deposition. These steeply NW-dipping beds are in the northern limb of the major anticline (Fig 12, section CC'). Unit tc3 will be examined at a later stop.
- 1350 m. 1f Unit tc4, packet 1. Highway cut through steeply NW-dipping beds (Fig. 23). Unit tc4 contains intercalated bed sets of two types: channelized amalgamated and single layer thick sandstones and pebbly sandstones of facies B and thin to medium bedded sandy and muddy turbidites of facies D and C. (Fig. 24). There are few evident vertical sequence trends. The unit includes a slump and many coarse sandstone dikes. Unit tc4 may represent thalweg and overbank deposits in a major inner fan channel relict from tc3 during retrogradation or waning input (Fig. 15). Proceed NW on highway past covered area above unit tc5, an abandonment facies, to unit tc6.
- 1600 m. 1g Unit tc6 of packet 1 at south end of Windy Hill (Fig. 25): Unit 6 contains thin and thick bedded turbidites of facies D and C and proximal outer fan association. It is abruptly gradational with tc5 and is thought to represent rejuvenation of fan deposition after a duration of bypassed sand inflow during tc5 deposition. Note wavetrain of north-vergent folds defined by sandstones in lower 3/4 of hill. A nappe of inverted disrupted terrigenous rock (broken formation) lies above the coherent sandstones and is folded with them (Fig. 25). Proceed NW on roadside; note northward shallowing of fold attitudes.
- 1850 m. 1h Unit tc6 of packet 1 at north end of Windy Hill (Fig. 25): Broken formation of unit tc6 with north-vergent late thrusts and refolded folds at reactivated northern tip of packet 1. Windy Hill as a whole overlies a probable S-dipping thrust which surfaces in the reactivated zone at stop 1h. (Fig.25). Retrace steps along highway past stop 1g and turn inland toward stop 1i at ruins.
- 2200 m. 1i Unit tc5 of packet 1: Unit tc5 consists of organic mudstone with occasional ungraded laminae and starved ripples of very fine sand. This is the fan abandonment facies. Folds are high harmonics to major fold pair of Chalky Mount.



Figure 21: Unit tc2 (near top) of packet 1. Channelized hard-pebble conglomerate; top to right. Stop 1e.

Figure 22: Same as Figure 21, closeup.



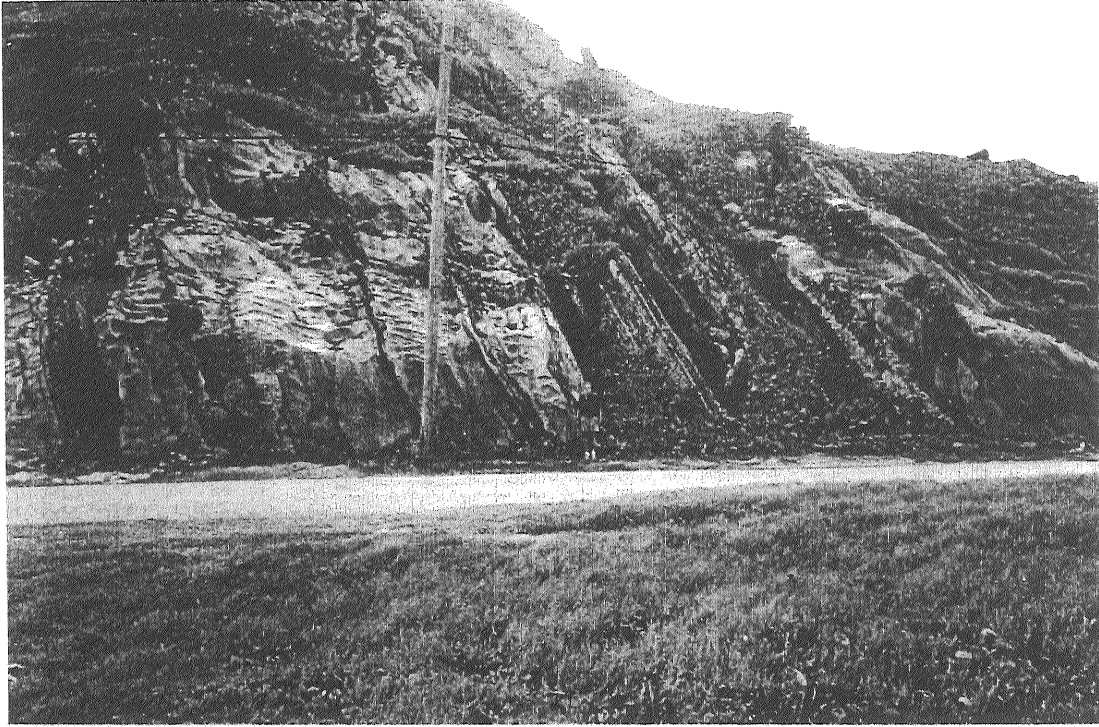


Figure 23: Unit tc4, packet 1, at roadcut on Ermy Bourne Highway at eastern base of Chalky Mt.; top to right. Stop 1f.

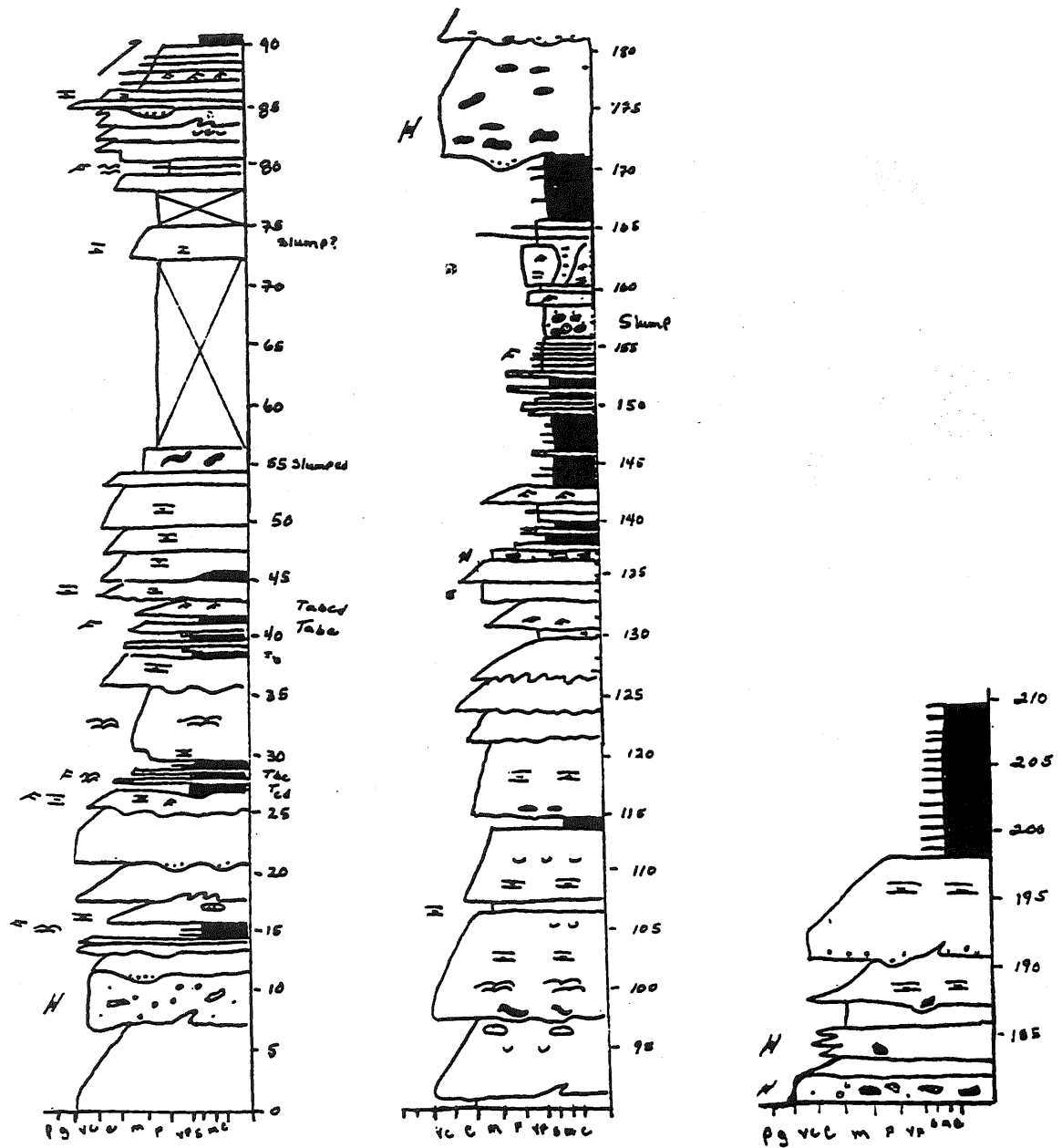


Figure 24: Unit tc4 packet 1. Columnar section showing maximum grain size. Courtesy of D.K. Larue.

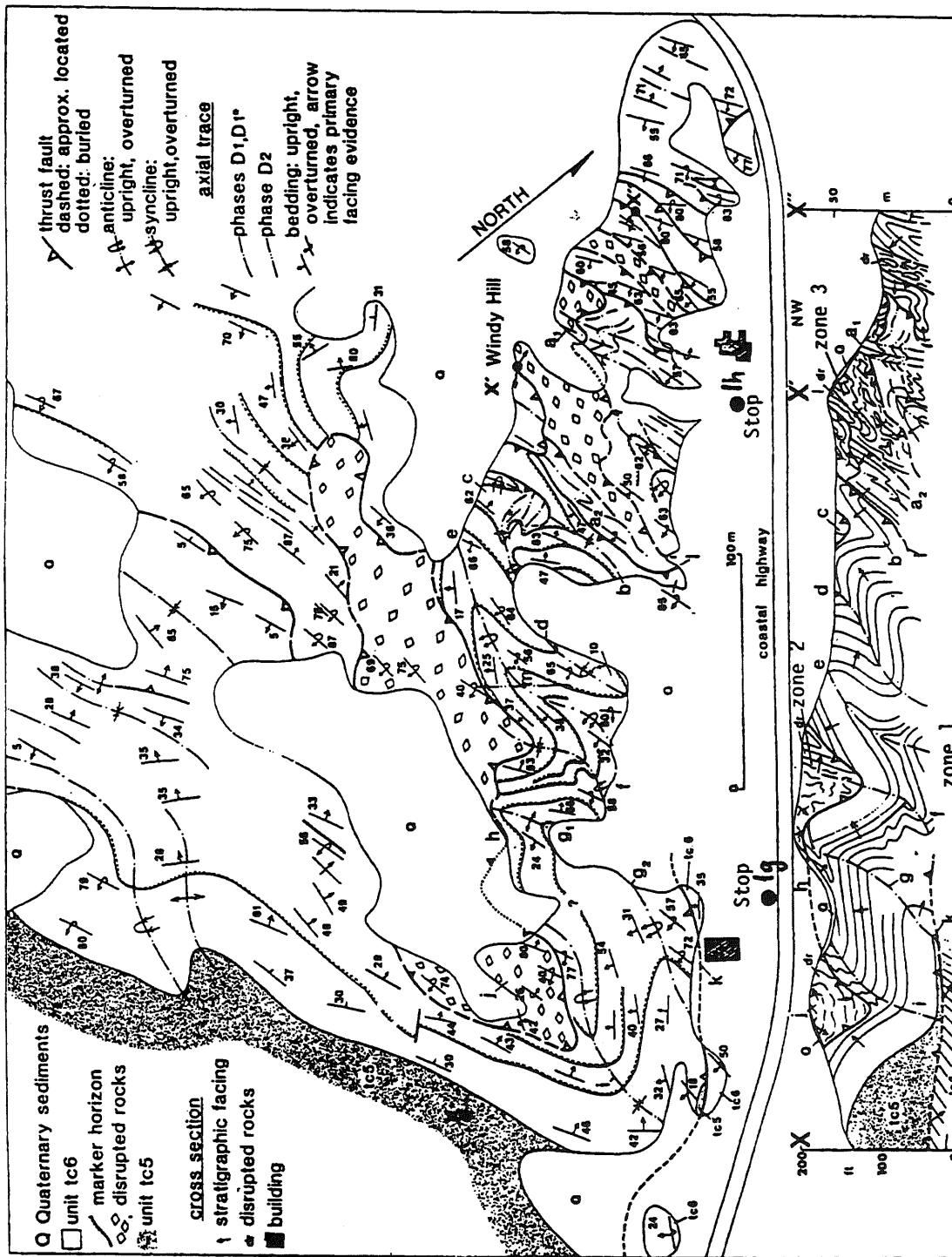


Figure 25: Geologic map and section of Windy Hill, at northern margin of Chalky Mt. area; stops 1g and 1h.

Ascend path heading S70W to a pass at 2400m. Turn left, ascend north slope of Chalky Mount to summit. Pass down-section from tc5 through tc4 to tc3.

- 2400 m. 1j Unit tc3 of packet 1 at summit of Chalky Mount: A complete traverse is made through the thickest (130m), purest sandstone at the surface of Barbados. The layers are facies B and possibly deposits in a wide inner fan channel. Note amalgamation, pebbly bottoms, occasional mudrapes, and concentrations of intraclasts (originally soft mud-and marlstone) above the Ta zones. The top of unit tc2 is 75m south of the summit on a path. The top is marked by lensy channelized conglomerate, as seen at stop 1e.
- 2600 m. 1k Unit tc2 of packet 1: View west to hinge region of major anticline defined by changing attitudes of unit tc3. Return on path to Chalky Mt. Village.

Site 2 Bissex Hill

Route (Fig. 10)

- 11.0 km Stop 1: return through Chalky Mount Village
- 12.2 km Intersection Chalky Mt. road; turn left.
- 12.5 km Intersection Cambridge—Less Beholden road; turn left
- 13.0 km T junction, turn right
- 13.2 km Cambridge estate house; park.

General

Bissex Hill affords a glimpse of tectonostratigraphy and two lithotypes of prism cover.

The tectonostratigraphy is illustrated in Figure 26. The lowest tier comprises vertical fault packets of basal complex (both terrigenous and radstone) and of diapir (packet 8). The second tier up is a thin sheet of prism cover, called Bissex Intermediate unit on Figure 26 and now called Cambridge beds (Fig.3). The Cambridge beds are Miocene and possibly, Oligocene.

The third tier up is the Bissex Hill nappe (Fig. 26), which includes deformed Oceanic beds of Eocene age overlain unconformably by the Bissex Hill Formation, a prism cover unit.

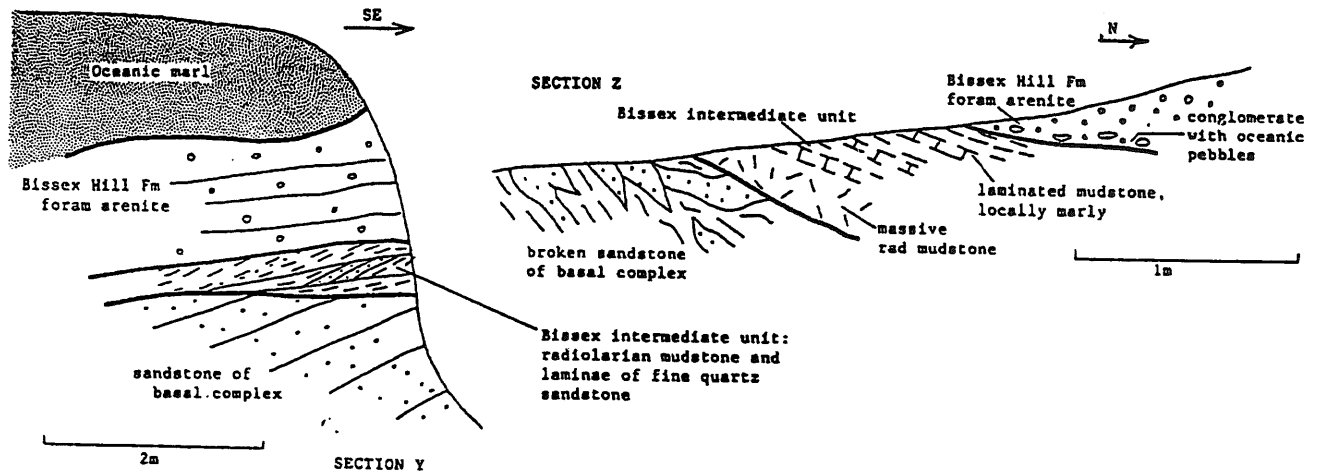
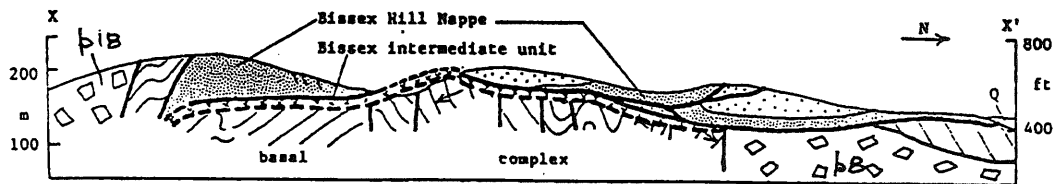
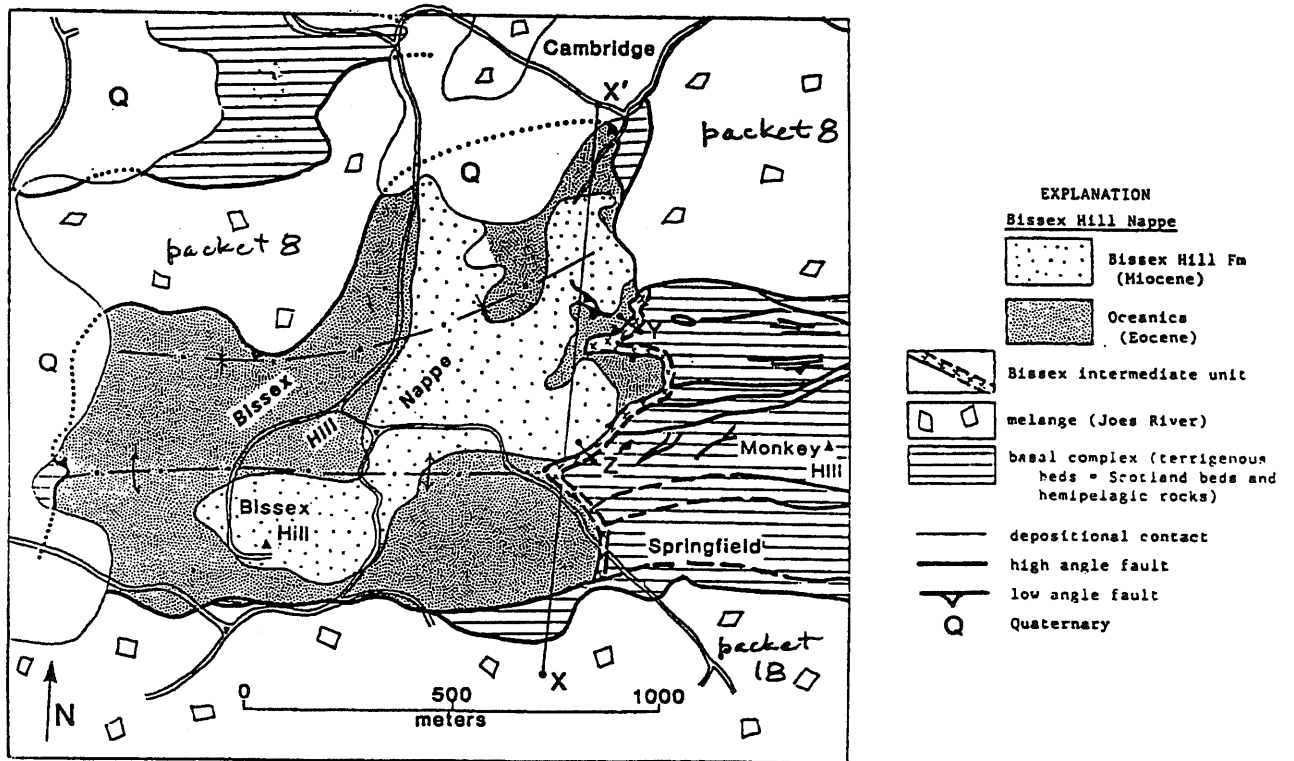


Figure 26: Bissex Hill area; Site 2 at Cambridge. Traces of sections XX: y, and z shown on map.

The base of the Bissex Hill nappe and the Cambridge beds are subhorizontal (although folded openly), as shown in sections X, Y, and Z (Fig 26). Diapiric packet 8 presumably was in place and cut by an unconformity before being overridden by the Bissex Hill nappe. This diapir is thus middle Miocene or older.

The highest tier is diapiric packet 18, which is interpreted to override the southern edge of the Bissex Hill nappe (Fig. 26).

The Bissex Hill Formation comprises two principal rock types: a lower crystalline micrite and an upper foram calcarenite (Fig. 27). Both can sometimes be seen in abandoned quarries A and B 200-300m south of the Cambridge estate house (Fig. 27). Crystalline micrite exists in discontinuous outcrop as thick as 10m. It is discontinuous and as thick as 10m. It is much brecciated and deformed. Thick-walled shells suggest shallow marine deposition. Sr isotopes indicate an early Miocene deposition or/and diagenesis. The foram arenite is massive and rarely, plane laminated. It contains compatible planktic forams of middle Miocene age but a wide range of incompatible nanno and radiolarian taxa. Benthic forams and ostracods are said to be shallow species.

I interpret the Bissex Hill Formation as a fully resedimented deposit. Its provenance was shoals at the crest of the moving Oceanic allochthon. Its site of deposition was probably a narrow basin on the east-facing slope of the allochthon. The micrite is probably olistostromal, and the arenite the product of grain flows.

Stops (Fig. 10)

From Cambridge estate house (Fig. 27), walk south on a track 300m to quarry B.

At quarry B, examine the basal micrite of the Bissex Hill Formation. The micrite, highly fractured, is in a tight synform overturned to the north (section, Fig. 27). The core of the synform is foram arenite. Oceanic beds are exposed (sometimes) below the micrite.

Return north 100m along the track. We shall attempt to access quarry A. There, a 12m section of foram arenite is exposed.

Upon return to the estate house, we shall inspect the highest levels of melange in the diapir of packet 8.

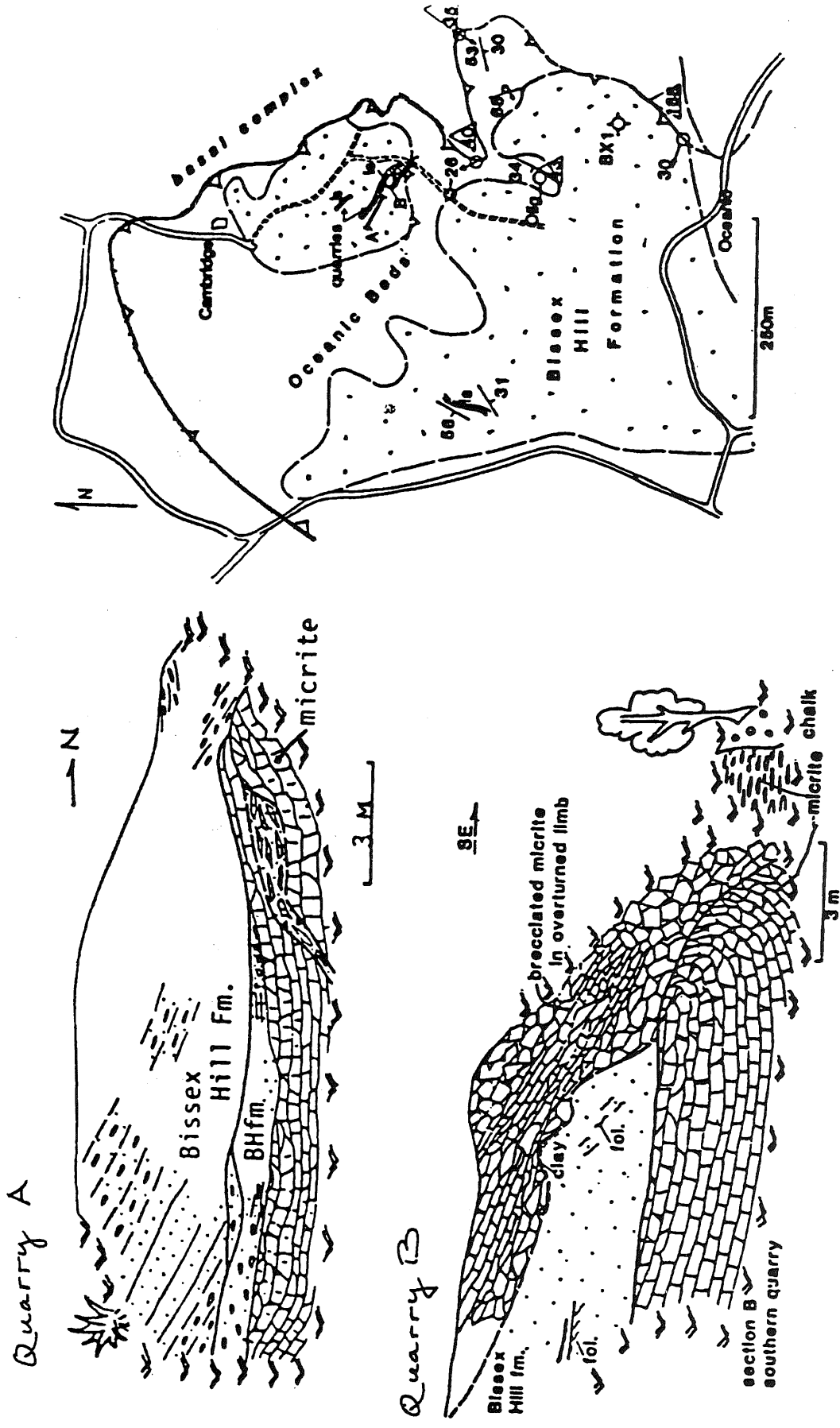


Figure 27: Map of northern Bissex Hill nappe showing Cambridge estate house (site 2) and locations of quarries A and B.

Site 3 Breedy's River Estate

Route (Fig. 10)

- 13.2 km: Site 2; Cambridge. Return to Chalky Mt. road.
- 13.9 km: Intersection Chalky Mt. road; turn right
- 15.6 km: Intersection Hwy2; turn right
- 17.6 km: Intersection Hwy 2 and Ermy Bourne Hwy in Belleplaine; go straight on Ermy Bourne Hwy.
- 19.9 km: 3-way intersection: Charles Duncan O'Neal Hwy, Ermy Bourne Hwy, and Morgan Lewis road; turn left on O'Neal Hwy.
- 21.1 km Breedy's brick factory, now Claytone Tiles; turn right into driveway.
- 21.3 km Continue NE around factory to claypit; park.

General

Site 3 is a NS traverse across four packets of terrigenous beds and a diapir (Figs. 28, 29, 33). The objectives are:

- 1) example of thick muddy turbidite section, the Claypit mudstone packet;
- 2) thick coarse sandstones of the Breedy sandstone packet, a probable inner fan facies association (Larue, 1985);
- 3) type area of Walker's beds of packet W, which include a spectrum of facies (B,C,D);
- 4) small, possibly plugform sand-rich diapir;
- 5) flat structures typical of the northern Scotland district. Flat structures include fault-bound homoclines of shallowly dipping beds, either upright or inverted; shallowly dipping faults; and subhorizontal axial planes of major folds. The fault-bound homoclines are almost certainly disconnected limbs of major isoclines.

The rocks and especially, the structures, of Site 3 contrast substantially with those of Site 1 (packet 1).

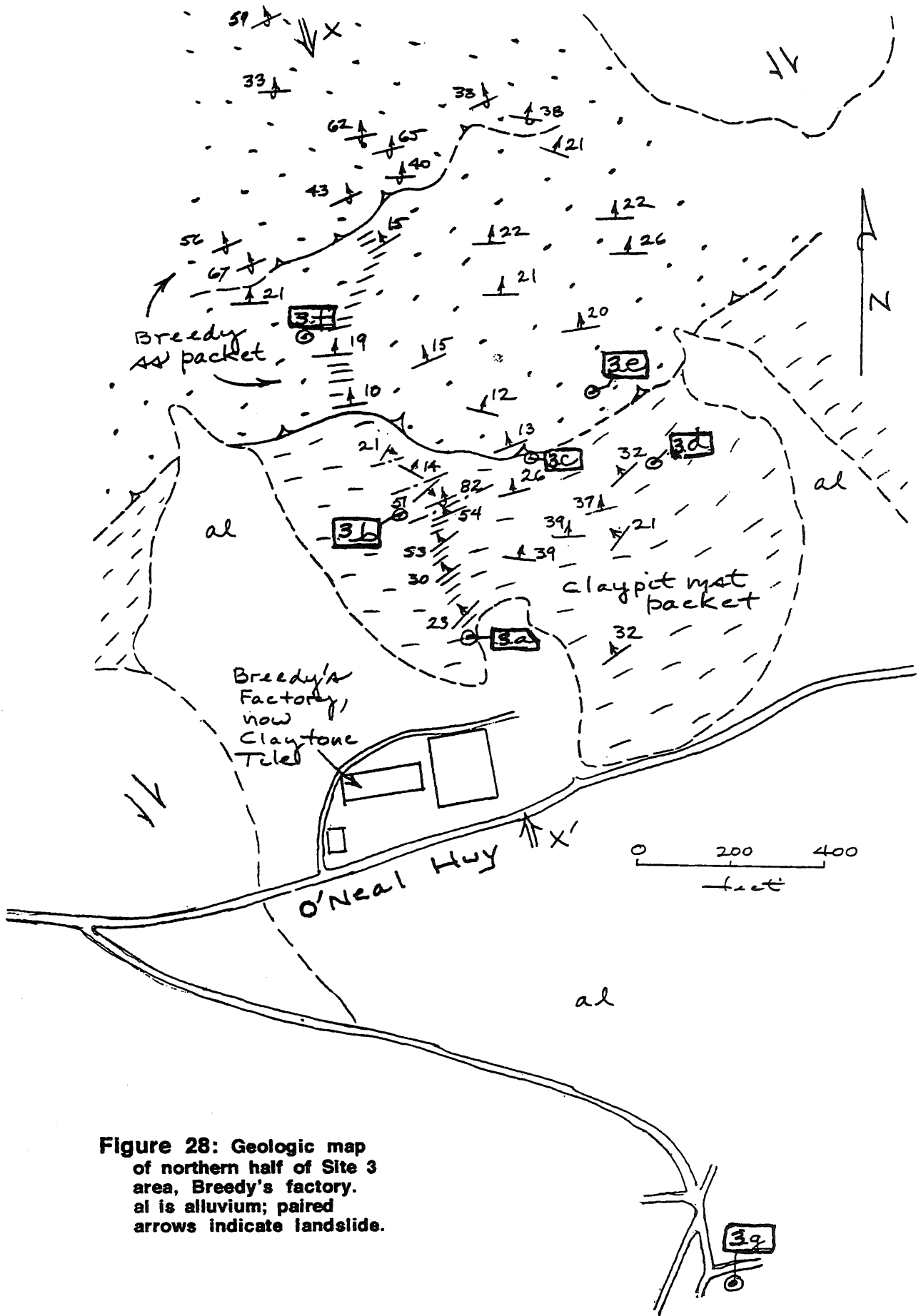


Figure 28: Geologic map of northern half of Site 3 area, Breedy's factory. al is alluvium; paired arrows indicate landslide.

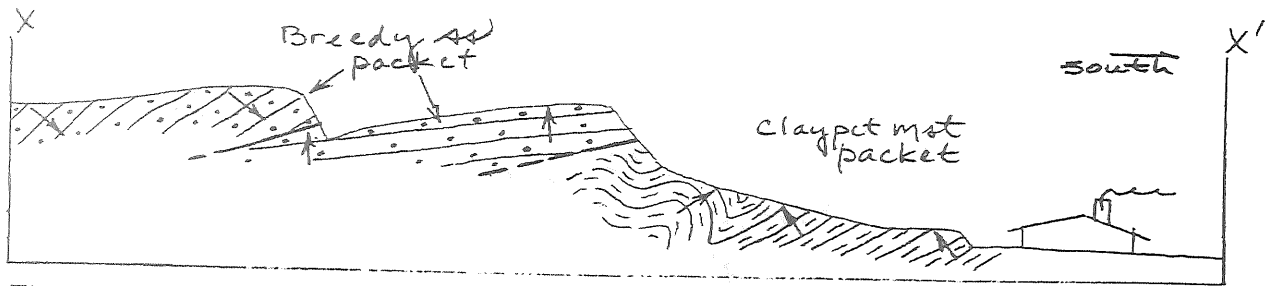


Figure 29: Cross section through packets at northern Site 3; section trace on Figure 28.

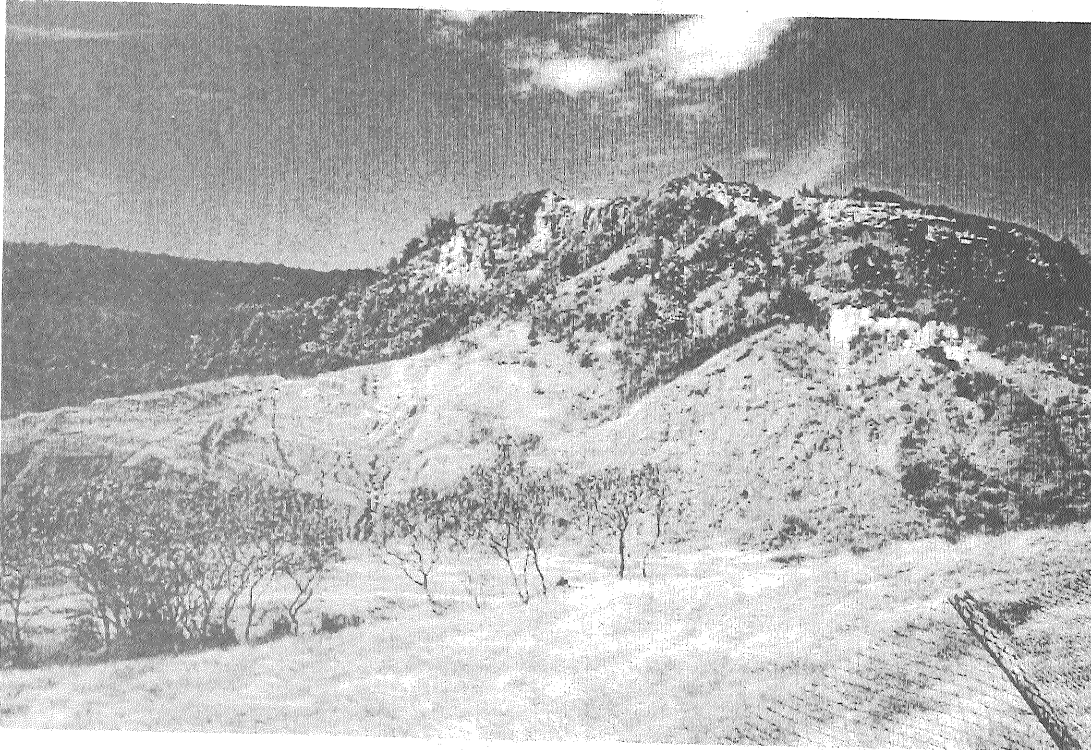


Figure 30: View north from Breedy's factory. Claypit packet below and Breedy sandstone packet above.



Figure 31: Thin mudrich turbidites (dark) and thin sandstones of lower packet.

- Stops (on foot, Fig. 28)
- 0 m 3a Southern end of western wall of clay quarry in Claypit mudstone packet. A roughly 100m thick section is exposed (Figs. 29, 30) The beds are mainly thin bedded mudrich graded sets between 3 and 15cm thick. Bouma zonation varies: Te (dark or brownish organic turbiditic layer and green organic-poor hemipelagic layer), Tde, and Tcde. Maximum grain size is fine grained sand, which occupies the Td or Tc bottoms of the thickest beds. Mudstone/sandstone is 6-8. Proceed NNW up to the quarry face to stop 3b.
- 120 m 3b Monotonous muddy turbidite section is punctuated in its middle by a thin lensy channelized coarse grained sandstone (Fig. 30). The upper half of the section contains many sets of thin bedded fine grained sandstones with tabular sharp boundaries and Tc Bouma zone features (convolutions, fluid-escape, ripples). Vertical thickness sequences are nonsystematic.
- The southern half of the succession is homoclinal whereas the northern half is folded with southerly overturning. The folding may be related to faulting of the overlying sandstone packet (Fig. 29).
- 200 m 3c Fault contact of Breedy's sandstone packet and claypit mudstone packet. Base of massive coarse-grained sandstone cuts bedding in muddy turbidites below. Scaly cleavage occurs in mudstone near contact.
- Walk down to quarry floor and NE to pass through muddy turbidites to stop 3d.
- 300 m 3d Eastern rim of clay quarry. Ascend NW across covered base of sandstone packet to stop 3e.
- 360 m 3e Breedy's sandstone packet. The packet comprises a lower upright section about 140m thick and a higher inverted section above a flat fault (Figs 28, 29). The rocks include grit to fine grained sandstone, conglomerate (minor), and thin bedded muddy turbidite (Fig. 31). Larue (1985) measured the upright section (Fig. 32) and assigned fan facies B,C, and D in repetitions. Layer thicknesses are as great as 6m. A 2m-thick conglomerate (facies A) lens occurs at one place at 10m above base. Interesting features of the sandstones are many horizons of abun-

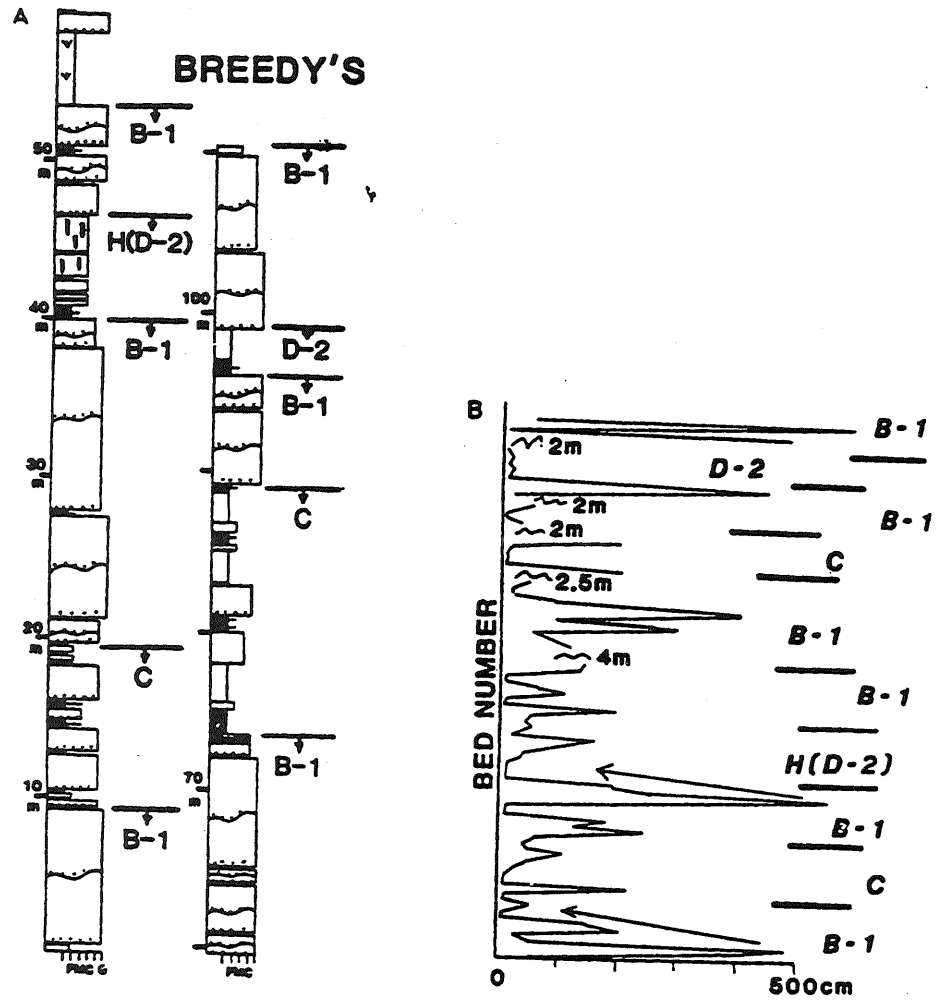


Figure 32: Columnar section (A) for Breedy's sandstone; width proportional to maximum grainsize. Thickness - height diagram; wiggly lines indicate covered intervals. H is bioturbated. From Larue (1985).

dant intraclasts (mudstone and marl), massivity, and organic richness of some muddy interlayers. Thickness-height plots imply two thinning-upward intervals (Fig. 32; Larue, 1985). The facies association is probably inner-fan channel.

Proceed upsection from 3e to 3 f.

- 450 m 3f End of safe passage through Breedy's sandstone. Return to cars. Drive out of quarry to O'Neal Hwy; turn right; drive 150m west; turn left on new gravel road (Fig. 28); drive to end of road or base of hill.
- 3g (Figs 28, 33), about 500 m from highway turnoff
- 0 m 3g Melange diapir with pluglike form (Figs. 33,34). This small diapir is distinguished lithologically from others by an especially sand-rich matrix and by the largest green mudstone granules (up to 5cm) found thus far. Tabular and diamond-shaped lithic blocks are well aligned and parallel a scaly spaced cleavage in the matrix.
- 70 m 3h Southern contact of diapir and beds of packet V (Fig. 33). Local isoclinal folding and shearing of packet V beds occur within 1m of contact
- 300 m 3i Packet V. Packet contains thin and very thick bedded turbidites. Structure is south-overtuned major tight anticline with generally EW axial trace. This early fold is refolded about NS axial traces (Fig. 33).
- 550 m 3j Packet W. This is the type locality of the Walker's beds of A. Senn. They have been much visited because of previously well displayed bottom marks on base-present sandy turbidites. The Walker's beds include many layer types, including base base-present sandstones with scoured and planar bases, amalgamated sandstones, and base-absent thin bedded sandy and muddy turbidites (Fig. 35). The facies association may be a midfan-proximal outer fan transition.

Packet W beds are deformed in a relatively coherent close fold train with flat axial planes (Fig. 33, section YY'). These characterize folds throughout much of the northern Scotland district. They are noteworthy because of the long homoclinal panels between axial planes and because the hinge regions are very small. Disruption of such folds along their axial planes would lead to homoclinal fault packets, which are commonly observed. The folds of packet W are

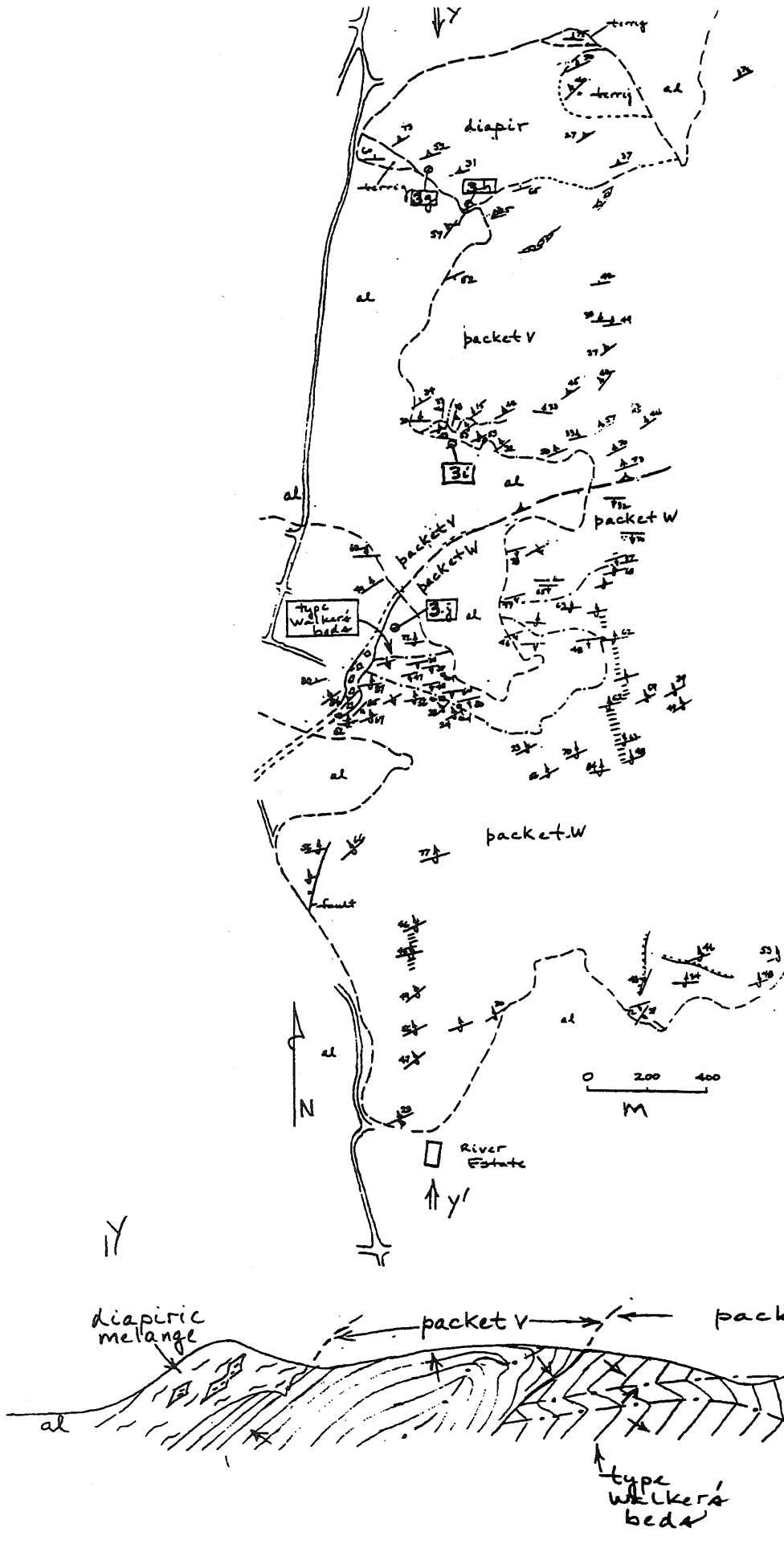


Figure 33: Geologic map and section for southern half of Site 3 area. Dash-dot lines in section are fold axial traces. Block pattern indicates broken formation and shear zone.

A foliation
 A bedding, top known
 // stack

South
 Y'
 ↑

~ 25m

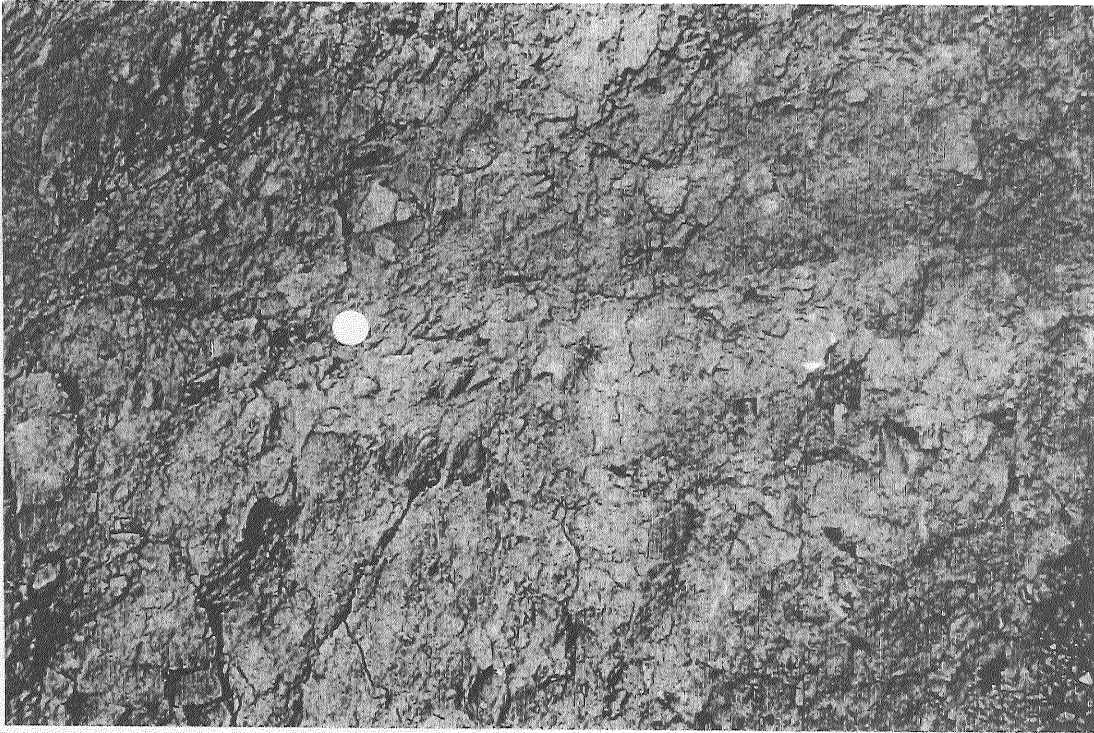


Figure 34: Diapiric melange at Site 3 (Fig. 33). Freshly exposed surface shows angular sandstone fragments (light grey), mudstone granules (greenish tinge), and matrix (light tan).

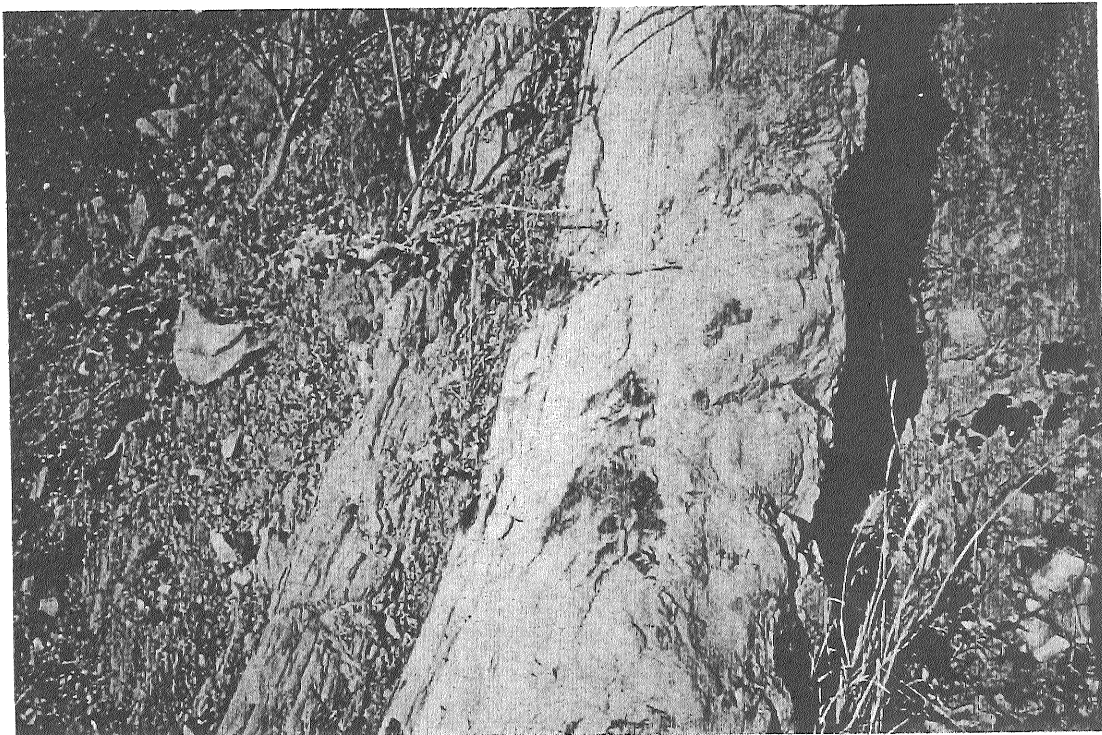


Figure 35: Thick sandstone in Walker's beds at type locality (Fig. 33). Thickness 3/4m. Bottom at left is plane-laminated, non-channelized, and base-absent. Top half contains fine sandstone and Tc zonal structures.

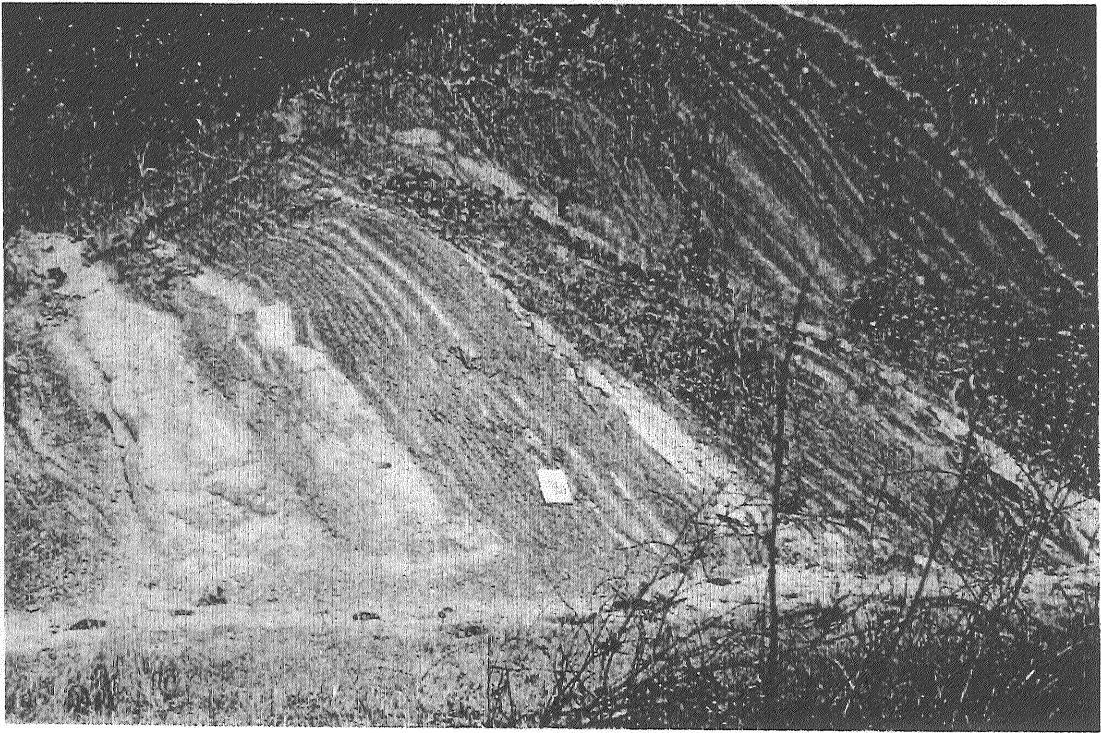


Figure 36: Layer sequence in Walker's beds; top to right.

interesting because the long limbs are overturned. This implies tht they may have been higher harmonic folds on the overturned limb of an originally even larger fold, now disrupted.

Return to cars; drive to O'Neal Highway.

Site 4 Walker's Savannah

Route (Fig. 10)

- 22.5 km O'Neal Hwy at Breedy's factory; head east on highway.
- 23.7 km Intersection O'Neal Hwy and Bourne Hwy; turn right on Bourne Hwy.
- 24.9 km Intersection unmarked dirt road leading to houses and a claystone dump; turn left; signs for Benjamin sand mine and St. Andrew's church are beyond the unmarked turnoff.
- 25.4 km Park just north of the rock dump.

General

Outcrops at Walker's Savannah provide a NS traverse across 9 fault packets of terrigenous rocks of the basal complex. Figures 37 and 38 show the detailed structure of the area.

Highlights

- 1) existence throughout of early (accretionary) flat faults and folds, typical of the basal complex in the northern half of the Scotland district;
- 2) existence among early structures of a duplex of sandrich packets;
- 3) exposures illustrating deformation gradients at packet boundaries and structures created by reactivation of packet boundaries;
- 4) existence of a thick section of strata in packet 35 (Green Hill) containing an outer fan progradation above basin plain.

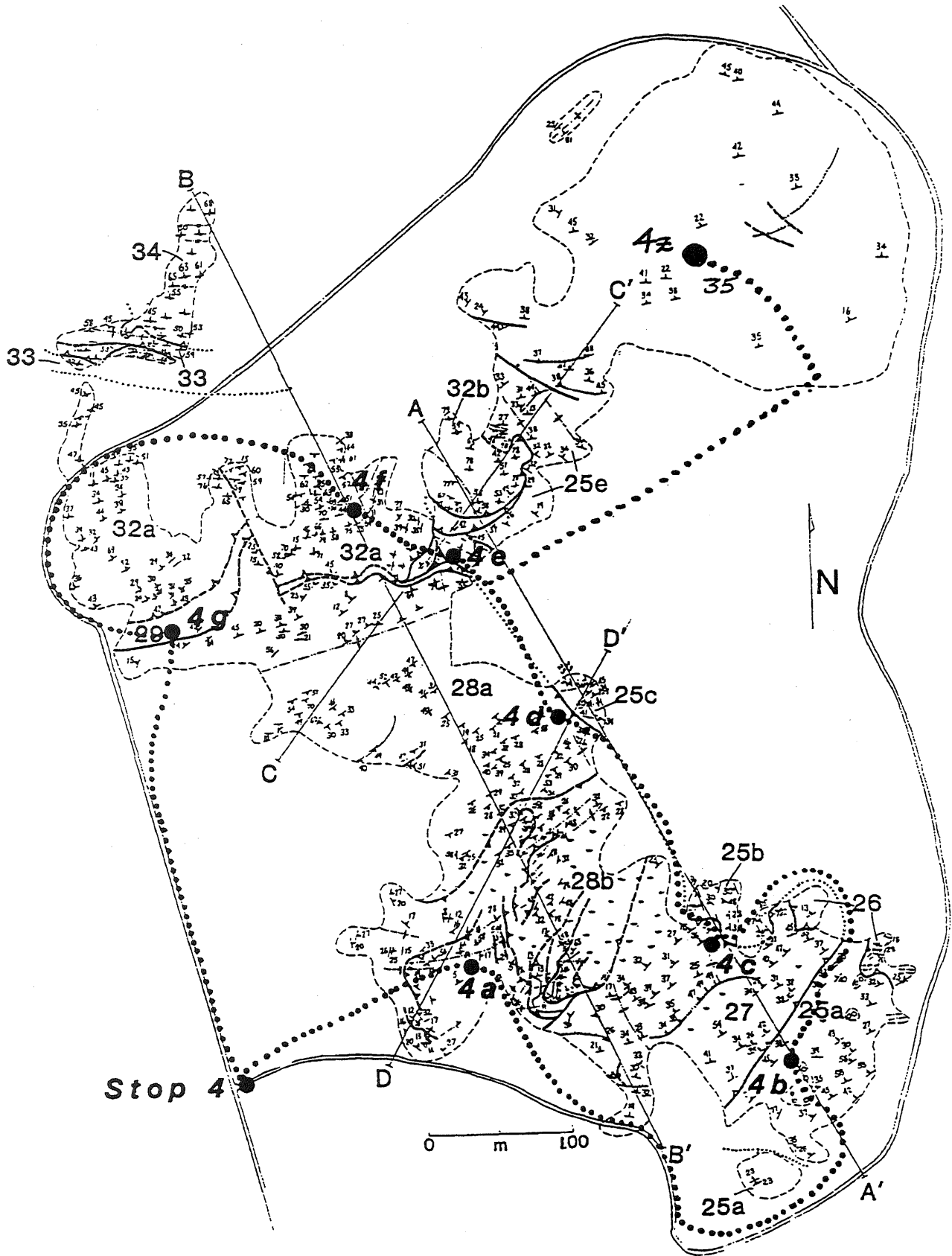


Figure 37: Geologic map of Walker's Savannah, showing packets 25 to 35. Letters attached to packet numbers indicate structural domains within packets. Dots are walking route for Site 4. Dash-one dot lines are early fold axial traces; dash - two dot lines are late fold axial traces. Finely dotted lines are buried fault traces.

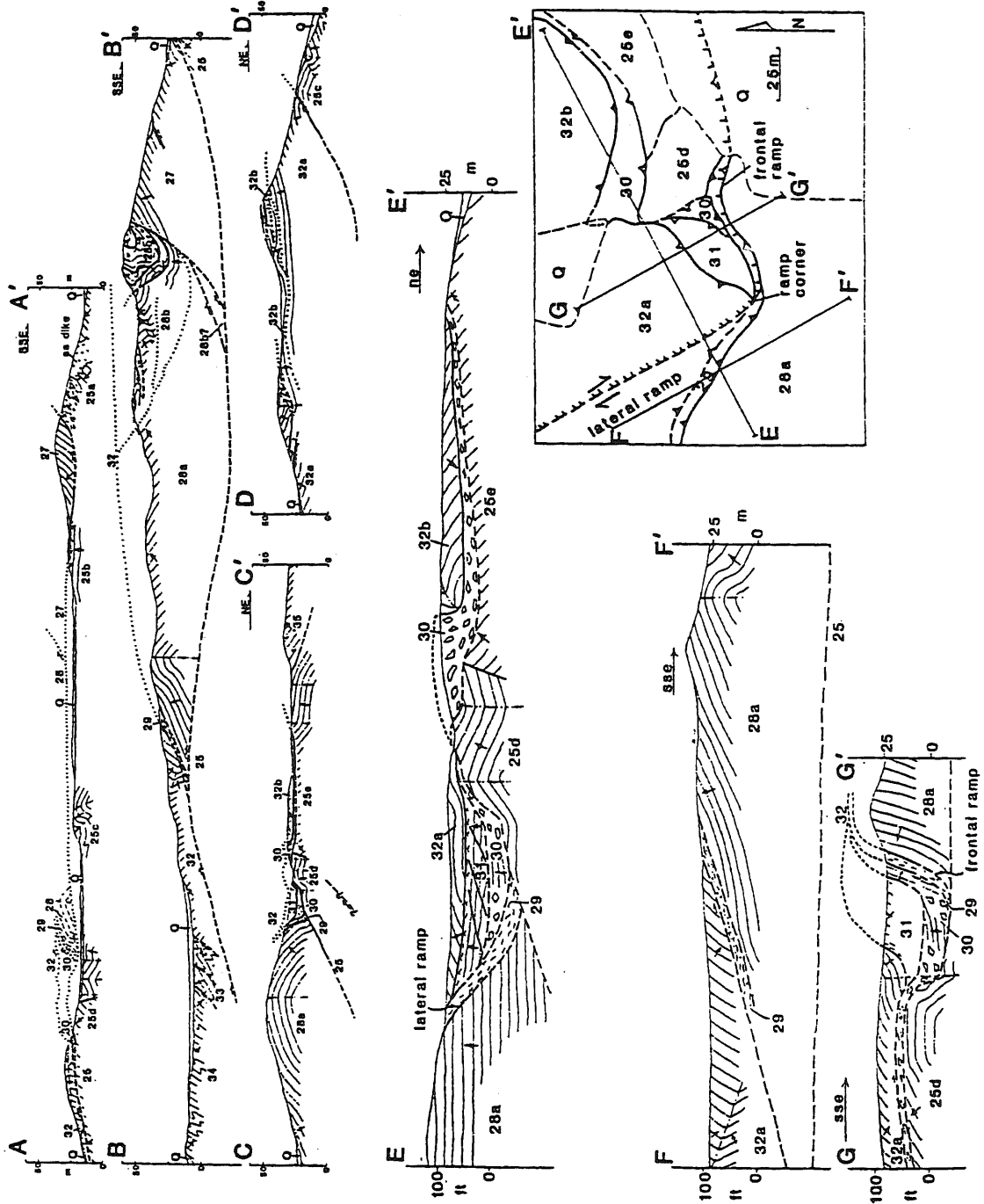


Figure 38: Cross sections at Walker's Savannah. Section traces on inset map and on Figure 37.

The kinematic history of rocks at Walker's Savannah is as follows.

- 1) early accretionary thrusting and folding about subhorizontal EW axes under NS contraction;
- 2) duplexing by subsurface imbrication of sandy packets 27-30 below the roof thrust sequence of muddy packets 32-35;
- 3) local homoaxial (EW) refolding of early folds and faults, still under NS contraction;
- 4) late superposition of NNW-SSE-trending folds.

Figure 39 gives a model of duplex formation at Walker's Savannah. The model assumes sandstones of packets 27-30 were a thick, wide channel fill and that muddy turbidite sections had high cohesion relative to that of sandstone.

<u>Stops</u>		(on foot, Fig. 37)
0	m 4	Begin traverse; head N70E upslope.
180	m 4a	Packet 28 (Fig. 37). This stop is within the duplex of packets 27-30; outcropping here are SSE-verging first fold and open late synform. In hill above and east is tight syncline (domain 28b, section BB', Fig 29) near top of duplex.
500	m 4b	Top of packet 25 near base of duplex. Large sand intrusion, and foliated broken formation.
700	m 4c	Packet 25 overlain by flat base of duplex (packet 28).
900	m 4d	Packet 25 overlain by duplex; between 4d and 4e, note major anticline in duplex sandstones (packet 28) on the left.
1000	m 4e	This stop is at the northern tip of the duplex, where mud-rich packets 29-34 directly contact the duplex base, packet 25, and are thrust above the duplex (Fig. 38, sections B, E, F, G). A lateral ramp on the lowest packet (25) can be seen.
1300	m 4z	Green Hill, packet 35. The structural position of this packet relative to the others at Walker's Savannah is unclear. It may be the highest. Its structure is an upright homocline except for a couple of narrow recumbent isoclines.

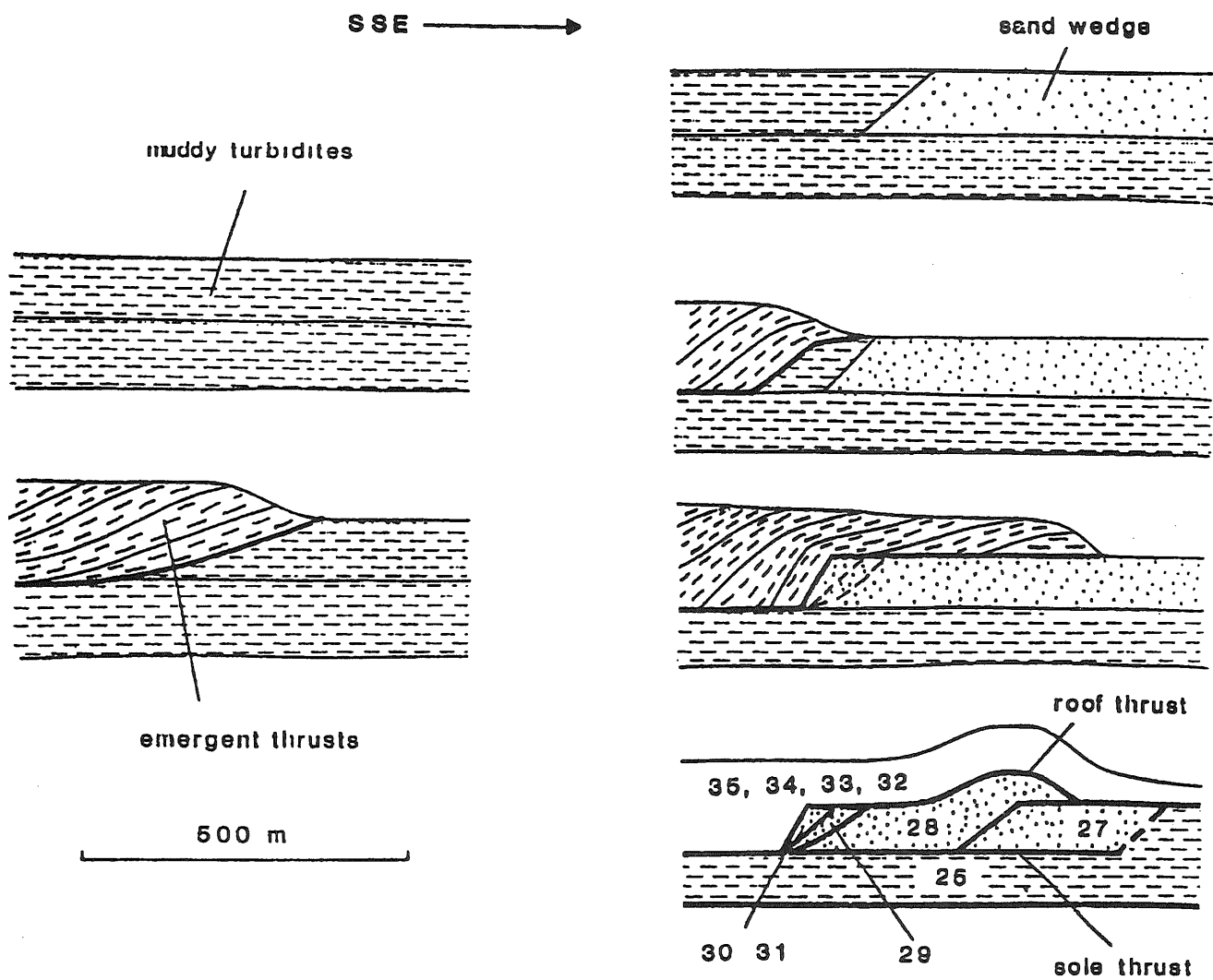


Figure 39: Model of duplexing at Walker's Savannah during accretion. Strata on left are uniformly muddy turbidites whose imbrication produces emergent flat packets. Strata on right include a sand-filled channel that has high frictional strength and is overridden by mudstone imbricate.

Green Hill exposes 120m of strata measured by Larue (1985). The section (Fig. 40) has mostly thin muddy turbidites of basin plain association (facies D1) in the lower half. These are succeeded by distal and proximal outer fan associations in most of the upper half (facies D2, C, Ch = C with scour). The bed thickness diagram shows a number of thin upward thickening sequences (Fig. 40).

The Green Hill strata can be interpreted as a prograding succession. Here as at many other places, however, the so-called basin plain association contains thin channelized beds of coarse sandstone. This confounds the basin plain interpretation and may suggest an environment beyond the levees of a major channel but subject to occasional levee break through.

1600 m	4f	Packet 32, duplex roof thrust; major recumbent fold.
1900 m	4g	Packet 29, foliated zone between roof thrust and duplex packets. Return to car

Site 5 Mount Hillaby

Route (Fig. 10)

25.9 km	Exit Walker's Savannah at Ermy Bourne Hwy, turn left.
27.0 km	Intersection Ermy Bourne Hwy and Hwy 2 in Belleplaine; go straight (south) on Hwy 2.
29.2 km	Intersection Hwy 2 and Hwy 3A; stay right on Hwy 2.
30.4 km	Intersection Mt. All road and Hwy 2; turn right.
32.6 km	White Hill; park car.

General

Mt. Hillaby, just west of White Hill, is the highest point of Barbados, about 330 m. The mountain is underlain by marl and ash of the Oceanic nappes. These rocks are crossed between White Hill and Stop 5 (Fig. 41).

Highlights at Mt. Hillaby are twofold. First, the basal complex is in a west-trending arch or culmination that crosses below Hillaby. A map of the Hillaby region (Fig. 41) indicates the complication of the culmination. The best model is that the culmination is the hangingwall or triangle zone above a N-verging

GREEN HILL

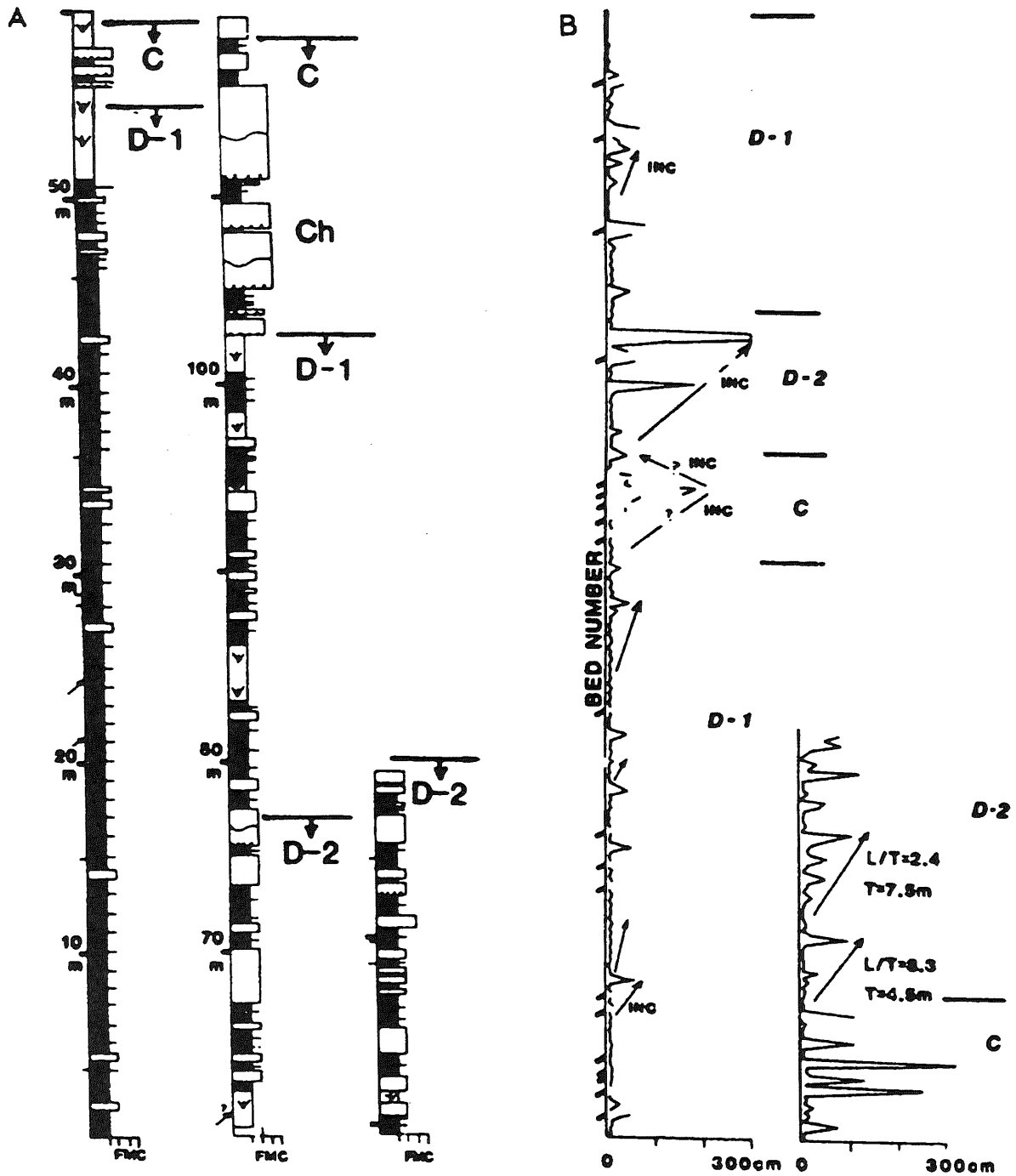


Figure 40: A . Columnar section at Green Hill, Site 4. D2 is sandier facies D than D1. Ch is channelized. B. Bed thickness vs height. From Larue (1985).

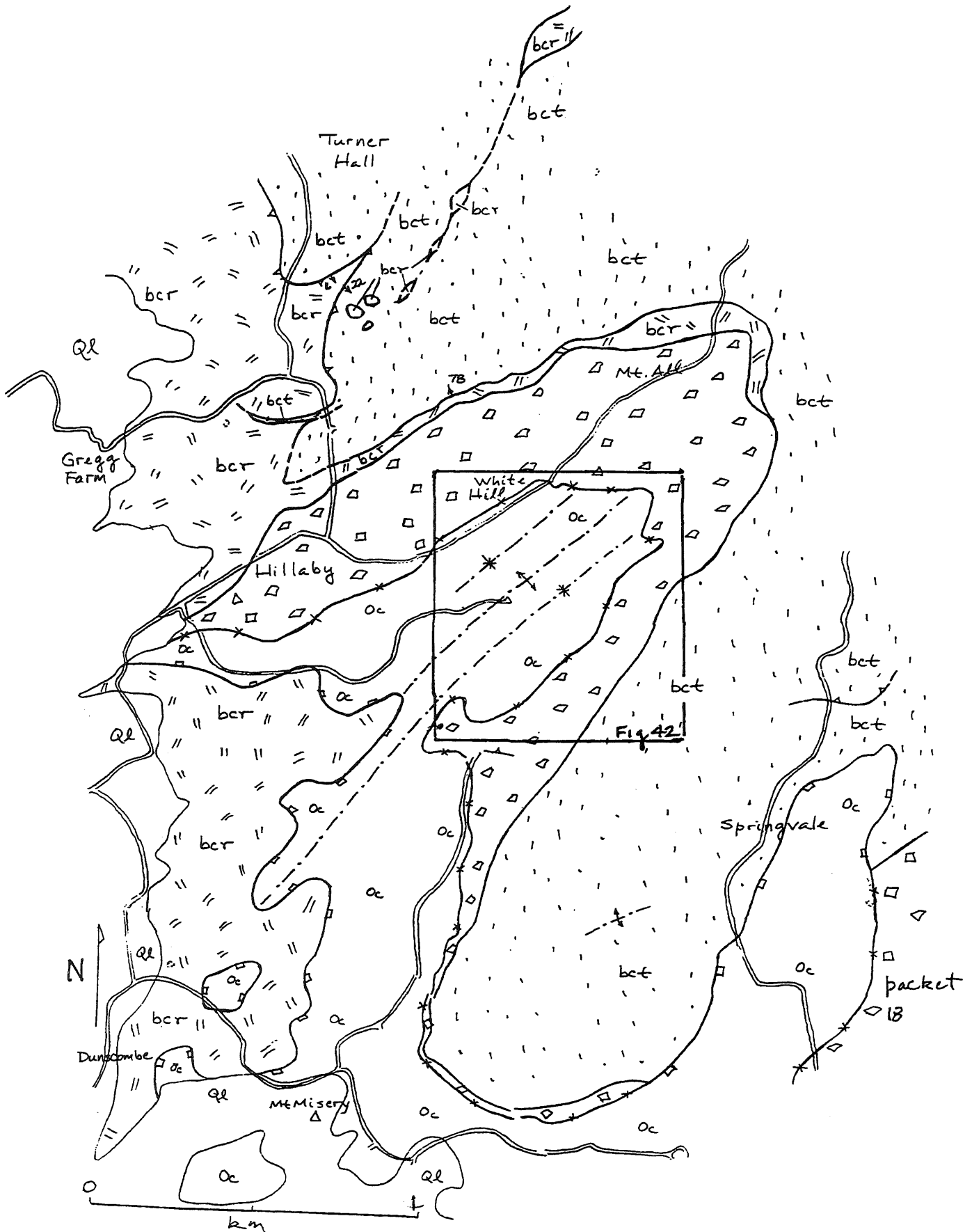


Figure 41: Geologic map of Mt. Hillaby area, which includes Site 5 near White Hill. Subhorizontal flap of diapiric melange (block pattern) extends NW from packet 18 (near Springvale) below Oceanic allochthon (Oc) and above basal complex (bcr, radstone, and bct, terrigenous).

backthrust. The culmination probably developed during late Neogene reactivation and S-vergent imbrication of the basal complex in northern Barbados (Fig. 6).

The second highlight is the existence of a sill or long flap of diapiric melange, which lies subhorizontally above the basal complex and its culmination (Fig. 41). The flap underlies the Oceanic nappes, and is continuous below them south 2.5 km to the top of the largest diapir, packet 18 (Fig. 9), which is probably a vertical dike.

The tentative structural sequence at Mt. Hillaby is: first, emplacement of Oceanic nappes above basal complex; second, intrusion of melange diapir along sub-Oceanic fault zone; and third, deformation of the structural stack with imbricate thrusting in the basal complex.

Stop 5 is at the base of the Oceanic nappes and above the diapir flap (Fig. 42). The contact is sometimes exposed. Note in the cross section that the nappe base and bedding within the nappe are greatly discordant. Over lengths of 1m, the diapir intrudes the basal nappes. Structures suggest the diapir intruded along the base of the Oceanic nappes, rather than the nappes having thrust above the diapir. Two nappes are distinguished in the Oceanics at Mt. Hillaby by dating (O₁ and O₂, Fig. 42).

Site 6 Coconut Grove

<u>Route</u>	Figure 11
0 km	Start, Bathsheba; north on Ermy Bourne Hwy.
0.7 km	Intersection, Saddleback road; turn left.
2.1 km	Intersection, Springfield road; continue on Saddleback road by left turn.
3.4 km	Coconut Grove, on south flank of Bissex Hill and 100m SW of intersection of Saddleback and Parks roads; park.

General

Site 6 is within diapiric melange assigned to packet 18 (Figs 9, 26, 43). This is the largest body of diapir at the Barbadian surface. Its form is a vertical dike of ENE strike and 3km width. Site 6 crosses the northern third of the dike's width. The elevation range of the site is from 230 to 100m. This same body continues WSW to the area south of Mt. Hillaby (Fig.41). There the upper reaches of the dike spread out laterally, at elevations of 250-300m. The diapir flap at Hillaby is apparently sourced from the dike to the south. At site 6, the

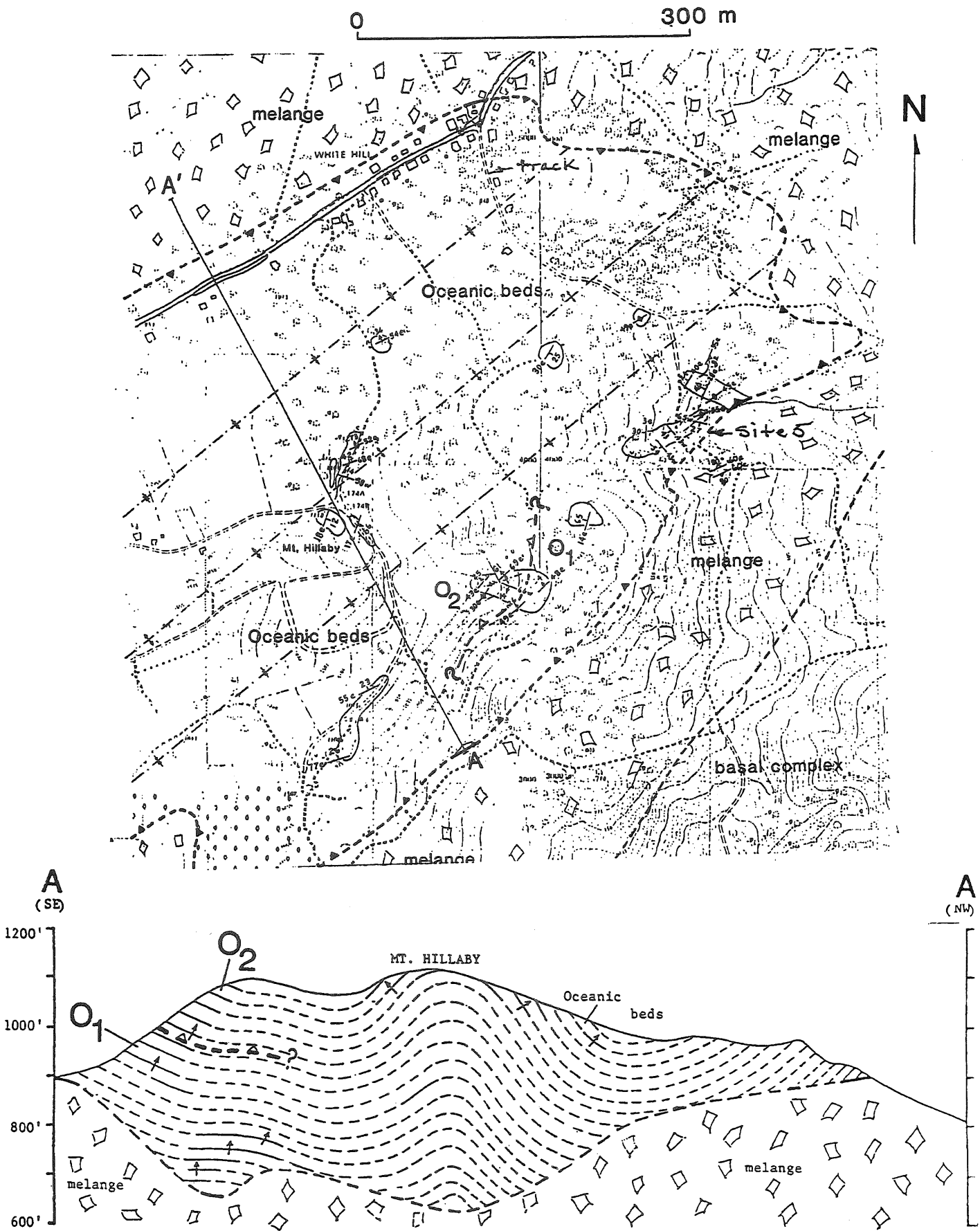


Figure 42: Geologic map and cross section of Oceanic allochthon and underlying melange flap at Mt. Hillaby. Map shows White Hill and path to reach Site 5.

△ Bissex Hill

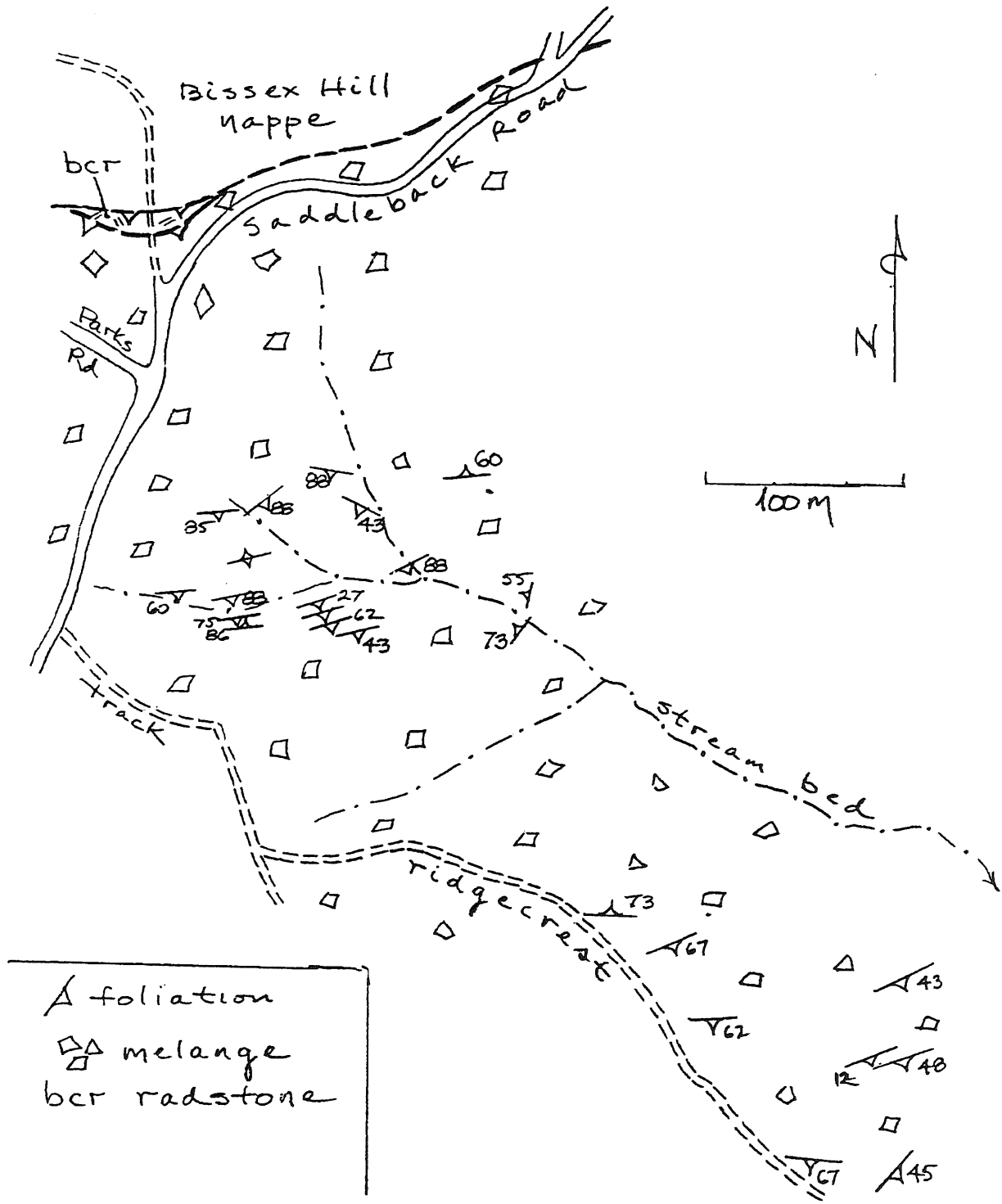


Figure 43: Map of Coconut Grove area (Site 6).

northern contact of the diapir is probably steeply south-dipping, (Fig. 26), suggesting that the diapir flap continued east but is now eroded east of Hillaby.

Melange at Site 6 comprises four components: lithic blocks, green mudstone granules, matrix, and fossils. Lithic blocks are mainly but not entirely hard rocks of the basal complex: clay ironstone, quartz sandstone cemented by carbonate or by bitumens, and calcitized radstone. Such blocks range in diameter from .01 to 25m. Granules of rocks unfamiliar in the basal complex, such as chert, also exist. The mudstone granules are mainly pure but occasionally sandy; they are as large as a few cm. They are major volumetric constituent and are important by the absence of an evident source bed in the basal complex.

Matrix is composed of quartz sand, clay, and organics, probably mainly bitumens. Sand sizes may be bimodal: fine and very coarse. The concentration of coarse sand is a puzzling feature of all Barbadian diapirs.

Megafossils at Site 6 are occasional scattered or concentrated clams, snails, and tubules. It was here that whole shells and fragments were found of a mollusc, named as a new oligotypic species *Nuculana senni* by P. Jung (Kugler and others, 1984). These occur in both the matrix and in blocks of calcitized radstone. If the megafossils are allochthonous, their transport on the seabed was probably not great. Melange matrix at Site 6 contains Eocene pollen.

Melange at Site 6 is well foliated. Foliation comprises spaced scaly cleavage and nonequant block orientation. Scaly cleavage consists of mm-thick panels of organic mudstone with slickenside and striae. Sandier lithons exist between the cleavages. The foliation generally strikes ENE (Fig. 43), parallel to the diapir walls. The foliation is folded, openly to isoclinally, on ENE-trending axial traces. I interpret the foliation to be the product of subhorizontal shortening in a NNW-SSE direction. Scaly cleavage may have begun as conjugate shears that took up strain and served as fluid-advection conduits within the diapir. With progressive shortening, the shears were rotated to parallelism. The cause of shortening may have been regional contraction or intrusion up into a progressively confined space or both.

Walk

Proceed from the Saddleback road southeast on a dirt track (Fig. 43). The track loses distinction after about 200m. Stay to the left on the crest of a spur, heading downhill. Outcrops of melange are on the north flank of the spur. Walk to base of spur, about 500m from paved road, and work up.

Site 7 Martin's Bay

<u>Route</u>	(Fig. 11)
3.4 km	Coconut Grove; drive back to Bathsheba.
6.8 km	Start; continue south through intersection onto East Coast Road.
11.6 km	Intersection Martin's Bay road; turn left and descend to shore.
12.1 km	Martin's Bay, south end; park.

General

The objective of Site 7 is a glimpse of the structure of the sub-Quaternary south of its major exposure and structural culmination in the Scotland district. As drawn on Figure 6, the top of the basal complex deepens markedly from the central arch southward into the Woodbourne Trough. Such deepening is linked with concomitant thickening of the Oceanic allochthon.

The coastal strip between Martin's Bay and Ragged Point exposes the top of the basal complex at elevations close to sea level (Fig. 44). Here too the Oceanic allochthon reaches thicknesses of 600m or more (inland from the modern eroded shoreline). This is a substantial contrast to the 100m thickness of the allochthon north of Martin's Bay (Fig. 44).

Martin's Bay thus may be an exposure of the northwestern flank of the Woodbourne Trough. If true, the flank is precipitous, and the Woodbourne Trough is indeed two-sided. In the 6km width of the Trough extension along the east coast (between Martin's Bay and Foul Bay, Fig. 44), isopachs of Oceanic allochthon define major structures (folds?) within the Woodbourne Trough. Such structures are also known by drilling downplunge to the SW.

The foregoing thoughts imply that prism cover (Woodbourne Fm) should exist between basal complex and Oceanic allochthon along the coastal strip. It apparently does not. To explain this, I postulate that the Trough plunge existed during Woodbourne Fm deposition or was imposed before arrival of the Oceanic allochthon.

Walk

Follow dirt track east for 150m through slides of Oceanic and Quaternary limestone (Fig. 45). Examine outcrops of basal complex and Oceanic allochthon over the next 150m. The basal complex consists of thin bedded muddy turbidites, folded about ENE-trending axes. The bc - Oa contact is folded. The hemipelagic tops of many of these turbidite beds have been examined for microfossils, none found.

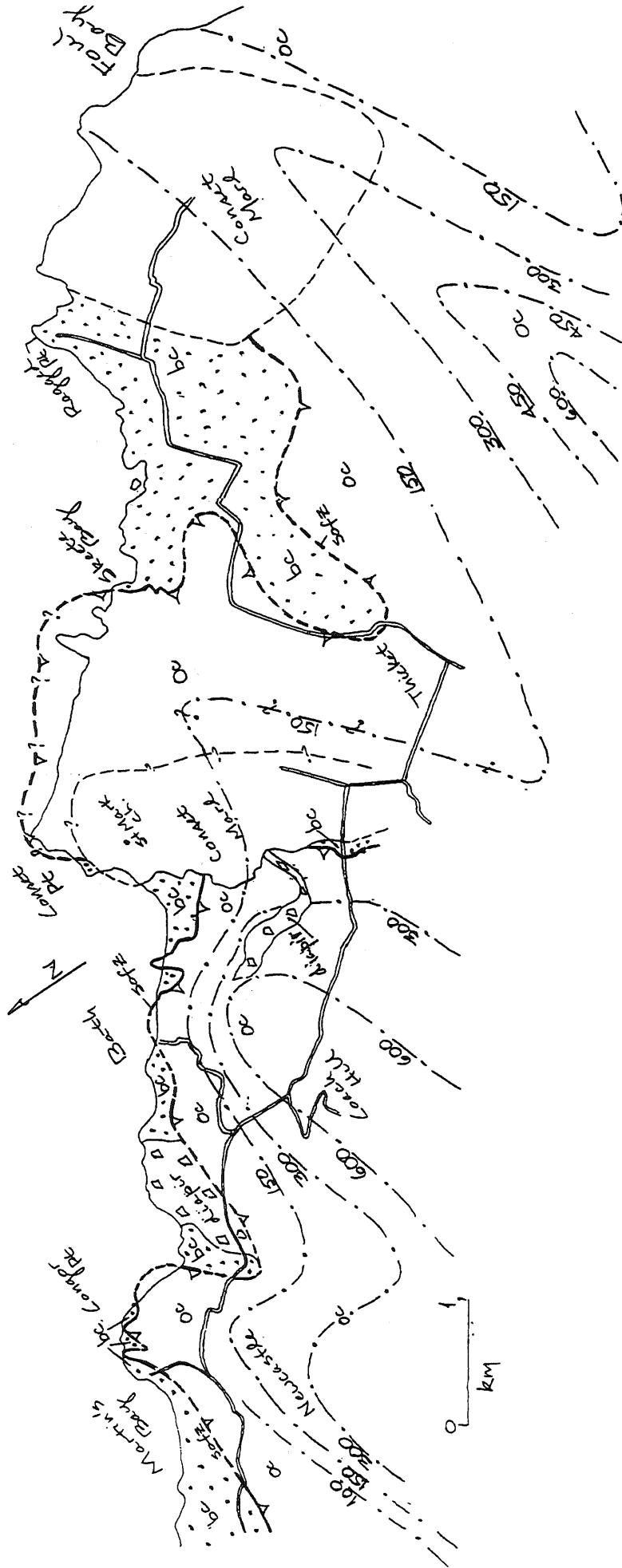
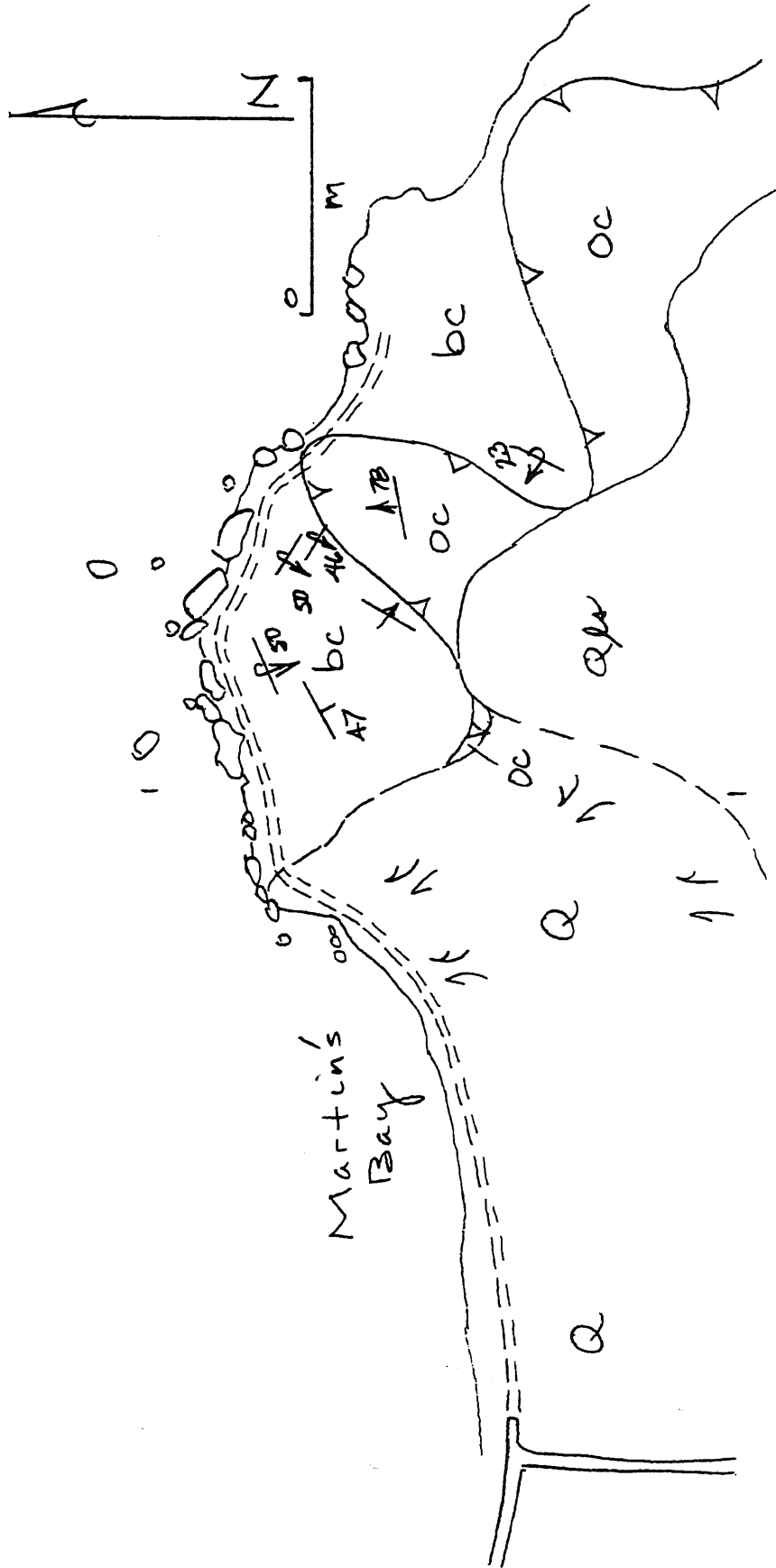


Figure 44: Regional map between Martin's Bay and Foul Bay of sub-Quaternary outcrop and subcrop. Nearly continuous fault trace is SOFZ — Sub-Oceanic Fault Zone, between Oceanic allochthon (Oc) and basal complex (bc). Contours are isopachs of Oceanic allochthon in meters.

Figure 45: Sketch map of Site 6 at Martin's Bay. Paired lines indicate cover by slides.



Site 8 Bath Cliffs

<u>Route</u>	(Fig. 11)
12.1 km	Martin's Bay; return to East Coast Road intersection
12.6 km	Intersection; turn left on East Coast Road.
14.8 km	Intersection Bath Beach road; turn left.
15.4 km	Bath Beach; T junction, turn right on track (Fig. 46)
15.6 km	End of track; park.

General

The Bath Cliffs provide good exposures of the Oceanic allochthon, SOFZ, and top of basal complex at what may be the axial region of the Woodbourne Trough (Figs. 2, 44). Highlights of Site 8 are:

- 1) structure and stratigraphy of the Oceanic allochthon;
- 2) structure and composition of the SOFZ;
- 3) late major folds that affect the Oceanic allochthon and basal complex together.

Figure 46 is a map of the Bath area showing the imbricated lower allochthon as nappes O₁ to O₅ and the thick highest nappe as O₆. Nappe O₆ contains 550m of beds which range from middle Eocene to late Oligocene age. The map array of substages in nappe O₆ is shown in Figure 46. The mid-Miocene Conset Marl lies unconformably on the Oceanic allochthon and basal complex at the southeastern margin of the Bath area (Fig. 46).

Well Conset 2 was drilled at point A (Fig. 46). Our study and dating of cuttings from Conset 2 indicates 515m vertical thickness of the allochthon, including two intervals of diapiric melange (Fig. 47).

Figure 48 shows detail and sections at the coastal cliffs, from Torrini and others (1985). Figure 49 gives a schematic of the structural stacking along section BB' of Figure 48. Note that the basal complex is divided between two units: radiolarian-rich (r) and radiolarian-poor (h).

Figure 50 gives age ranges of various units at Bath Cliffs from radiolarians and forams. It is not clear whether the basal complex and Oceanic beds are age discrete or narrowly age overlapping in the middle Eocene.

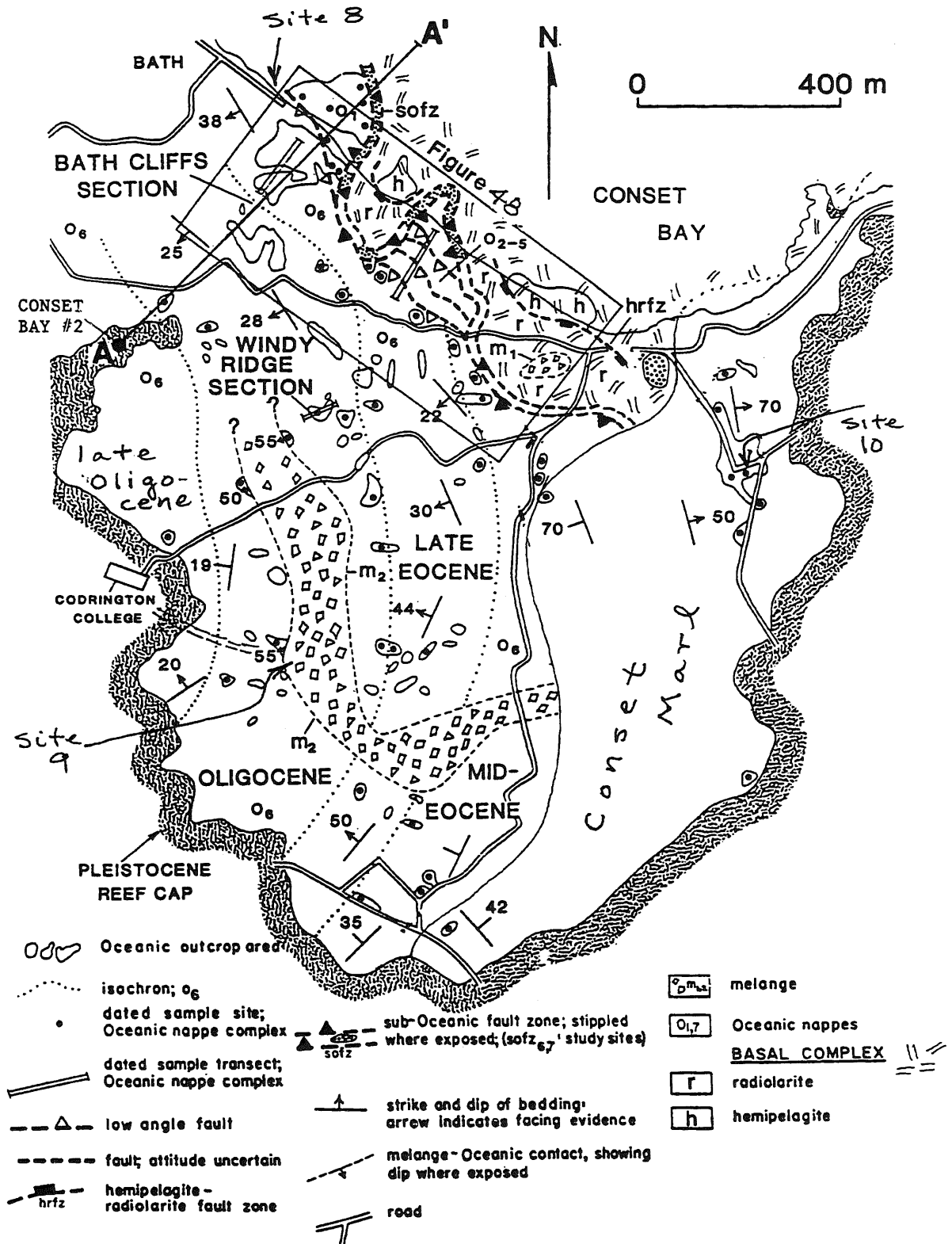


Figure 46: Geologic map of the Bath area, which includes Sites 8, 9, and 10.

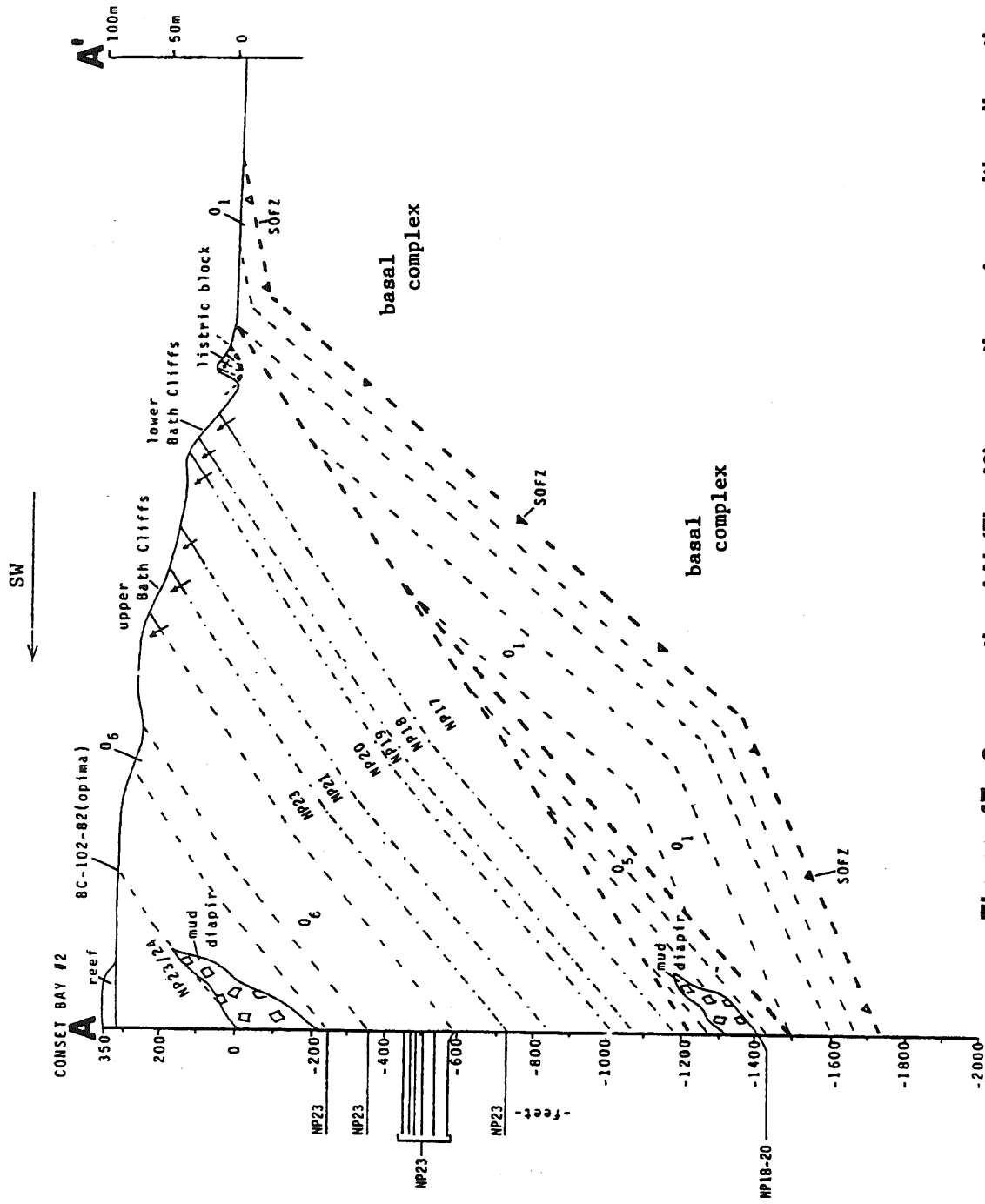


Figure 47: Cross section AA' (Fig. 46) connecting outcrop with well section of Conset Bay 2. Heavy dashed lines are boundaries of nappes in Oceanic allochthon. Light dashed lines are stratal layering. Dash-dot lines are nannofossil zonal boundaries.

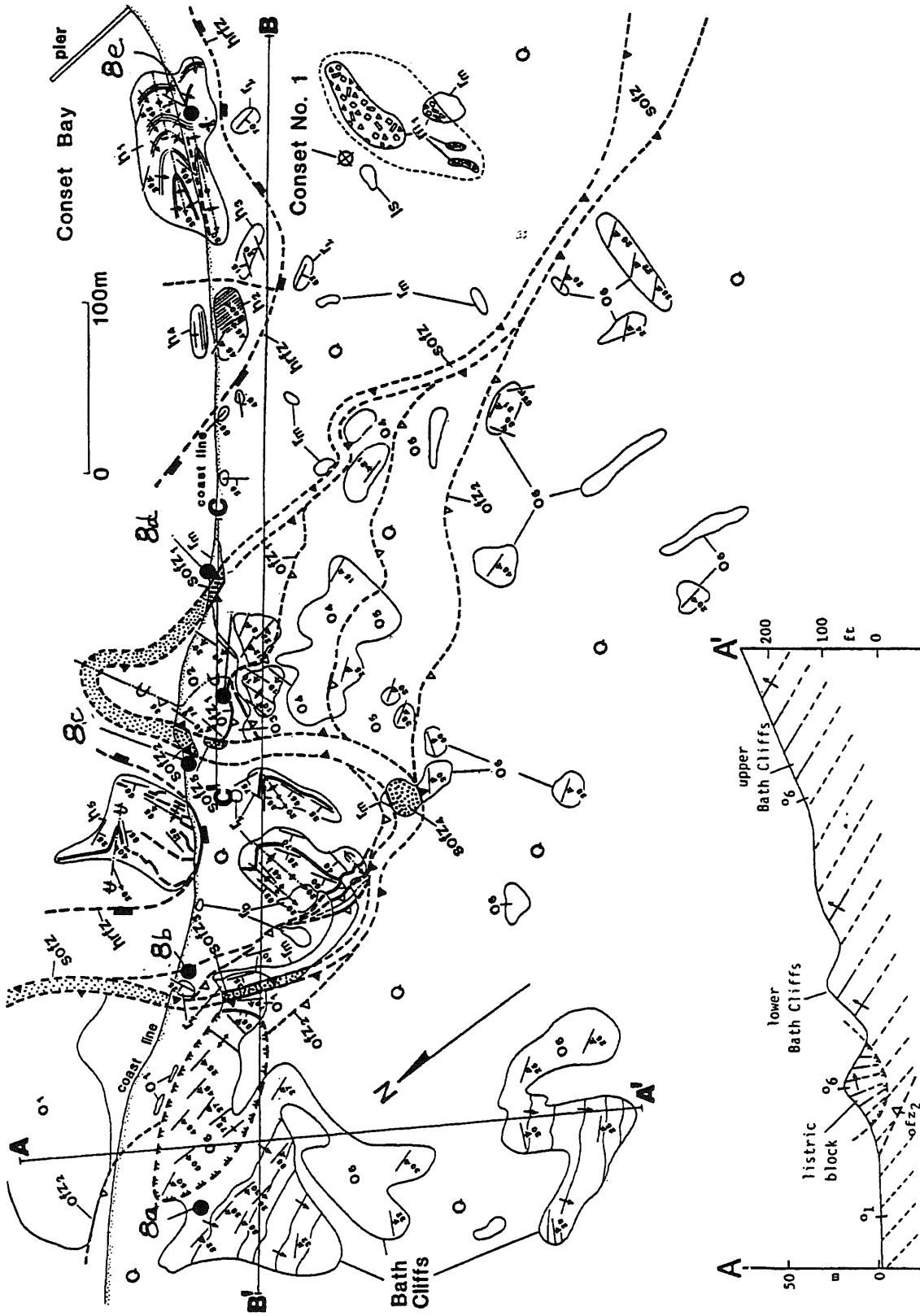


Figure 48: Geologic map and sections of Bath Cliffs, located in Figure 46
Stops on walking tour are 8a - 8e.

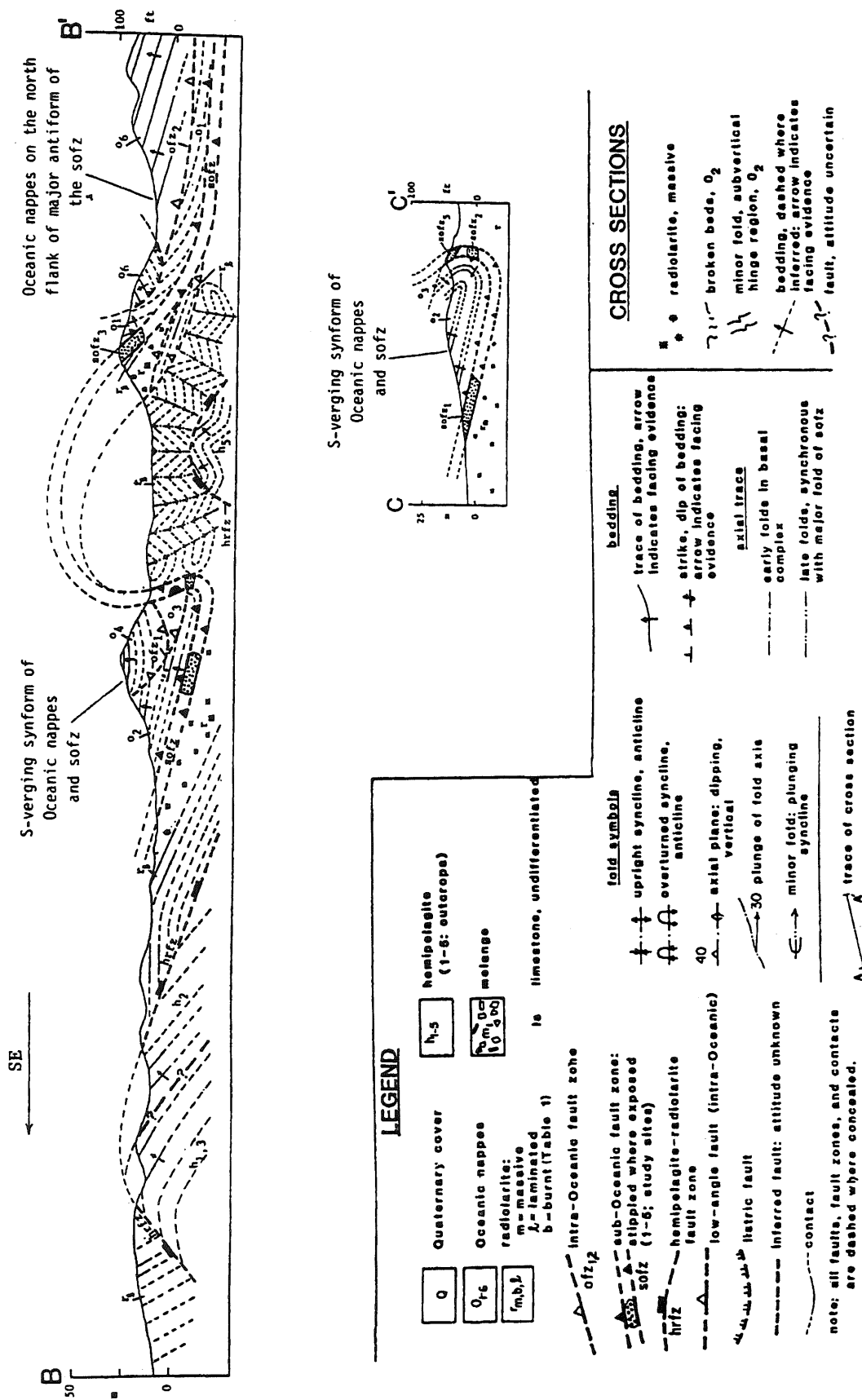


Figure 48: Geologic map and sections of Bath Cliffs, located in Figure 46. Stops on walking tour are 8a - 8e.

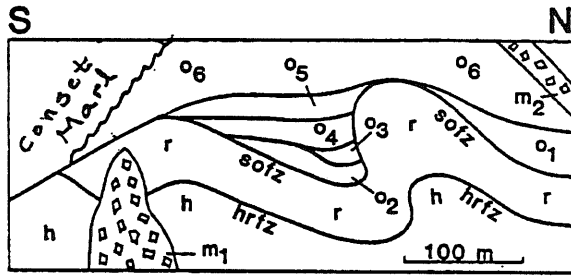


Figure 49: Diagrammatic tectonostratigraphy of the Bath area; O₁-6, Oceanic nappes; basal complex: r, radiolarite; h, hemipelagite; m₁, 2, diapiric melange. All contacts except those bounding melange are faults; SOFZ, sub-Oceanic fault zone; HRFZ, hemipelagite/ radiolarite fault zone within basal complex.

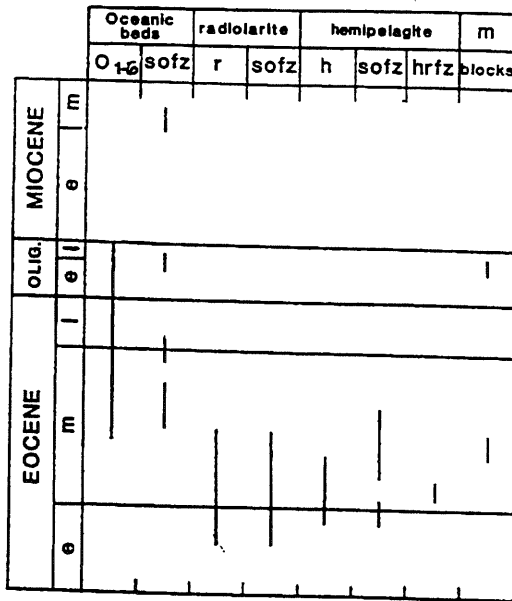


Figure 50: Ages (radiolarian and foraminiferal) of pre-Pleistocene rocks of Bath area; lines indicate ranges of ages of major lithic suites. O₁-6, Oceanic nappes; r, radiolarite; h, hemipelagite and fault zone rocks (SOFZ, sub-Oceanic fault zone; HRFZ, hemipelagite/radiolarite fault zone); lines in melange column (m) are dates of blocks.

Figures 51 and 52 show measured section and analytic data for Oceanic beds of nappe O₆ from Torrini (1986) and Saunders and others (1984).

Table 2 describes the basal complex at Bath Cliffs.

Detailed sections of the SOFZ at three places are in Figure 53.

<u>Stops</u>		(Fig. 48)
0m	8a	Cliff west of car park (Fig. 52). This is the section of Figure 51 where 175m of marl and ash were examined at 1-2m resolution in outcrop and trenches.
150	8b	Cross SOFZ into basal complex. Note thin beddedness, absence of bioturbation and high organic content of radstones. This stop is on the north-dipping flank of a major late antiform which verges SE..
300	8c	Intermediate limb of late major fold pair. SOFZ is vertical (SOFZ-2), Fig. 53). Just south are steeply dipping Oceanic beds of nappe O ₂ . Continue south on abrasion terrace above Oceanic beds. Note graded ash layers and bioturbation, partly escape burrows. Cross axial trace of late major synform.
400	8d	South limb of late major synform. SOFZ at SOFZ-1 (Fig. 48)
800	8e	Basal complex. Thin bedded graded sets of radiolarian mudstones (Table 2). Strata are deformed in NW-plunging syncline with subvertical axial plane.

Site 9 Codrington College

<u>Route</u>		(Fig. 11)
15.6	km	Bath Beach; return to East Coast Hwy.
16.2	km	Intersection East Coast Hwy and Bath Beach road; turn left.
17.4	km	Intersection Codrington College road and East Coast Hwy; turn left.
17.7	km	Turn right into parking lot; park.

General

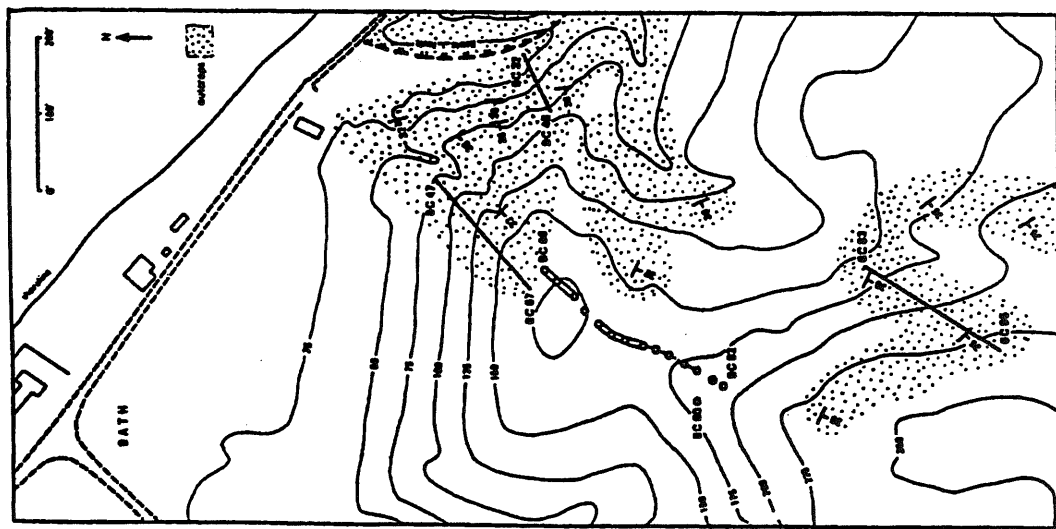
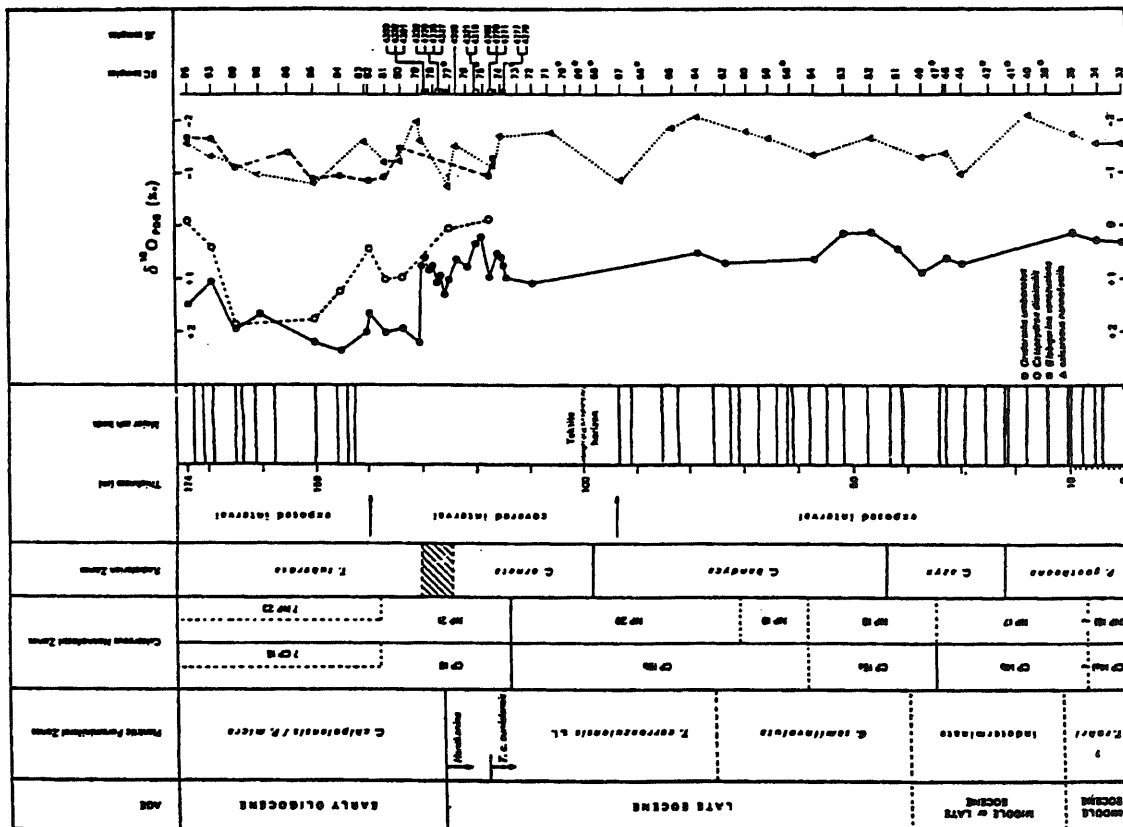


Figure 51: Stratigraphy of Oceanic beds in nappe Og of Bath Cliffs. Map shows sampling traverses. Data from Torrini (1986) and Saunders and others (1984). Black is poorly calcareous.

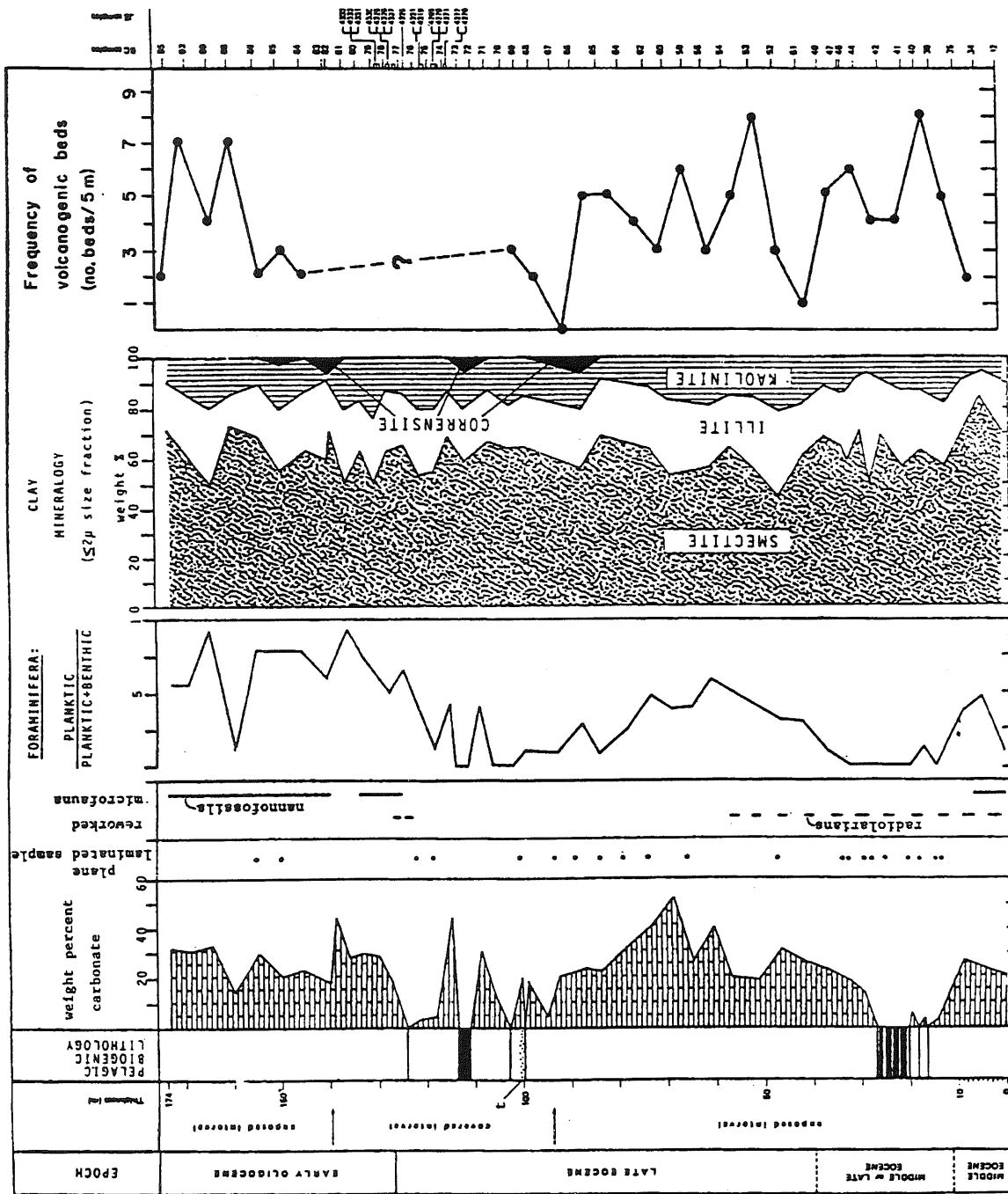


Figure 51: continued.

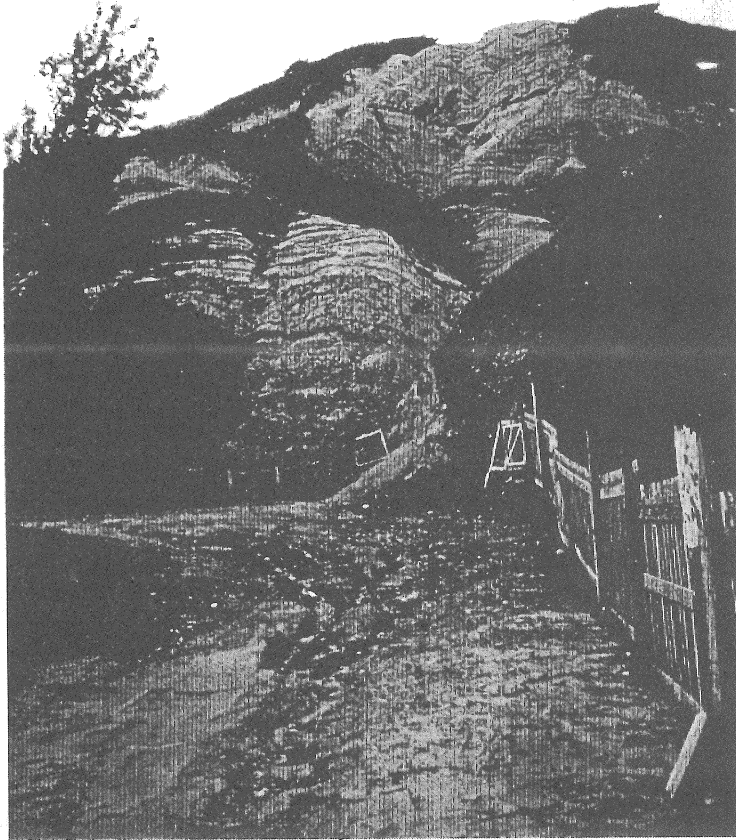


Figure 52: View west to Bath Cliffs from stop 8a; beds are marl (white) and ash (dark) of nappe O₆.

Table 2: Lithic properties of two suites in the basal complex at Bath Cliffs.

	<u>RADIOLARITE SUITE</u>	<u>HEMPELAGIC SUITE</u>
age	early - middle Eocene	early - middle Eocene
particle constituents	mostly siliceous fauna and clay, with minor dispersed silt-clay sized quartz; calcareous fauna and terrigenous and volcanogenic particles are notably absent	siliceous fauna and clay along with quartz (dispersed or in laminae or beds); turbidites contain quartz, K-spar, plagioclase, glauconite, mica, plant debris, mudclasts, shell fragments, and resedimented radiolaria and foraminifera of Late Cretaceous age
beds	massive or plane-laminated; laminated rocks consist of alternations of test-framework and test-floating layers between 0.4 and 3 mm thick; bioturbation is absent in laminated rocks and undetected in massive rocks	plane- and cross-lamination and bioturbation pervasive; interbedded quartzose turbidite, mudstone, laminated radiolarian mudstone and radiolarite, and mudclast breccia; turbidites are tabular and plane-bottomed with ss/mud ratios ≤ 1 and maximum particle size of fine-grained sand; beds of mudclast breccia are tabular and ungraded
organic content	organic carbon rich; total organic carbon = 1.9 - 10.7 %, but probably migrated	organic carbon rich; hydrocarbons may be migrated
diagenesis	local breccia of brick-red vesicular glass associated with solid hydrocarbon veins and columnar-jointed radiolarite; interpreted as a product of fusion around vents of burning hydrocarbon gas (mapped as r_b , Fig. 21)	siliceous tests are opal-A, opal-CI, quartz filled, or zeolitized; zeolites are members of heulandite group, none indicative of elevated P or T; clays are mostly mixed layer smectite/illite with minor discrete illite, kaolinite, and chlorite; mixed layer clays contain 70 - 100 % expandable layers

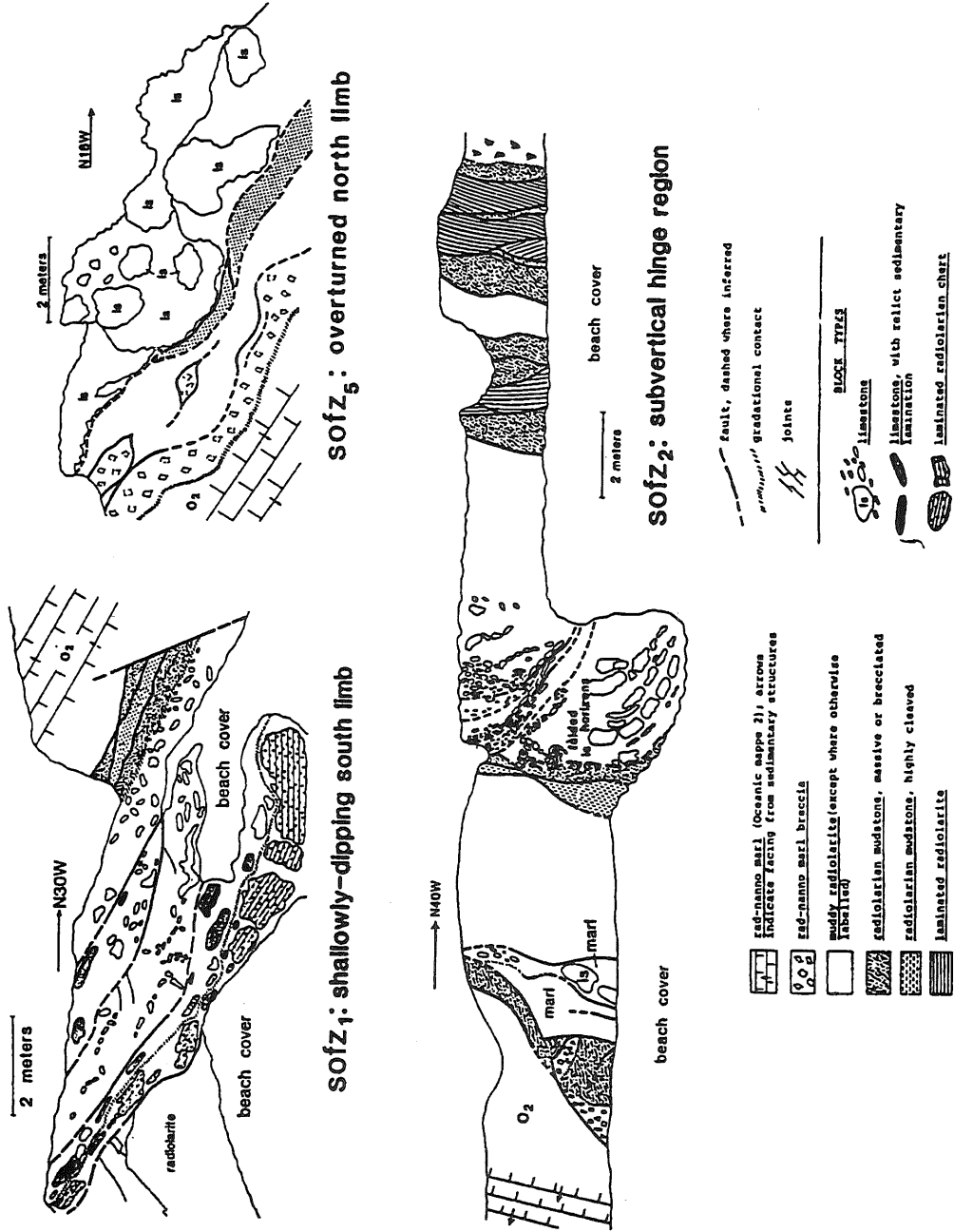


Figure 53: Outcrops drawings of SOFZ at three positions, located on Figure 48. Blocks are mainly concretionary limestone and cherty radstone. Elongate blocks are better aligned and more concentrated in horizons than equant blocks. Block horizons and foliation are folded.

D) NAPPE EMPLACEMENT MODEL

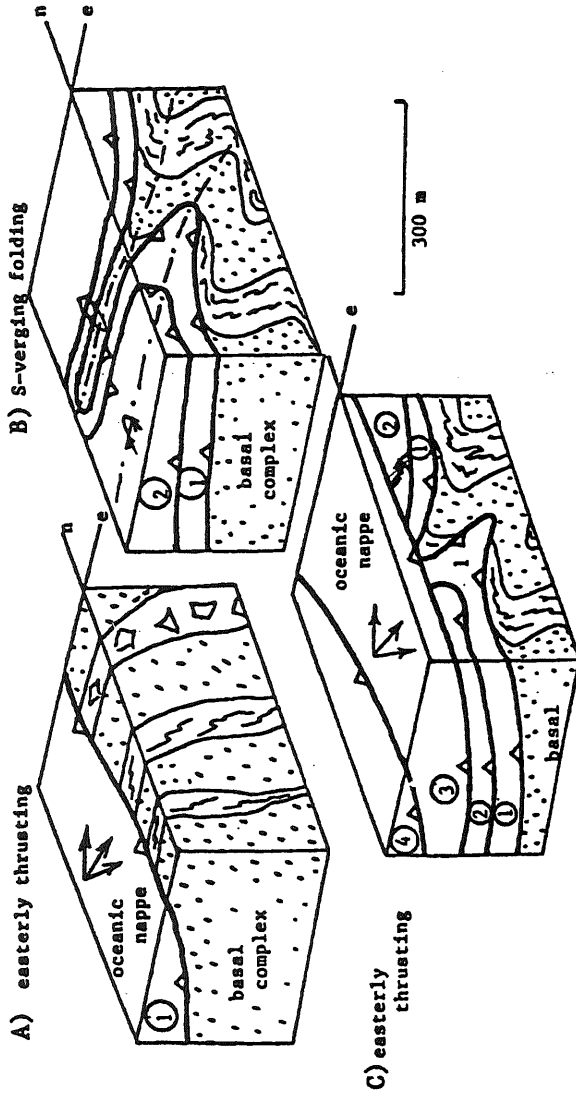
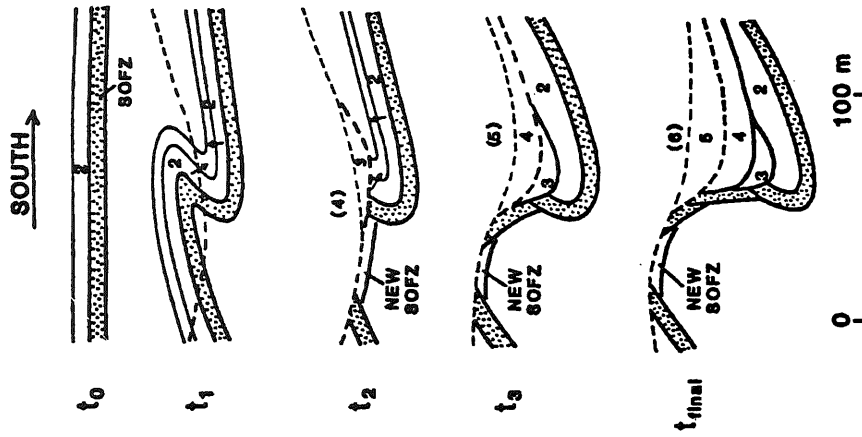


Figure 54: Model of emplacement of Oceanic allochthon at Bath. A,B,C: three stages of thrusting and folding. D shows sequential upward propagation of nappes from base (SOFZ) into allochthon. Allochthon transport normal to page. Heavy lines are active and extinct faults. Light, dashed lines are faults to be.



Site 10 provides a view of an important prism cover unit, the Conset Marl. The unit is very poorly exposed and has only recently been investigated by trenching. The outcrop area of Conset Marl is shown on Figure 46. Figure 44 shows this together with a suspected subcrop region of Conset Marl to the south of Ragged Point.

The Conset Marl consists of three lithotypes:

- 1) pelagic marl and ash;
- 2) arenitic carbonate turbidites;
- 3) debris flow.

Marl and ash form the topographically higher tier of the unit. The 40m thick succession of beds at St. Mark's roadcut is the only significant exposure (Fig. 54). These beds appear much like Oceanic beds and are distinguished from them by middle Miocene (*G. peripheronda*) ages.

Arenitic carbonate turbidites punctuate the roadcut section at two horizons (Fig. 55). They occur preferentially in the topographically lower tier of the unit together with debris flows. The turbidites contain microfossils of Eocene to Miocene age, but the dominant sand-framework species are early Miocene and the same as those which constitute the arenite of the Bissix Hill Formation.

Debris flow occurs low in the unit and consists of blocks and matrix of Oceanic beds and basal complex, together with minor Miocene components, including calcarenite.

The base of the Conset Marl lies unconformably on the Oceanic allochthon, basal complex, and SOFZ. its deposition thus followed the emplacement of the Oceanic allochthon.

The Conset Marl was probably deposited across the oceanward edge of the Oceanic allochthon, sourced initially by slides from the allochthon's front and by density currents that brought cover sediments from the shoaled crest of the allochthon edifice. With time the proportion of pelagic downfall relative to sediment-gravity transport increased, yielding the upper tier of the unit.

Walk

Examine the roadcut section of marl and ash on the road fork heading west from the 3-way intersection.

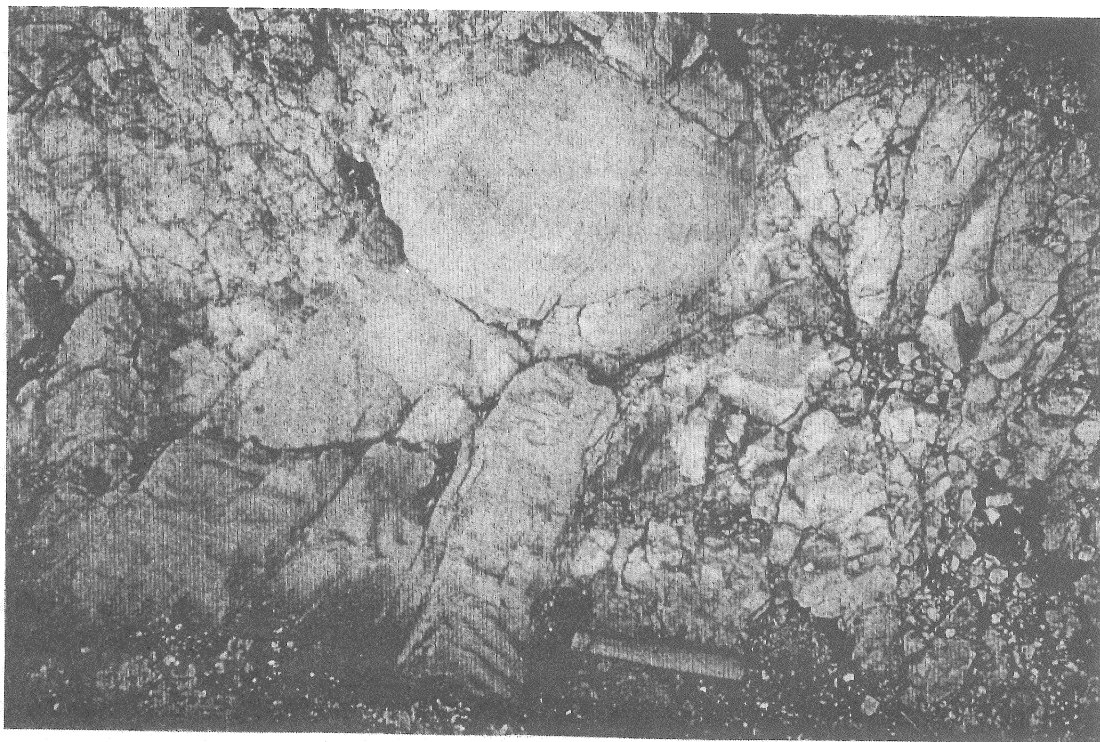
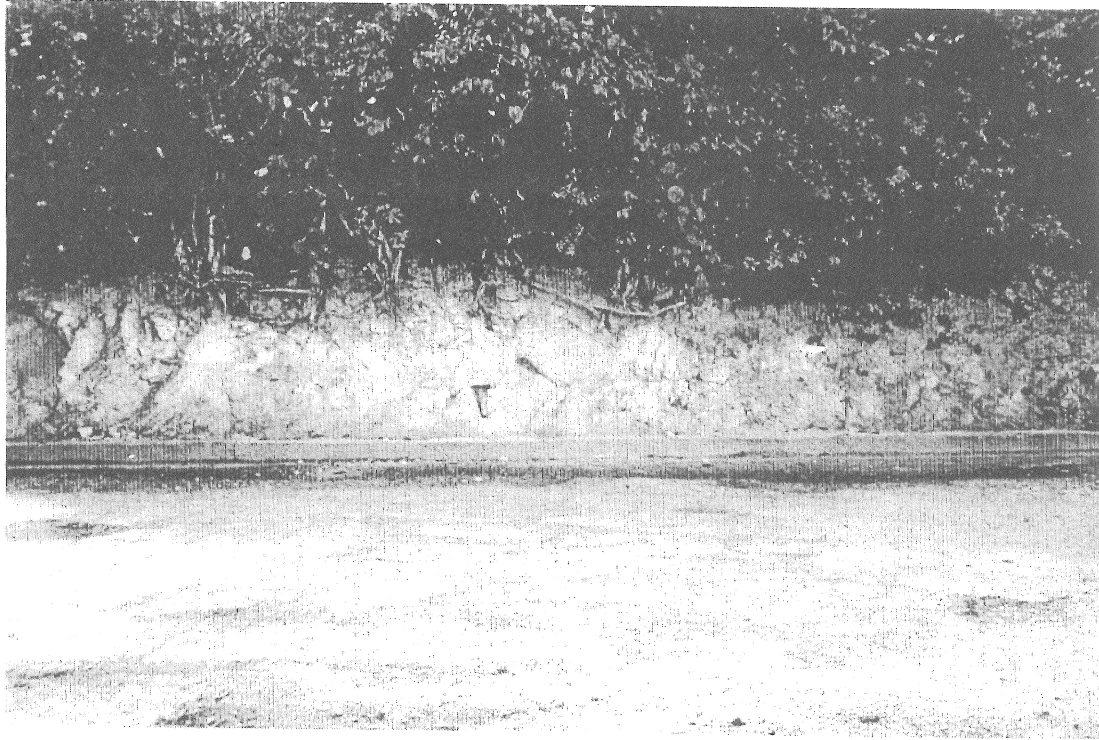


Figure 55: St. Mark's roadcut, Site 10. Upper photo shows Conset Marl in 15m thick section of beds dipping left (east) and overturned. White rocks are marl; orange bed is carbonate turbidite. Lower photo is closeup of turbidite; top to right (west).

Site 11 Ragged Point

<u>Route</u>	(Fig. 11)
21.1 km	Intersection near St. Mark's Church, Site 10; return to East Coast Highway.
22.8 km	Intersection East Coast hwy and Blades Hill – College Savannah road; turn left.
23.8 km	Thickets intersection; turn left; follow East Coast Hwy past Three Houses Spring, Bayfield, and Marleyvale
27.9 km	Intersection East Coast Hwy and road to Ragged Point lighthouse; turn left.
28.4 km	Ragged Point lighthouse; park.

General

Ragged Point provides the southernmost outcrop of basal complex on Barbados (Figs 2, 44). It is almost certainly within the axial region of the Woodbourne Trough up plunge from the Woodbourne oilfield. Ragged Point is a culmination or structural high within the Trough's axial region (Fig. 44).

The rocks at Ragged Point are terrigenous and principally quartz sandstone (Fig. 56). The beds from an inverted homocline, about 250m thick. Sandstones are anomalously coarse and thick compared to other sites in the basal complex. They are also unusual because of massivity, evidently due to bioturbation, and because of intercalated muddy units but without beds of transitional size ranges.

Figure 57 is a section at Ragged Point measured by Larue (1985). Facies low in the section are D, E, and B whereas the higher beds are 140m of mainly facies B. These are overlain by facies C and D, implying upward fining and thinning. Based on this finding, the sandstones at Ragged Point may be an inner fan channel deposit.

The inverted homocline of Ragged Point may be overturned limb of a major south-vergent fold (section, Fig. 56).

The basal complex at Ragged Point either was never covered by Oceanic allochthon or the allochthon was there but denuded before deposition of Conset Marl on Ragged Point's southern flank. In either case, the basal complex was relatively high at Ragged Point in mid-Miocene time. Since then, Ragged Point has risen further, perhaps forming an island in the Quaternary.

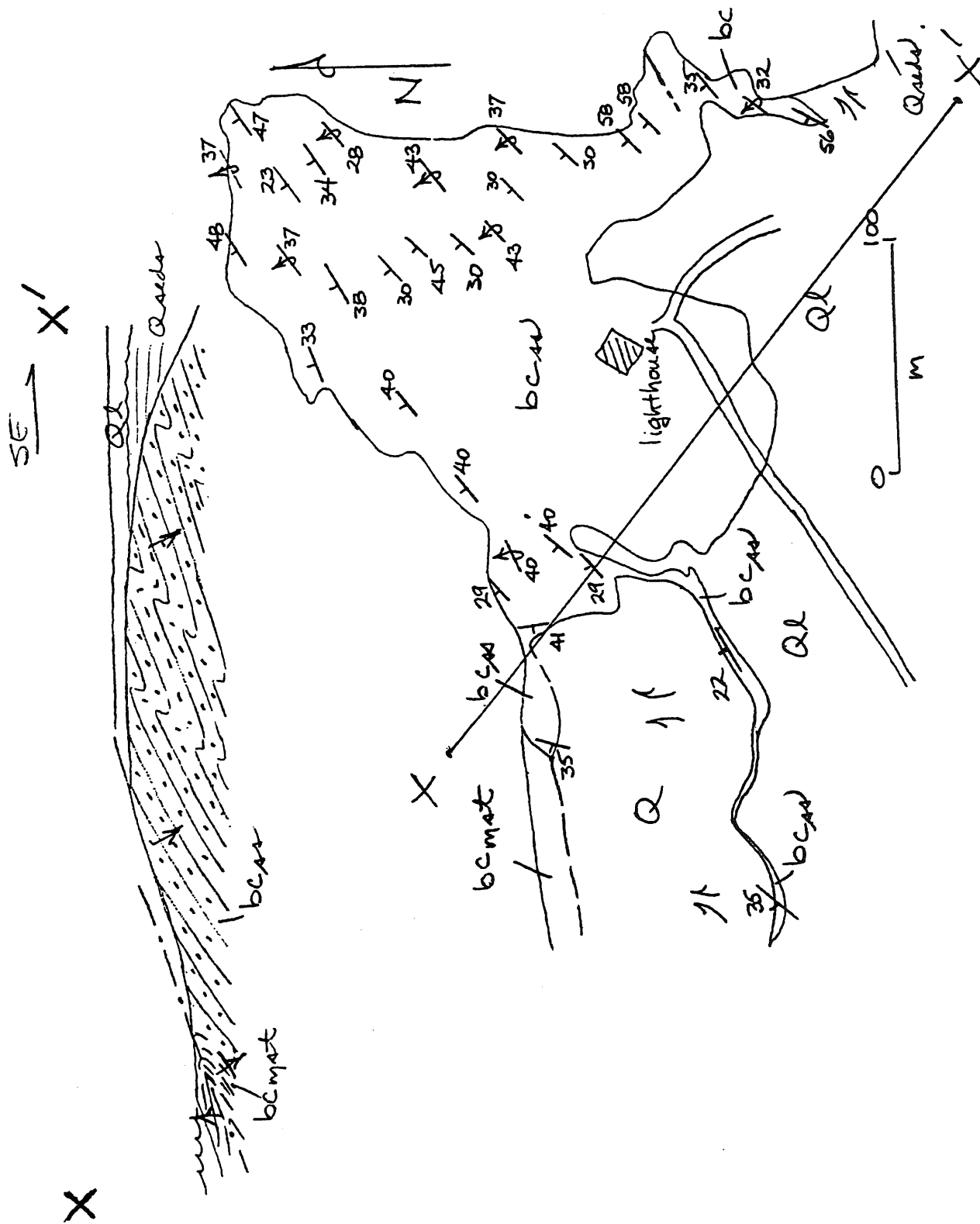


Figure 56: Geologic map and section of Ragged Point. Arrows in section show facing.

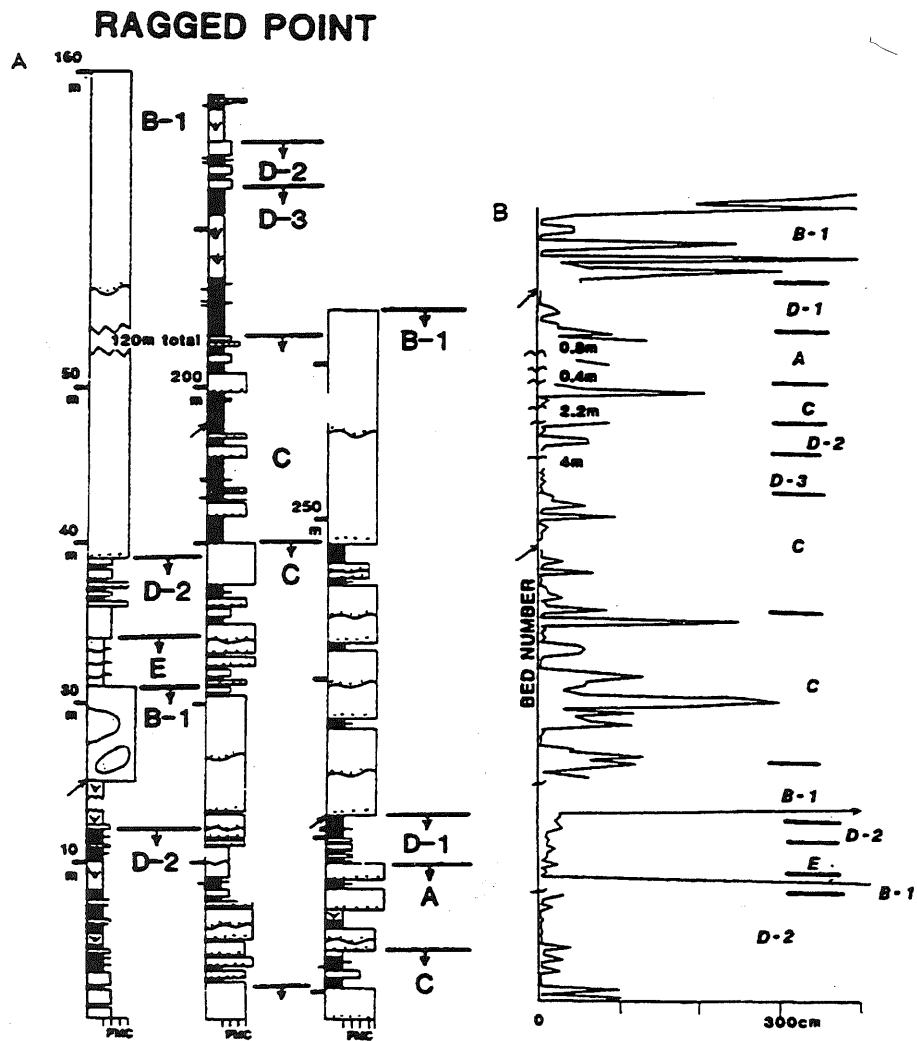


Figure 57: Columnar section and thickness vs height of beds in basal complex at Ragged Point; from Larue (1985).

Evidence is the thin coating of reefal limestone on the Point's crest whereas thick Quaternary clastics underlie the limestone on the southern flank (section, Fig. 56). The record at Ragged Point may suggest episodic or continuous movements within the Woodbourne Trough through Neogene time.

Walk

Walk NE from lighthouse to Point, about 200m; observe thick coarse grained sandstones.. Return 150m toward lighthouse, turn left, proceed on foot path SE and downhill, going upsection through coarse sandstones. Intervals of muddy beds are seen near base of cliff.

References

- Barker, L.H., J.M. Gordon, and R.C. Speed, A study of the Barbados intermediate unit, surface and subsurface; Transactions 11th Caribbean Geological Conference, Barbados, p. 36, 1-24, 1986.
- Bender, M.J. and others, Uranium-series dating of Pleistocene reef tracts of Barbados, Geological Society of America Bulletin, 90, 577-594, 1979.
- Fairbanks, R.G., and R.K. Matthews, The marine oxygen isotope record in Pleistocene coral, Barbados, Quaternary Research, 10, 181-196, 1978.
- Gallup, C.D., R.L. Edwards, and R.C. Johnson, The timing of high sea levels over the past 200,000 years; Science, 263, 796-8800, 1994.
- Jansma, P.E. and R Speed, Subhorizontal structures and duplex in the accretionary complex of Barbados at Walker's Savannah; Trans 11th Caribbean Geological Conference, 16:1 to 16:14, 1986.
- Kugler, H.P., P. Jung, and J. Saunders, The Joe's River Formation of Barbados and its fauna; Ecological geol Helvet. 77, 675-705, 1984.
- Larue, D.K., Nappe dismembered by melange intrusion, Cattlewash, Barbados; Trans 11th Caribbean Geol. Conf., 30:1 to 30:14, 1986.
- Larue, D.K., and R.C. Speed, Quartzose turbidites of the accretionary complex of Barbados, I: Chalky Mount succession, Journal Sedimentary Petrology, 53, 1337-1352, 1983.
- Larue, D.K., and R.C. Speed, Structure of the accretionary complex of Barbados, II: Bissex Hill, Geological Society of America Bulletin, 95, 1360-1370, 1984.
- Matthews, R.K., Relative elevation of late Pleistocene high sea-level stands, Barbados, Quaternary Research, 3, 147-153, 1973.
- Mesoella, K.J., H.A. Sealy, and R.K. Matthews, Facies geometries within Pleistocene reefs of Barbados, American Association Petroleum Geologists Bulletin, 54, 1899-1917, 1970.
- Poole, E., and L.H. Barker, Geologic map of Barbados, Govt. of Barbados publication, 1982.
- Saunders, J.B., and seven authors, Stratigraphy of the late Middle Eocene to Early Oligocene in the Bath Cliff section, Barbados, Micropaleontology, 30, 390-425, 1984.

- Senn, A., Die Geologie der Insel Barbados B.W.I. (kleine Antillen) und die Morphogenese der umliegenden marinen Grosformen, *Ecologiae Geologicae Helvetiae*, 40, 199-222, 1948.
- Sedlock, R.L. and R. Speed, Structural evolution of the accretionary complex of Barbados in the Morgan Lewis area; *Trans 11 Caribbean Geo. Conf.*, 17:1 and 17:14, 1986.
- Speed, R.C., Geology of Barbados: Implications for an accretionary origin, *Proceedings 26th International Geological Congress*, 259-265, 1979.
- Speed, R.C., Structure of the accretionary complex of Barbados, 1: Chalky Mount, *Geological Society of America Bulletin*, 94, 92-1126, 1983.
- Speed, R.C., Volume loss and defluidization history of Barbados, *Journal Geological Research*, 95, 8983-8996, 1990.
- Speed, R.C., Geological history of Barbados: A preliminary synthesis, *Transactions 11th Caribbean Geological Congress*, 29, 1-11, 1988.
- Speed, R. and L. Barker, Quaternary terrace and uplift history in St. Philip, Barbados; *Transactions 14th Caribbean Geological Conference.*, Trinidad, 1997, in press.
- Speed, R.C., and D.K. Larue, Barbados: Architecture and implications for accretion, *Journal Geophysical Research*, 87, 3633-3643, 1982.
- Taylor, F. MS Thesis, Brown Univ., 1974.
- Torrini, R., Structure and kinematics of the oceanic nappes, Barbados, *Transactions 11th Caribbean Geological Congress Barbados*, 16, 1-14, 1988.
- Torrini, R., and R.C. Speed, Tectonic wedging in the forearc basin-accretionary prism transition, Lesser Antilles forearc, *Journal Geophysical Research*, 94, 10, 549-10, 584, 1989.
- Torrini, R., and R.C. Speed, and G.S. Mattioli, Tectonic relations between forearc basin strata and the accretionary complex at Bath, Barbados, *Geological Society of America Bulletin*, 96, 861-873, 1985.